Talanta 302 (2026) 129373

Contents lists available at ScienceDirect

Talanta

journal homepage: www.elsevier.com/locate/talanta

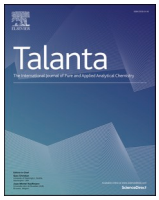

Recent advances in electrochemical genosensing

Alnilan Lobato [a,b,*], Mitja Koderman [a,c], Nika Vranešič [a], Samo B. Hočevar [a], Nikola Tasić [a,**]

[a] Department of Analytical Chemistry, National Institute of Chemistry, Ljubljana, Slovenia
[b] International Postgraduate School Jožef Stefan, Ljubljana, Slovenia
[c] Faculty of Chemistry and Chemical Technology, Ljubljana, Slovenia

ARTICLE INFO

Keywords:
Electrochemical genosensor
Nucleic acid detection
Nanomaterials
Capture probe
Signal amplification
Target sequences

ABSTRACT

Electrochemical genosensing finds applications across a wide range of fields, including clinical diagnostics, forensic science, food safety, agriculture, biotechnology, cancer research, defense, environmental monitoring, etc. It focuses on the detection of specific DNA or RNA sequences, often called target sequences, rather than target analytes as in conventional (electro)analysis. Since the groundbreaking contributions dating back to the late 1990s and early 2000s, nearly 500 articles have been published elucidating various important aspects of this research field. This review aims to provide an overview of the current state of knowledge, serving as a comprehensive synthesis of the most recent literature on electrochemical genosensors, published in the last five years. Hopefully, it will also serve as a valuable resource for students, young researchers, scientists, non-academics, or other professionals seeking a consolidated understanding of the key aspects behind this research area, without delving into a collection of individual and scattered studies.

1. Introduction

Electrochemical genosensing emerges as a versatile approach for detecting genetic material, specifically nucleic acids, making it an evolving alternative to conventional central laboratory techniques such as polymerase chain reaction (PCR) [1], reverse transcription PCR (RT-PCR) [2], quantitative PCR (qPCR) [3,4], loop-mediated isothermal amplification (LAMP) [5,6], Northern and Southern blotting [7,8], and fluorescence in situ hybridization (FISH) [9]. This innovative approach merges electrochemistry with sophisticated molecular biology methods and reportedly offers rapid, sensitive, and selective detection of nucleic acids. The main goal of this rapidly growing technology is to eventually revolutionize various fields, including clinical diagnostics and environmental monitoring, due to its noteworthy electroanalytical performance, portability, and potential for multiplexed analysis. In the most typical setup, electrochemical genosensing operates on the principle of molecular recognition between complementary DNA (deoxyribonucleic acid) or RNA (ribonucleic acid) strands [10]. DNA is the fundamental genetic material of all living organisms [11], containing the sequence that encodes the instructions for protein formation, the maintenance of cellular functions, and the inheritance of genetic traits across generations [12]. The ability to accurately recognize and analyze DNA sequences is crucial for understanding genetic diseases, identifying pathogens, and studying genetic variation [13,14].

Similar to affinity biosensors, the main components of an electrochemical genosensor typically include a recognition element, such as DNA or RNA capture probes, a transducer (supporting electrode), and a signal-processing unit [15]. Capture probes are short, single-stranded sequences of nucleotides that are complementary to the target sequence [16]. In the most typical "direct" architecture, these probes are immobilized or anchored on the surface of the supporting electrode by various immobilization techniques. After the hybridization with the target sequence, the electrochemical properties of the electrode interface are altered so that the target sequence can be detected and quantified using various electrochemical approaches. Alternatively, the hybridization event can be carried out ex situ and then transferred to the electrode surface, where the degree of hybridization is measured electrochemically. The state-of-the-art in the field of electrochemical genosensors offers far more diversified sensor architectures and detection principles, and will be thoroughly presented in this review article. The article will also provide a concise theoretical introduction to the common electrochemical techniques used, motivated by their ability to detect swift and small changes in relevant electrochemical processes, thereby enabling the detection of very low concentrations of target

* Corresponding author. Department of Analytical Chemistry, National Institute of Chemistry, Hajdrihova 19, SI, 1000, Ljubljana, Slovenia.
** Corresponding author. Department of Analytical Chemistry, National Institute of Chemistry, Hajdrihova 19, SI, 1000, Ljubljana, Slovenia.
E-mail addresses: alnilan.lobato@ki.si (A. Lobato), nikola.tasic@ki.si (N. Tasić).

https://doi.org/10.1016/j.talanta.2026.129373
Received 17 November 2025; Received in revised form 25 December 2025; Accepted 7 January 2026
Available online 13 January 2026

sequences that were beyond belief for decades. The high sensitivity of electrochemical techniques is particularly advantageous in clinical diagnostics, where early detection of genetic mutations or infectious agents is crucial for timely intervention and treatment. In addition, owing to the specificity of the DNA hybridization event, e.g., a pairing of complementary single-stranded DNAs (ssDNAs) to form a double-stranded DNA molecule, electrochemical genosensors exhibit excellent selectivity towards the target sequence. The complementary base pairing between the DNA probe and the target sequence ensures that only the desired sequence is detected, while non-specific binding is minimized through precautionary measures taken during sensor fabrication, which involve the introduction of various blocking agents [17]. This specificity minimizes false-positive results and enhances the accuracy of the genosensing platform, making it potentially reliable for practical applications.

In electrochemical genosensing, a recurring but not essential step is the use of a signal amplification process, such as enzyme-based amplification, secondary nucleic acid amplification, and nanomaterial-based amplification. Enzyme-based amplification involves the use of enzymes to produce redox-active products that provide a relatively high electrochemical response [18]. In nucleic acid amplification, enzymes or nucleic acids are used to replicate, elongate, or break the DNA chain to affect the corresponding electrochemical signal [19,20]. In nanomaterial-based amplification, nanomaterials, which can be carbonaceous, magnetic, metallic, metal-oxides, zero-to three-dimensional, etc., are incorporated into one or more layers of the sensor architecture, which can serve both to amplify the electrochemical signal and as a support for more stable immobilization of the biological recognition elements [21,22].

The versatility of electrochemical genosensing aims to extend beyond laboratory settings, as these sensors can be miniaturized and integrated into portable devices for on-site and point-of-care diagnostics/applications. The simplicity and cutting-edge miniaturization of the electrochemical instrumentation, coupled with the potential for automation and multiplexed analysis, make electrochemical genosensing a good candidate for resource-limited circumstances and decentralized healthcare systems. More importantly, the swift turnaround time of electrochemical genosensors facilitates real-time monitoring of biological processes, such as disease progression, enabling timely decision-making and intervention. Moreover, these devices hold promise for various other fields, including food safety [23], environmental monitoring [24], and forensic analysis [25]. This is particularly relevant for the detection of foodborne pathogens, environmental contaminants, and genetic markers associated with advanced forensic investigations. As research in the field of genosensing is spread across various disciplines and has progressed to the point where we can anticipate further advancements that will enhance the overall genosensing performance and broaden real-life applications, there is a need for a comprehensive and systematic review article on recent electrochemical genosensing, reflecting a broader selection of reports and criteria compared to already available review articles.

2. Available review articles on genosensing

The first review on electrochemical genosensors dates back to 2011. The authors revised the existing literature concerning different PCR-amplification strategies [26]. The amplification step is often considered necessary due to very low concentrations of the target nucleic acids, which are below the detection limits of conventional analytical techniques. Thus, the amplification with the PCR protocol usually guarantees comfort against false negative results. This review article gathered 29 published studies, related to the (i) direct sensing of the target nucleic acids, (ii) nucleic acid detection through electroactive indicators, i.e., methylene blue (MB), meldola blue, Hoechst 33258 redox-active molecule, transition metal complexes, and (iii) nucleic acid detection via enzyme amplification schemes, e.g., by using alkaline phosphatase (ALP), horseradish peroxidase (HRP), other peroxidases (POD), or glucose-6-phosphate dehydrogenase (G6PDH). The same group has also published a review article that focused on thus far existing ca. 25 research reports on the subject of cancer-related micro RNAs (miRNAs) detection [27]. In a more recent review, Mohammadi et al. provided an updated version on the electrochemical genosensing of miRNAs, covering ca. 20 articles, mainly dealing with different amplification strategies [28]. A couple of years later, Campuzano et al. published a comprehensive review concerning the genosensing of circulating biomarkers holding different roles, such as risk screening, prognostic, predictive, diagnostic, and disease monitoring [29]. At the time, the review provided valuable perspectives on recent progress and future prospects in the electrochemical detection of biomarkers related to bacterial infections, viral infections, neurodegenerative diseases, and cancer, involving a selection of 44 articles. The same group contributed two more review articles, one on the matter of electrochemical genosensing of circulating tumor DNA and its specific features [30], and the second on the advances in electrochemical sensing targeting epigenetic modifications of nucleic acids [31]. In addition, Prof. Ferapontova wrote a concise and critical review on the trends of constructing label-free DNA hybridization genosensors, focusing on the electrical properties of nucleic acids, reviewing 51 articles [32].

An updated review on the DNA-based electrochemical sensing of cancer biomarkers was published by Sadighbayan et al. [33]. It is important to highlight that this review stands out as the most comprehensive one, encompassing over 150 articles on various types of cancer, including colorectal, cervical, breast, prostate, lung, pancreatic, oral, acute lymphocytic leukemia (ALL), and others. The authors opted for the term “DNA-based biosensing” in the title, while the term “genosensor” was extensively utilized throughout the manuscript, which focused on contemporary DNA-hybridization sensors in a very systematic manner.

Manzanares-Palenzuela et al. have compiled an extensive review discussing electrochemical DNA-hybridization sensors designed for genetically-modified organisms (GMOs) [13]. The review encompasses various facets, including the choice of electrochemical transducers, target sequence selection, immobilization strategies, and detection methods. The article summarized 35 articles related to the subject matter.

In a very specific review article, Orozco et al. dealt with the electrochemical genosensing tools for monitoring blooms in toxic algae [34]. Besides the short review that involved ca. 10 articles, the authors also presented their own work within the same scope and provided a respectful critical overview concerning limitations and future prospects behind the technology.

Similarly, Hasanzadeh et al. published a narrow-scoped review on the nanomaterials and signal enhancement methods for the genosensing of p53 tumor suppressor protein [35]. In a very detailed manner, the authors reviewed ca. 20 electrochemical genosensors and provided comparative tables with the relevant fabrication and analytical performance data, including signal amplification components, linear range, limit of detection (LOD), capture or target sequences, nanomaterials used, etc. Babaei et al. reviewed electrochemical, optical, and surface plasmon resonance genosensors for the detection of viral species, and the approaches, limitations, and developments, with a review spanning almost 300 articles [36]. Thapa et al. focused on describing capture/signaling probe immobilization and signal amplification strategies in electrochemical genosensing, reviewing ca. 140 articles [37].

A mini 3-page review was published by El Goumi, in which the author briefly reviewed the definition and fields of application [38]. Finally, another review worth mentioning covers the usage of nanomaterials in electrochemical genosensing, covering various important aspects [39].

3. Supporting electrodes for electrochemical genosensing

The choice of an appropriate supporting electrode is critical in

genosensing because it might influence the sensitivity, selectivity, reproducibility, and overall electroanalytical performance of the genosensor. The supporting electrode serves as the substrate on which the capture probe is immobilized, and its properties significantly affect the interactions with the target sequence and the consequent signal transduction. When selecting a suitable supporting electrode, researchers should consider various key physicochemical properties and aim to address as many of them as possible. These properties include surface roughness, the chemical composition of the electrode surface, the presence of functional groups, electrical conductivity, compatibility with commonly used immobilization chemicals, biocompatibility with the sample, ease of functionalization, electrochemical reproducibility, stability, fabrication costs, etc. As in conventional biosensing, two major types of supporting electrodes are mostly utilized, i.e., **one-shot/disposable** and **conventional solid electrodes**. Disposable electrodes are typically designed for on-site, real-time analysis, prioritizing ease of use and integration into portable potentiostats. In contrast, conventional solid electrodes are generally used in laboratory settings, offering higher reproducibility, stability, and versatility for detailed electroanalytical as well as fundamental studies. A variety of electrode materials and designs are commonly employed in genosensing, each offering unique advantages tailored to specific applications and operating settings, including glassy carbon electrodes (GCE) [21,40–48], carbon electrodes (CE) [49,50], gold electrodes (AuE) [51–64], gold microelectrodes (μAuE) [65], 3D-printed electrodes [66,67], paper-based electrodes [68], pencil graphite electrodes (PGE) [69,70], aluminium-based electrodes [71], carbon paste electrodes (CPE) [72], screen-printed carbon electrodes (SPCE) [73–80], screen-printed gold electrodes (SPAuE) [17,81–92], "in-house" produced electrodes [93–95], fluorine-doped tin oxide (FTO) electrodes [96–98], and others [99–101].

Gold electrodes (AuEs) are probably the most preferred option, particularly for their biocompatibility and ability to form strong thiol-gold bonds, which reportedly enhance the stability of the immobilized capture probe. Otherwise, it goes without saying that gold electrodes are the most utilized electrodes in the general field of electrochemical biosensing, with applications ranging from detecting DNA and RNA sequences [102], monitoring glucose levels in diabetes management [103], identifying cancer biomarkers [104], tracking environmental pollutants [105,106], performing drug screening [107], analyzing protein interactions [108], etc. **Glassy carbon electrodes (GCEs)** are widely used due to their excellent chemical inertness, high conductivity, and smooth surface, which assures efficient probe immobilization [109]. Interestingly, over the past several years, this type of supporting electrode was solely used in direct detection approaches, characterized by modification of the electrode surface with the appropriate nanomaterials, followed by the immobilization of the capture probes, and a subsequent electrochemical detection typically based on the presence of selected redox active species. On the other hand, advancements in thick film technologies have led to the development of **screen-printed electrodes** (SPEs), such as SPAuE and SPCE, which stand out for their affordability and suitability for large-scale manufacturing. These features make SPEs particularly suitable for tailoring portable and disposable genosensors. However, while the intrinsic irreproducibility is a persistent problem, their ease of functionalization is highly appealing and attracts considerable attention.

It should be noted that AuEs, GCEs, and SPEs have been extensively studied and widely employed in electrochemical sensing platforms for many years. While they offer reliable performance and established protocols for modification, their long-standing use limits their novelty and innovative appeal in the context of emerging genosensing principles. As such, this review will prioritize studies that utilize less conventional or newly engineered electrode substrates, which offer good surface functionalization possibilities, adaptability for the integration of functional nanomaterials, and potential for improved sensitivity and selectivity in genosensing applications.

3D-printed nanocarbon electrodes were recently developed in Pumera's group by using the fused deposition modeling (FDM) method. Nanocarbon/polylactic acid (PLA) filament was extruded at 220 °C from the printing device nozzle into a 3D working electrode shape, and the electrical conductivity of the printed electrodes was further enhanced through the N,N-dimethylformamide-activation procedure reported elsewhere [67]. Electrodes were used to monitor the DNA hybridization process via enzyme-linked linear sweep voltammetry (LSV). Similarly, the same group reported on the fabrication of a needle-like 3D-printed working electrode included in a system comprising a polydimethylsiloxane (PDMS) microfluidic channel and the 3D-printed electrochemical cell. The electrode material was also based on nanocarbon/PLA filaments, as mentioned above. The electrode was used to immobilize ssDNA capture probe targeting the N gene sequence of SARS-CoV-2, and the differential pulse voltammetry (DPV) was used to follow adenine oxidation upon the desorption of the hybridization product [66]. The fabrication procedure of such a sensor is depicted in Fig. 1a.

Pencil graphite electrodes (PGEs) are low-cost, disposable, and conductive platforms that have recently been used in electrochemical sensing due to their ease of modification and availability. Flauzino et al. used a graphite disk electrode in the standard three-electrode electrochemical setup for the detection of meat adulteration via electrochemical impedance spectroscopy (EIS) and square-wave voltammetry (SWV) to quantify a specific target sequence [80]. Kivrak et al. exploited PGEs by incorporating carbon nanotubes (CNTs), creating a working electrode within the conventional three-electrode setup for detecting specific point mutations in the genome using the **CRISPR-Cas9 protocol** [70]. CRISPR stands for clustered regularly interspaced short palindromic repeats, wheras CRISPR-Cas9 is a revolutionary genome-editing tool, enabling precise modifications in DNA sequences [110]. The capture probe was immobilized via 1-ethyl-3-(3-dimethylaminopropyl) carbodiimide (EDC) and N-hydroxysuccinimide (NHS), i.e., EDC/NHS chemistry, and the detection of the sequence was carried out by DPV. PGEs were also modified with graphene oxide (GO) via a slightly modified Hummers' method [111], followed by the electrochemical reduction to obtain reduced graphene oxide (rGO). The electrode was then electropolymerized with 3-hydroxybutyric acid (BHB) monomer via cyclic voltammetry (CV), while the immobilization of the capture probe was performed by EDC/NHS protocol. In another report on the usage of PGE for genosensing, Moattari et al. modified the PGE with rGO, followed by electrodeposition of Au from the corresponding chloride solution [69]. Single-stranded DNA capture probe with 5′-thiol group was immobilized onto the gold support, and the target sequence was detected via EIS upon the hybridization event.

Magneto-actuated graphite-epoxy composite electrodes (*m*-GEC) leverage the incorporation of magnetic nanoparticles within the electrode matrix, enabling precise manipulation and orientation under an external magnetic field. These electrodes can be particularly advantageous in biosensing applications, as magnetic actuation allows for controlled sensor-sample interaction and reduces nonspecific binding, resulting in higher sensitivity and selectivity. However, they have somewhat complex operating principles and laborious protocols. These electrodes were used by Pallares-Rusinol et al. for the detection of specific exosomes, which are highly regarded for their role as biomarkers for breast cancer [91]. The measurement procedure included the usage of antibodies with the magnetic particles, amplification of the target sequence with double-tagging RT-PCR, using primers tagged with biotin and digoxigenin (DIG). DIG is a small steroid-like molecule derived from the foxglove plant (*Digitalis purpurea*), commonly used as a non-radioactive labeling molecule in molecular biology for detecting nucleic acids [112]. The primer tagged with DIG served for labeling with anti-DIG HRP conjugate, and electrochemical detection was performed using an amperometric readout on the *m*-GEC, with HRP acting as the reporter probe. The scheme is presented in Fig. 1b.

Carbon paste electrodes (CPEs) are made from a mixture of carbon powder and a binder, typically a viscous oil-like liquid [113]. Known for

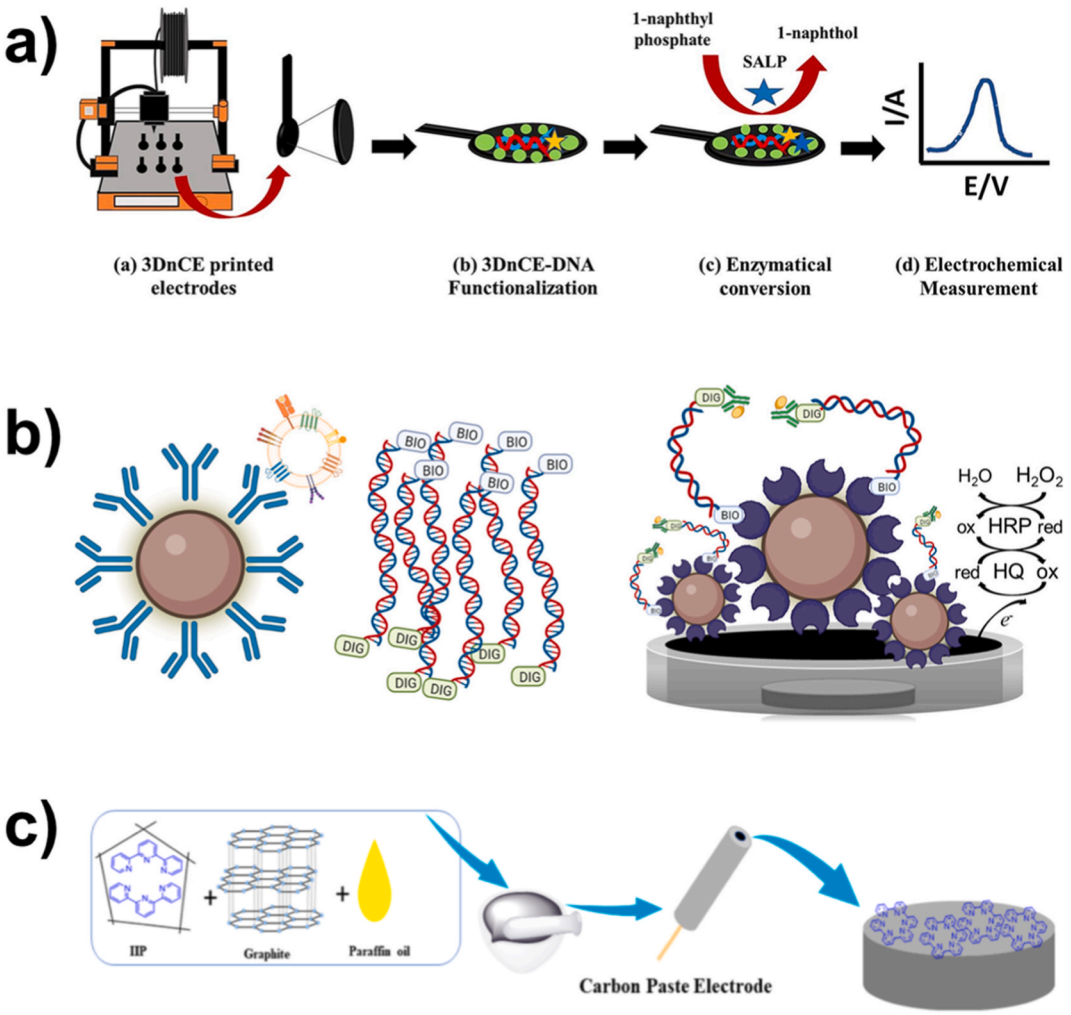

Fig. 1. a) Fabrication process of 3D nanocarbon electrodes along with the simple detection scheme (image reproduced from Ref. [67] with permission from *Wiley*), **b)** magneto-actuated graphite-epoxy composite electrodes (*m*-GEC) along with the signal generation scheme (image reproduced from Ref. [91] with permission from *ACS Publications*), **c)** carbon paste electrodes (CPEs) used for genosensing of HIV-1 pol gene (image reproduced from Ref. [72] with permission from *Elsevier*).

their versatility, low cost, and ease of bulk modification, CPEs are widely used for detecting biomolecules, environmental pollutants, and trace metal ions [114–116]. Recently, they have been investigated in electrochemical genosensing for the DPV detection of the HIV-1 pol gene of the human immunodeficiency virus type 1 [72], which is responsible for encoding key enzymes such as reverse transcriptase (RT), protease (PR), and integrase (IN). For this purpose, the surface of CPE was impregnated with lead ion-imprinted polymer nanoparticles, followed by the electrochemical deposition of Au nanoparticles and the immobilization of the corresponding ssDNA capture probe via a tris(2-carboxyethyl) phosphine (TCEP)-based protocol (Fig. 1c).

Indium tin oxide (ITO) glass is a transparent and conductive material commonly used as an electrode in biosensors and optoelectronic devices due to its excellent electrical conductivity and optical transparency. Javed et al. report on the use of ITO as the supporting electrode for further modification with a GO/chitosan composite, and subsequent DPV detection of the *Mycobacterium tuberculosis* target sequence. The capture ssDNA probe was immobilized using 1 % glutaraldehyde (GA), while bovine serum albumin (BSA) served for blocking the remaining non-specific binding sites. The sensor was used in the conventional three-electrode electrochemical cell [117]. **Fluorine-doped tin oxide (FTO) glass** is also a transparent, conductive material used as an electrode in (photo)electrochemical applications due to its high electrical conductivity, chemical stability, and optical transparency. In a recent study, Shishegari et al. used FTO glass as the supporting electrode for multi-step modification. Firstly, sulfur-doped reduced graphene oxide (S-rGO) was cast on the electrode surface to enhance conductivity, followed by electrodeposition of dendritic palladium nanostructures (Den-PdNS) to increase (electro)catalytic activity. Afterwards, a cerium-based metal-organic framework (Ce-MOF) was added to provide a high surface area with (electro)catalytic cerium sites. Finally, the electrode was functionalized using EDC/NHS chemistry to enable the immobilization of ssDNA capture probes, and a blocking agent was used to prevent non-specific binding [96]. In a similar study, Heidari et al. used an FTO electrode modified with a palladium-aluminum layered double hydroxide (Pd–Al LDH) film. This modification provided high conductivity and (electro)catalytic activity. A ssDNA probe was immobilized on the LDH film, followed by the deposition of 6-mercapto-1-hexanol (MCH) to prevent non-specific interactions. The final step involved the hybridization of target DNA to assess the electroanalytical performance of the genosensor [97].

Paper-based electrodes have recently gained significant attention in the general field of electroanalysis due to their low cost, flexibility, biodegradability, and suitability for point-of-care applications, enabling the fabrication of portable and disposable sensing platforms [118–120]. In electrochemical genosensing, a recent contribution from Zhan et al. draws particular attention [121]. Carbon paper was modified with gold nanoparticles to provide a high-surface-area scaffold, further functionalized with DNA hairpins and GOx on the bioanode and DNA tetrahedra on the biocathode, creating a dual-electrode system that drives catalytic

hairpin assembly and electron transfer for ultrasensitive miRNA-21 detection. A study published by Bishoyi et al. reports the development of a low-cost, paper-based genosensor for Zika virus detection, where the supporting electrode, a paper-based graphene platform printed with carbon conductive ink, was strategically modified by drop-depositing AgNPs to enhance electron transfer kinetics and provide a biocompatible surface, followed by immobilization of a DNA probe specific to Zika virus, enabling sensitive detection through CV changes upon target DNA hybridization [68].

A recent work proposed by Aldea et al. centers on the fabrication and use of innovative **gold-coated electrospun polymeric fiber electrodes** (Au/PMMA/PET), whose three-dimensional fibrous architecture dramatically increases electroactive surface area and enables robust immobilization of phosphorothioated oligonucleotides via strong Au–S bonds, outperforming conventional planar Au/Ti/SiO_2/Si electrodes in sensitivity, selectivity, and stability for electrochemical genosensing of the BCR/ABL fusion gene [100].

Finally, an original genosensor was recently demonstrated in which a **conical glass micropipette served as an electrode**; the inner surface of the pipette was modified with amino-functionalized silica nanowires covalently linked to complementary probe DNA, enabling ultra-sensitive miRNA detection through ionic current changes [101]. Meanwhile, the outer surface is coated with AuNPs, which were further functionalized with aptamers and MB to allow protein detection via surface-enhanced Raman scattering (SERS). This dual-surface architecture provides distinct and independent detection mechanisms without cross-interference.

As a final point, although the supporting electrode largely defines the baseline electrochemical performance, it is the interface between the transducer and the biological recognition element that ultimately dictates functionality of the genosensor. From the selection of the supporting electrode, the focus naturally shifts to the immobilization of nucleic acid capture probes, a critical step that directly governs probe density, orientation, accessibility, and long-term stability. It should be emphasized that the physicochemical properties of the electrode, particularly surface chemistry and roughness, impose clear constraints on the anchoring and immobilization strategies that can be adopted. Accordingly, probe immobilization should not be regarded as an isolated fabrication step, but rather as an integral extension of electrode engineering that links electrode selection to molecular recognition and electrochemical signal transduction.

4. Anchoring strategies in electrochemical genosensing

The process of immobilizing the biological recognition element, i.e., the capture probe, represents a crucial step in the development and fabrication of a sensitive and selective electrochemical genosensor. An efficient immobilization method plays an important role in ensuring the overall applicability and performance of the genosensor. On the other hand, poor anchoring of the biological recognition element can produce incorrect, false, and unreliable signals, which may result from substrate defects, undesired aggregation, or the presence of non-specifically adsorbed substances [122]. Since this topic has already been thoroughly reviewed in detail [123], this review article will only provide a brief update on very recent related contributions, along with important fundamental insights. Notably, and in addition to the more common strategies where the biological recognition element is immobilized first, some reported approaches begin by binding the target sequence directly to the electrode surface. Subsequent steps are then applied to generate an electrochemical signal corresponding to the presence of the target sequence and its concentration.

Various strategies of probe immobilization are available and widely used, including physisorption, chemisorption, covalent binding, affinity binding, indirect probe immobilization techniques, π-π stacking, diazonium coupling, glutaraldehyde crosslinking, etc.

Physisorption relies on the electrostatic attraction between the probe and the electrode surface and does not require special nucleic acid modification protocols [124]. This method is widely accepted and frequently employed because of its straightforward and simple nature, as shown in Fig. 2a. However, it is associated with some limitations, as the probe's accessibility to the target analyte may become restricted due to the close interaction of the probe with the electrode surface, ultimately leading to suboptimal analytical performance of the genosensor. A potential approach to address and mitigate this disadvantage involves the modification of the electrode surface with a polymeric layer, possessing suitable properties, such as biocompatibility, stability, or the ability to protect the electrode from non-specific adsorption of analytes [16]. There are several recent studies reporting on the physisorption principles; for example, Bishoyi et al. immobilized DNA capture probes onto the paper-based carbon SPE modified with silver nanoparticles (AgNPs). The immobilization process involved drop-casting the AgNPs on the surface of the working electrode, followed by the deposition of the DNA probes on the AgNP-modified surface [68]. In a more recent study, Jyoti et al. firstly deposited the target DNA sequence (t-DNA) onto the 3D-printed nanocarbon electrode using the drop-casting technique, followed by blocking the non-specific binding sites with BSA, and subsequent drop-casting of the complementary biotinylated oligodeoxynucleotide [67]. In the final step, streptavidin-alkaline phosphatase (SALP) was added, enabling the enzymatic conversion of the added 1-naphtyl phosphate into electroactive 1-naphthol, and the electrochemical signal was obtained with LSV. Jaroenram et al. used physisorption to attach LAMP products mixed with Hoechst-33258 redox molecules onto the surface of the screen-printed graphene electrode (SPGE), followed by measuring the current response generated from the interaction between the target molecules and the SPGEs using cyclic voltammetry (CV) [93].

Chemisorption refers to a process in which the interaction between the capture probe and the surface is stabilized and maintained through the formation of reportedly strong chemical bonds. The most extensively studied and commonly utilized method within this category involves the formation of a self-assembled monolayer (SAM) of DNA probes, achieved through the process of chemisorption of the SAM onto either gold electrode or gold nanoparticles (AuNPs). This particular technique is widely adopted for immobilization purposes due to a strong interaction and binding between thiolated nucleic acids and the gold surface [128]. The Au–S bond is known for its strength, stability, and reproducibility; therefore, this interaction is extensively exploited in the field of genosensing [129]. In Fig. 2b–a recently proposed electrochemical genosensor based on this immobilization principle is shown [126].

Covalent binding is based on attaching a chemically modified end of the DNA capture probe onto the activated supporting electrode surface, achieved through the creation of strong and stable covalent bonds between the two components (Fig. 2c and d) [128]. In contrast to physisorption, the sensing layer based on covalent binding exhibits enhanced stability and strength, making it more durable and reliable for genosensor applications. Moreover, this method offers the advantage of achieving a favorable vertical orientation of the DNA capture probes, contributing to increased efficiency during the DNA hybridization step. Pyrrole and its derivatives are frequently used in covalent binding processes; they can be electropolymerized by CV, resulting in the formation of polymeric films that establish a covalent bond with the nucleic acid probes, enhancing the overall binding efficiency and stability [130]. In addition, the application of carbodiimide reagents is widely practiced in the covalent immobilization of DNA probes, with the combination of NHS and EDC being the most commonly used. These reagents function as carboxyl activators, facilitating the covalent attachment between carboxyl groups and amines, thereby improving the efficacy and reliability of the immobilization process [129]. Glutaraldehyde (GA) is also widely utilized in the design of genosensors as a cross-linking agent, playing a key role in stabilizing the attachment of the DNA capture probe and enhancing the overall performance and durability of the genosensor. It acts by forming covalent links between

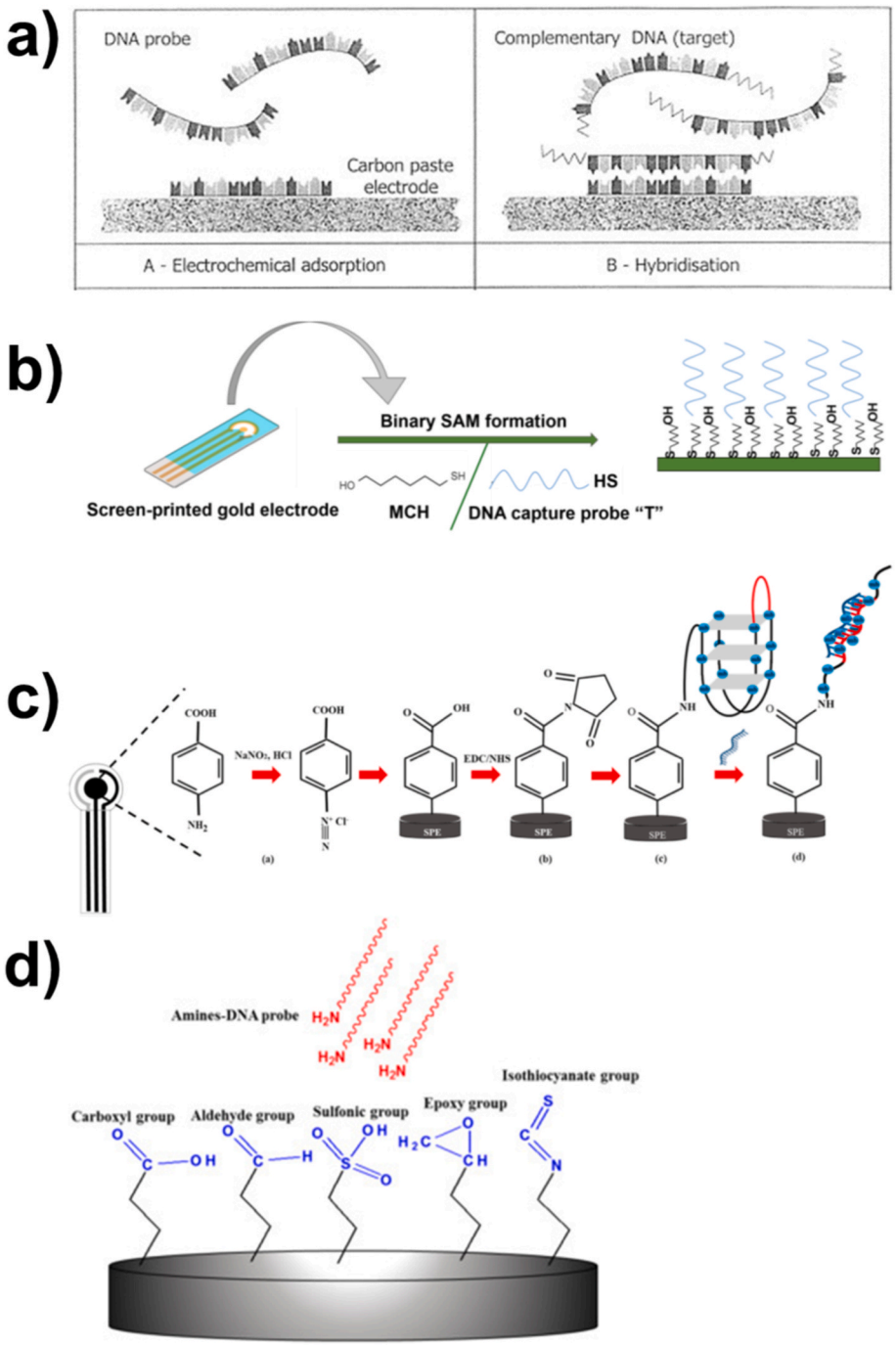

Fig. 2. Different techniques for immobilizing capture probes onto the supporting electrodes: **a)** physisorption (image reproduced from Ref. [125] with permission from *Elsevier*), **b)** chemisorption via formation of the SAM (image reproduced from Ref. [126] with permission from *MDPI*), **c)** covalent binding of the G-quadruplex serving as the capture probe (image reproduced from Ref. [127] with permission from *Elsevier*), **d)** various covalent binding options with the aminated capture probe (image reproduced from Ref. [123] with permission from *Elsevier*).

amine groups on the DNA capture probes and the substrate/surface, ensuring robust binding and improving the genosensor's sensitivity, reproducibility, and resistance to time-degradation [131]. In a recent study, GA facilitated immobilization of the MY09 DNA capture probe by linking the amine groups on the poly(amidoamine) (PAMAM)-G5 dendrimer-coated gold nanoparticles (PAMAM-G5-AuNPs) to the aminated DNA capture probe via Schiff base formation. This step was essential to ensure stable capture probe binding for subsequent hybridization with the target human papillomavirus (HPV) sequences. The crosslinking step using GA was crucial to maintain the structural integrity and sensing performance of the proposed genosensor [54]. In a similar study, GA was used to activate aminated silica nanospheres, facilitating the conjugation of aminated DNA capture probes. The aldehyde groups of GA reacted with the primary amines on both the DNA capture probe and the silica surface to form imine bonds (Schiff bases). This linkage strategy was validated using Fourier-transform infrared spectroscopy (FTIR), which showed characteristic imine bond peaks. The GA-mediated immobilization step was critical for the construction of the genosensor for detecting GMOs, ensuring strong and stable attachment of the DNA capture probes to the nanomaterial-modified support [75].

Diazonium coupling is a surface functionalization technique in

which diazonium salts are electrochemically or chemically reduced to generate reactive aryl radicals that form strong covalent bonds with carbon-based electrodes, creating a stable organic layer with functional groups for the robust and controlled covalent immobilization of biomolecules such as DNA capture probes. In a recent study, Ibrahim et al. employed a diazonium-based electrografting strategy to modify the surface of an SPCE with 4-carboxyphenyl groups. This was achieved by generating diazonium salts in situ from 4-aminobenzoic acid and sodium nitrite under acidic conditions, followed by electrochemical reduction to form aryl radicals. These radicals covalently bonded to the carbon electrode surface, forming a stable organic layer rich in carboxyl groups. This functional layer was then activated using EDC/NHS chemistry to enable the covalent attachment of a human telomeric G-quadruplex DNA capture probe, which served as the biorecognition element [127]. **G-quadruplexes** are noncanonical nucleic acid secondary structures formed in guanine-rich regions of DNA or RNA, consisting of stacked planar arrangements of four guanine bases, called G-tetrads, and stabilized by Hoogsteen hydrogen bonding and monovalent cations, typically potassium or sodium [132]. These structures can adopt diverse topologies, such as parallel, antiparallel, or hybrid, depending on sequence context, strand orientation, and environmental conditions. Their structural polymorphism and functional importance have made G-quadruplexes attractive targets for therapeutic intervention, but they have also recently found applications in electrochemical genosensing.

Affinity binding is another non-covalent immobilization technique that occurs when molecules attach to the electrode surface through a specific biorecognition event [43]. A well-known example of affinity binding is the avidin-biotin system, where the DNA probe is biotinylated to bind with avidin or streptavidin molecules that are anchored on the electrode surface [21,133]. Notably, the biotin-streptavidin interaction is one of the strongest known non-covalent bonds, with an exceptionally high affinity (dissociation constant of ca. 10^{-15} M) [134]. This system is favored for its stability and mechanical resistance [37]. Additionally, supramolecular interactions have also been explored in affinity binding. For instance, Ortiz et al. developed a DNA sensor based on the interfacial complexation between a bifunctionalized carboxymethylcellulose (CMC) polymer backbone, containing ferrocene units, and a DNA probe on a cyclodextrin-functionalized surface [135]. In recent years, several articles have been published demonstrating the use of affinity binding as the primary immobilization strategy, highlighting its effectiveness and growing popularity in the development of biosensing platforms. Chaturvedi et al. reported on the genosensor utilizing an ssDNA probe functionalized with biotin, which was immobilized on an avidin-modified reduced graphene oxide–polydopamine–gold nanoparticle-modified glassy carbon electrode (rGO–PDA–AuNP/GCE). The high specificity of the avidin-biotin system ensured stable attachment of the probe, allowing for selective hybridization with complementary *Mycobacterium tuberculosis* (MTB) DNA sequences [44]. In a study conducted by Alzate et al., the biotinylated capture probe was anchored onto streptavidin-coated magnetic beads. The hepatitis E virus (HEV) target RNA hybridized with this capture probe and a DIG-labeled signal probe, forming a sandwich complex. An anti-DIG antibody labeled with HRP then bound to the signal probe, forming the complete detection complex [83]. Chaibun et al. report on a multi-analyte electrochemical genosensor, in which affinity binding played a central role through streptavidin-biotin interactions. Specific DNA probes for HPV-16 and HPV-18 were labeled with biotin and immobilized onto streptavidin-coated magnetic beads. Target DNA sequences from oral and cervical cancer samples were then hybridized with these immobilized capture probes to form DNA duplexes. After the hybridization, the signal was amplified using a biotinylated signaling probe and streptavidin-HRP conjugate, which bound specifically to the biotin-labeled DNA [136]. The assay proposed by Fortunati et al. employed PNA (peptide nucleic acid) capture probes immobilized on carboxylated magnetic beads by covalent binding strategies, enabling high-affinity hybridization with DNA targets (KRAS p.G12D mutation and wild-type). Then, a biotin-labeled signal probe was hybridized to the DNA-PNA duplex, followed by streptavidin-ALP binding to the biotin moiety. The biotin-streptavidin-ALP complex enabled enzymatic generation of an electroactive product, i.e., hydroquinone, for voltammetric detection [99].

In addition, commercial binders are ready-to-use immobilization agents that create strong covalent links between functionalized electrode surfaces and biomolecules like DNA probes, ensuring stable, oriented, and efficient attachment for reliable genosensing. In the article by Krishnan et al., a commercial linker, i.e., Mix&Go™ binder, was used as a ready-to-use bioaffinity layer to activate the chitosan-butein (CSB)-modified electrode surface and enable robust covalent immobilization of the aminated DNA capture probe for the exosomal CD24 genosensor; this commercial binder reportedly acted as a strong crosslinker, thereby ensuring high probe density, proper orientation, and enhanced hybridization efficiency for detecting target DNA at ultra-low concentrations [79].

Alternatives to the previously discussed methods are **indirect probe immobilization techniques**, which utilize structures like DNA nanoobjects, one-dimensional arrays, and 2D or 3D crystalline materials to anchor the probe. These structures enable interactions with the target analytes without the need for direct contact with the electrode surface [37]. A DNA tetrahedron was designed to immobilize a DNA capture probe to a gold surface; three thiol groups in each tetrahedron vertex were used for binding to the gold surface, whereas the DNA probe was attached to the fourth vertex [137]. The 3D tetrahedron structure provided enhanced accessibility of the capture probes, maintaining their upright orientation that led to elevated efficiency of the target hybridization and consequently high sensitivity and selectivity of the genosensor [37,137].

π-π stacking has been proposed as an efficient way to immobilize DNA sequences onto carbon-modified supporting electrodes in recent years. In the work by Crevillen et al., a microfluidic genosensor was developed for rapid detection of SARS-CoV-2 RNA using a fully 3D-printed electrochemical cell. The working electrode, fabricated with a graphene/PLA filament, provides a π-rich carbon surface that enables the physical adsorption of the ssDNA antisense probe through π–π stacking interactions between the DNA nucleobases and the graphene structures at the 3D-printed electrode. This non-covalent immobilization keeps the probe firmly attached, yet allows it to be released upon hybridization with the target RNA, causing a measurable change in the oxidation signal of adenines. This simple π–π stacking approach makes the system label-free, fast, and easy to regenerate for repeated testing [66]. Asaadi et al. developed a genosensor using a porous carbon--metal–organic framework (PCMOF) derived from ZIF-8 carbonization. The graphene-like π-rich PCMOF surface enables strong non-covalent hydrophobic and π–π stacking interactions with ssDNA capture probes. The interaction anchors the ssDNA onto the PCMOF without chemical modification, forming a biogate-keeper that traps MB inside the PCMOF pores. Upon target DNA hybridization, the ssDNA forms double-stranded DNA (dsDNA) with lower affinity for π–π stacking, releasing MB and changing the electrochemical signal [45]. Another electrochemical genosensor was designed using ferrocene-functionalized graphene oxide (Fc-GO) nanosheets. The ssDNA capture probe was adsorbed onto the Fc-GO via π–π stacking between the nitrogenous DNA bases and the graphene oxide nanosheets. The non-covalent immobilization created a stable complex that produced an electrochemical signal due to the ferrocene's redox activity. When the target miRNA hybridized with the capture probe, the π–π interaction was disrupted, which reduced the redox peak current, providing a sensitive mechanism for the detection of miR-200a [42]. Eskandari et al. also reported on the DNA immobilization using a double mechanism, i.e., electrostatic interaction between the negatively charged DNA backbone and the positively charged CeO_2, and crucially, π–π stacking between the nitrogenous bases of the DNA and the π-conjugated rGO sheets. This dual binding improves probe orientation and

hybridization efficiency for the target sequence detection [138].

Once the capture probes are effectively immobilized, the genosensor architecture is completed at the molecular level, but its analytical performance is ultimately realized through the chosen electrochemical detection technique. The manner in which nucleic acids are anchored and organized at the electrode surface directly influences electron transfer pathways, and kinetics at the interface. The following section therefore focuses on electrochemical detection techniques, examining how different transduction and amplification approaches translate molecular recognition events at the functionalized interface into measurable and analytically meaningful electrical signals.

5. Electrochemical techniques and detection schemes

Electrochemical detection techniques offer several advantages for sensitive and selective measurement of biochemical interactions (Figs. 3–4). Techniques such as amperometry (Fig. 3a), (pulse) voltammetric techniques (Fig. 3b–d), and EIS (Fig. 4) each provide unique benefits, including rapid response times, ease of operation, and portability. In recent years, their adaptability to miniaturized systems and suitability for multiplexed detection have greatly increased their appeal, leading to a surge in biosensing-related research and publications. This subsection provides a concise overview of the most prominent electrochemical techniques, with particular focus on their recent applications in the field of genosensing.

Electrochemical Impedance Spectroscopy (EIS) is commonly used for studying the electrical properties of materials and interfaces in electrochemical systems, such as batteries [139], fuel cells [140], solar cells [141], or as a tool in understanding the protective qualities of coatings and kinetics of corrosion processes [142], for corrosion monitoring [143], supercapacitor studies [144], electrocatalysis [145], biomedical and biological applications [146,147], fundamental kinetics studies [148], etc. The versatility and non-destructive nature of EIS make it a valuable tool in both fundamental research and application studies. However, interpreting EIS data requires a deeper understanding of theory and often involves complex equivalent circuit modeling to accurately represent the physical and chemical processes occurring within the system under investigation. Nevertheless, with the appropriately chosen equivalent circuit and data interpretation, its ability to provide detailed information about charge transfer, diffusion processes, and surface properties makes EIS a powerful tool for designing highly sensitive and selective (bio)sensors for environmental [149], medical [150], and other applications. It is generally accepted that the EIS measurements are a non- and/or least-destructive electrochemical technique; however, some studies suggest that repetitive EIS measurements on the same electrode can lead to irreproducible signals [151]. The fundamental principle of genosensing using EIS is illustrated in Fig. 4.

Recently, our group has demonstrated how EIS can be used in electrochemical genosensing of *Citrus bark cracking viroid* (CBCVd) in real total RNA samples obtained from infected plants [21]. The supporting GCE was modified in such a manner that the hybridization event between the immobilized ssDNA capture probe and the target circular RNA sequence from the total RNA sample resulted in an increase of the charge transfer resistance (R_{ct}), quantifiable by EIS (Fig. 5a). The EIS measurements were carried out in the frequency range of 10^5–10^{-1} Hz, at a potential of +0.14 V, with an amplitude of 5 mV, in a solution containing the external $[Fe(CN)_6]^{4-/3-}$ redox probe. The potential of +0.14 V represents the thermodynamic equilibrium between the oxidized and reduced redox species under given experimental conditions, i.e., the formal potential of the redox couple. It is defined as the potential at which the concentrations of the oxidized and reduced species are equal, and was determined from the midpoint of the anodic and cathodic peak potentials in CV. As an analytical signal, the change in R_{ct} before and after the hybridization event was used, i.e., $\Delta R_{ct} = R_{inc}$-R_{blank}. The recorded Nyquist spectra ($-Z''$ vs Z') exhibited a typical semicircle spanning from higher to medium frequencies, which corresponds to the charge transfer process, followed by the diffusion tail at lower frequencies. The R_{ct} parameters were obtained by nonlinear least squares fitting (NLSF) using the Randles-type equivalent circuit model ($R_S([R_{ct}Z_W]Q_{dl})$), which represents the real physicochemical processes at the genosensor/electrolyte interface. Herein, R_S corresponds to the solution resistance, Q_{dl} is the constant phase element accounting for the non-ideal double-layer capacitance, R_{ct} is the charge transfer resistance of the genosensor/electrolyte interface, and Z_W is the Warburg element that models the diffusion phenomenon. The corresponding fit was characterized by the chi-squared (χ^2) factor, being $<10^{-3}$. In a recent study, Moattari et al. used the EIS technique to detect viral hemorrhagic septicemia virus (VHSV) genome in a label-free operation mode. The measurements were performed in the presence of the external $[Fe(CN)_6]^{4-/3-}$ redox probe, at the potential of +0.15 V. The ΔR_{ct} value was, presumably, extracted from the recorded impedimetric spectra using a fitting procedure and a Randles-type equivalent circuit [69]. In another report, EIS was used to investigate the analytical performance of the genosensor for safe and early diagnostics of fetal gender, based on the composite nanostructures loaded onto the GCE [47]. The proposed genosensor was successfully used to determine the fetal sex in real DNA samples obtained from pregnant individuals. Ansah et al. used EIS as an electrochemical detection technique for *P. falciparum*, *P. malariae*, and *P. ovale*, three malaria-related species [65]. The authors opted for the relative response as the analytical signal, i.e., $RR = [(R_1–R_0)/R_0]$, where R_0 and R_1 represent the R_{ct} before and after the addition of the target sequence, respectively. The measurements were performed in the presence of the external $[Fe(CN)_6]^{4-/3-}$ redox probe at the potential of +0.15

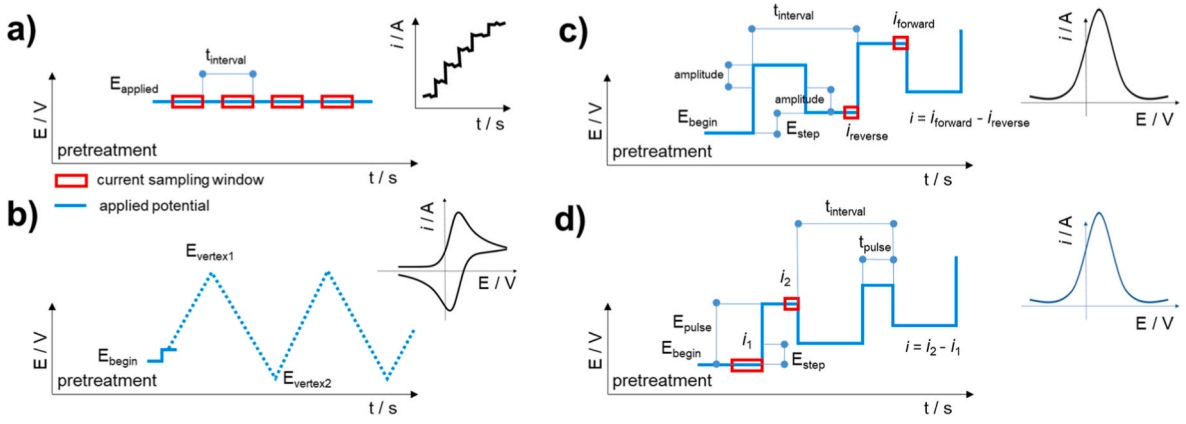

Fig. 3. Schematics of the applied potentials along with the typical current responses of different electrochemical detection techniques predominantly used in contemporary genosensing: **a)** chronoamperometry (CA), **b)** cyclic voltammetry (CV), **c)** square-wave voltammetry (SWV), **d)** differential pulse voltammetry (DPV).

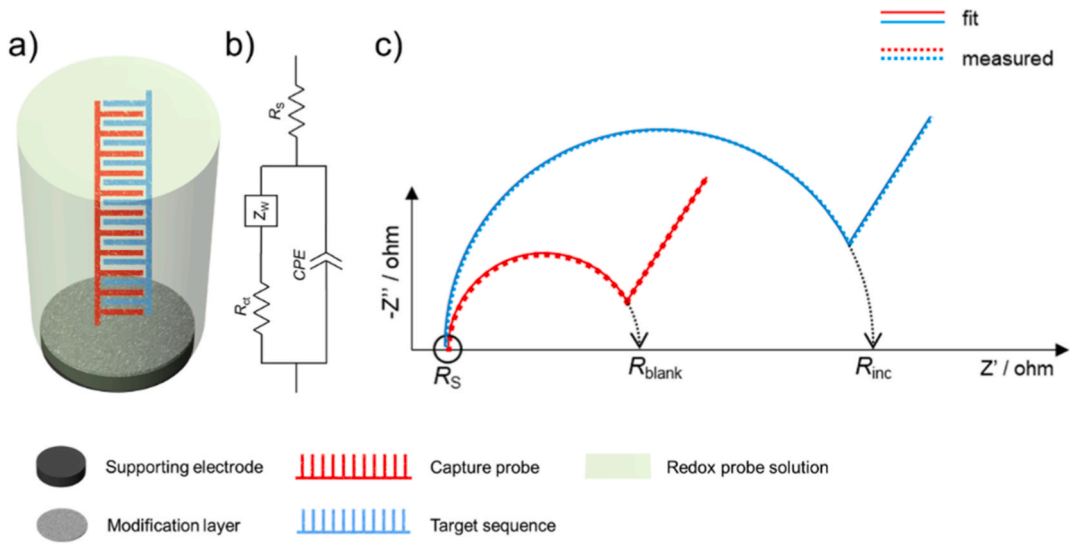

Fig. 4. General principle of the genosensing by EIS in the Faradaic operating regime: **a)** a simplified presentation of the hybridization event between the capture and target sequences on the modified supporting electrode, **b)** an example of Randles-type equivalent circuit used to fit the obtained impedimetric spectra, **c)** Nyquist plots recorded for the blank and the incubated genosensor in the Faradaic operating mode, i.e., in the presence of the external redox (signaling) probe.

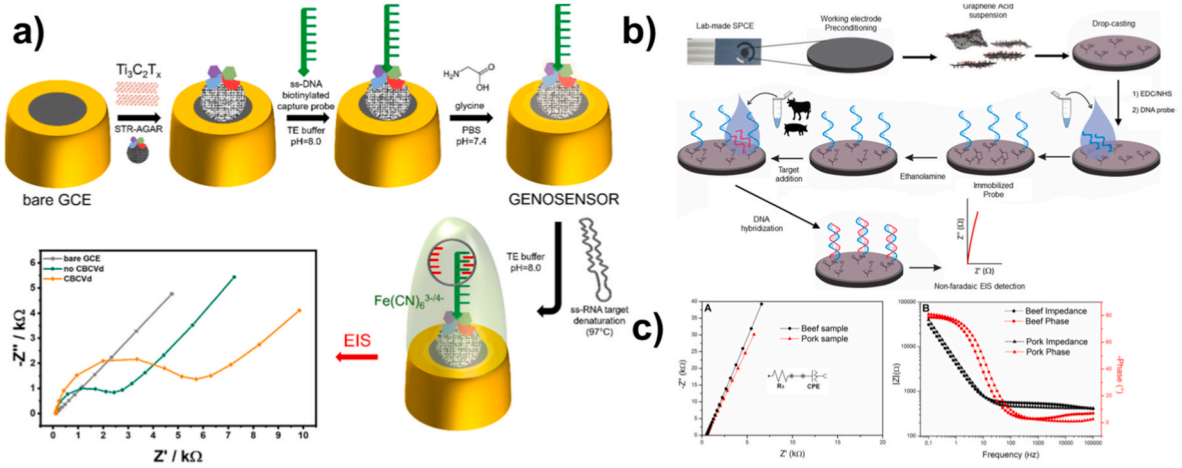

Fig. 5. **a)** EIS detection of the CBCVd recently presented by our group (image from Ref. [21] with permission from *Elsevier*), **b)** and **c)** non-Faradaic EIS detection of meat adulteration proposed by Flauzino et al. (image from Ref. [152] with permission from *Elsevier*).

V.

It is widely accepted in the electrochemistry community that EIS is a powerful tool to monitor discrete changes at solid-liquid interfaces; therefore, its applicability extends across many fields. In genosensing, EIS can also serve for efficient monitoring of the step-by-step fabrication of the sensor layers [42,56,73,96,97,127], as well as to optimize its architecture. Recently, Bonaldo et al. investigated the influence of different types of BSA buffers, i.e., native or fragmented BSA, on the electroanalytical signal using EIS [17]. BSA is commonly used to prevent excessive non-specific binding in genosensing. It has been shown that the detection sensitivity is limited when using native BSA, whereas the use of fragmented BSA lowers steric hindrance, leading to higher signals, as evidenced by EIS. The measurements were carried out in the Faradaic regime, using the external $[Fe(CN)_6]^{4-/3-}$ redox probe, and the obtained data were fitted with the Randles equivalent circuit.

Notably, the EIS technique also allows measurements in the non-Faradaic regime. In such measurements, no redox probe is needed, as the electroanalytical signal does not correspond to any oxidation or reduction process in the investigated system, but is related to changes in the capacitive properties of the (bio)sensing interface. In a recent study by the group of Merkoçi [17], a non-Faradaic EIS detection was used to determine adulteration of beef by detecting a particular DNA sequence (Fig. 5b and c). The obtained impedimetric spectra were fitted using the equivalent circuit R_S-Q_{dl}, in which R_S corresponds to the solution resistance, while Q_{dl} corresponds to the constant phase element, accounting for the non-ideal double-layer capacitance [153]. The overall impedance (Z_{CPE}) can be calculated as the inverse of its admittance (Y_{CPE}), which is easily extracted using fitting software; the change in Y_{CPE} before and after the hybridization event between the capture and the target probe was used as an analytical signal. The measurements were performed at 0.0 V, with an amplitude of 10 mV in phosphate-buffered saline (PBS) solutions with and without the target sequence. In this case, the recorded Nyquist spectra did not exhibit a typical semicircle because no charge transfer occurred in the system. Instead, the spectra exhibited only a straight line emerging from the R_S, related to the electrostatic interactions of the hybridization conjugate and the electric double layer.

Amperometric sensors are a class of electrochemical sensors that measure the current produced by the oxidation or reduction of an analyte or the redox/signal probe at the electrode surface; they operate by

applying a constant potential to the working electrode relative to the reference electrode, prompting the electrochemical reactions. The resulting current is related to the concentration of the analyte, enabling quantitative analysis. Despite their advantages, amperometric genosensors face challenges such as fouling of the electrode surface [154,155], limited selectivity in complex matrices, and potential interference from other electroactive species. Ongoing research aims to address these issues through the development of advanced electrode materials, improved sensor designs, and advanced signal processing techniques [156]. Amperometric genosensors mostly rely on more complex and less robust detection schemes, including the utilization of TMB, i.e., 3,3′,5,5′-tetramethylbenzidine coupled with H_2O_2 enzymatic system [83,88,95,157], HRP-based protein-enzyme complexes [82], GOx-based enzymatic system with Prussian blue as the mediator [77], HRP-H_2O_2 interactions [126], and hydroquinone (HQ)-H_2O_2 redox systems [91]. Due to the complexity and high originality of these detection schemes, they will be explained in detail in this section.

For example, Alzate et al. report on the amperometric biosensor for the detection of HEV genotype 3 in wastewater [83]. The detection principle is as follows: a biotinylated capture probe is first immobilized on streptavidin-coated magnetic beads (Fig. 6a). The target sequence is then prehybridized with a DIG-labeled signalling probe before being introduced to the capture probe-coated magnetic beads. The detection scheme relies on the complementary pairing of DNA/RNA strands in the sample; final recognition occurs through the signalling probe, which binds to an anti-DIG monoclonal antibody labeled with the HRP enzyme. The beads are then magnetically drawn to the surface of a SPAuE, where the electrochemical detection is performed using chronoamperometry (CA), with H_2O_2 as a reactant and TMB, a chromogenic substrate commonly used in enzyme-based assays, as a mediator [158]. To obtain the electrochemical signal, TMB is added, along with a fixed concentration of 10 mM H_2O_2, and a constant voltage of 150 mV is applied. After 30 s of signal stabilization, the chronoamperometric detection lasts for 60 s. The obtained current is directly proportional to the concentration of the target sequence.

Streptavidin-coated magnetic beads, deposited onto *m*-GEC, were also used by Pallares-Rusiñol et al. to sequester double-tagged amplicons, produced through a somewhat time-consuming procedure, involving the preconcentration and lysis of exosomes [91]. Through 32 PCR cycles and double tagging with DIG and biotin, the double-tagged amplicons were transferred to the streptavidin-coated magnetic beads, followed by incubation with anti-DIG antibodies labeled with HRP (Fig. 6b). The chronoamperometric detection was carried out in the presence of HQ as a mediator and H_2O_2 at the potential of −0.1 V vs. AgIAgCl.

Similarly, Cajigas et al. demonstrated amperometric genosensing of SARS-CoV-2 using a sandwich-type architecture [82]. The genosensor was assembled on top of maleimide-modified magnetic beads (MMB) by linking a thiol-labeled capture probe via a strong covalent bond [159]. Then, the viral RNA target sequence was hybridized between the thiolated capture probe and a biotinylated signaling probe. Three different protein-enzyme complexes, i.e., streptavidin-HRP, streptavidin poly-HRP20, or streptavidin poly-HRP80, containing different quantities of HRP molecules, were specifically bound with biotin from the signaling probe to complete the genosensing platform. Finally, the genosensor performance was investigated using TMB in two ways: either

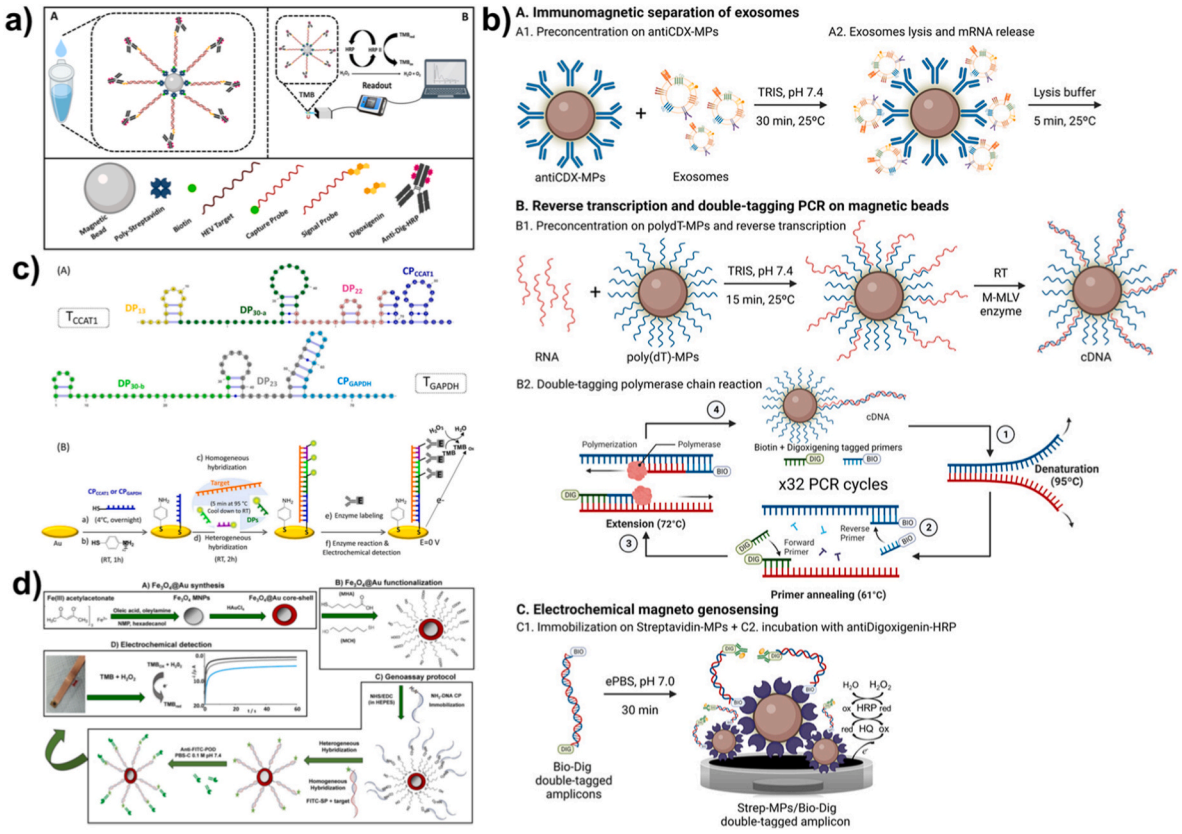

Fig. 6. State-of-the-art amperometric genosensors: **a)** detection of HEV genotype 3 in wastewater by an amperometric genosensor (image from Ref. [83] with permission from *Elsevier*), **b)** detailed fabrication and detection schemes of an amperometric genosensor for the detection of overexpressed glyceraldehyde 3-phosphate dehydrogenase (GAPDH) transcripts in breast cancer exosomes (image from Ref. [91] with permission from *ACS Publications*), **c)** an amperometric platform for the relative quantification of the circulating RNA sequence to aid in the diagnostics of colorectal cancer (image from Ref. [88] with permission from *Elsevier*), **d)** a scheme of the amperometric genosensor fabrication and detection principle for high-mobility group protein (HMGA) maize endogenous gene (image from Ref. [95] with permission from *Elsevier*).

colorimetrically, by following the formation of its oxidized colored product in the presence of hydrogen peroxide, or chronomperometrically, by monitoring the TMB reduction at a constant voltage of −150 mV for 60 s.

Caldevilla et al. firstly modified the SPAuE with a binary SAM, followed by the immobilization of the thiolated ssDNA capture probe [126]. In the next step, the target sequence was ex situ prehybridized with the fluorescein isothiocyanate (FITC)-labeled signalling probe and then transferred onto the sensor surface for hybridization with the immobilized capture probe. In the next step, anti-fluorescein antibodies labeled with peroxidase (anti-FITC-POD) were added, followed by chronoamperometric measurements in the presence of TMB/H_2O_2 commercial substrate system at a potential of −0.1 V.

Another similar study was published by Morais et al., demonstrating the detection of the toxic dinoflagellate, *Alexandrium minutum* [157]. SPAuE was first modified with SAM and the capture probe with a high specificity towards the target. The latter was also ex situ prehybridized with the FITC-labeled signalling probe and then transferred onto the sensor surface for hybridization with the immobilized capture probe. Finally, the anti-FITC-POD was added, followed by the chronoamperometric measurements using the TMB/H_2O_2 system at −0.1 V for 60 s.

Sánchez-Salcedo et al. also used a similar approach, which included the formation of SAM on the SPAuE, and the immobilization of the capture probes for two different target sequences that were recognized as biomarkers for colorectal cancer [88]. The ex situ homogeneous prehybridization of the targets was carried out simultaneously with two different FITC-labeled signalling probes, allowing for the incorporation of multiple anti-FITC-POD moieties and, consequently, better sensitivity of the genosensor. The chronoamperometric measurements were carried out in the presence of TMB/H_2O_2 (Fig. 6c). More recently, Barbosa et al. used the same approach for sensitive detection of VKORC1 1639 G > A and CYP2C9*2 polymorphisms for pharmacogenetic applications [160, 161].

A recent contribution came from Souza et al., starting from the carboxylation of Fe_3O_4@Au core-shell magnetic particles, followed by the immobilization of the aminated capture probe onto them. In the following steps, the target sequence and FITC-labeled signalling probe were first prehybridized ex situ, and then added to the particle-capture probe conjugate (Fig. 6d). In the final step, the core-shell particles functionalized with this DNA duplex were resuspended in anti-FITC-POD and transferred onto the home-made gold electrode for the amperometric measurements in the presence of TMB/H_2O_2 [95].

An enzymatic system, centered around **rolling circle amplification (RCA)** in combination with RCA and chronoamperometry, was used by Ciftci et al. for the detection of Ebola viral sequence [77]. The Padlock-probe-target conjugate was attached to the commercially available streptavidin-coated magnetic beads, followed by the amplification of the attached conjugate. In the next step, the amplified product was hybridized with the complementary biotinylated capture oligonucleotide sequence. Then, the streptavidin-conjugated GOx was added, and the amplified and labeled product was transferred onto the surface of the SPCE with integrated Prussian blue mediator. The chronoamperometric detection was conducted at +0.80 V vs. pseudo Ag reference electrode, to monitor the oxidation of H_2O_2 released from the enzymatic reaction in the presence of 10 mM glucose in PBS (Fig. 7a). Notably, **RCA** is an isothermal nucleic acid amplification technique that exploits the ability of DNA polymerases to generate long single-stranded DNA or RNA products from a circular template. Initiated by a short primer hybridized to the circular DNA, the polymerase continuously extends the strand, displacing the previously synthesized sequence and producing a long concatemer containing tandem repeats which are complementary to the template. Notably, unlike PCR, RCA operates at a

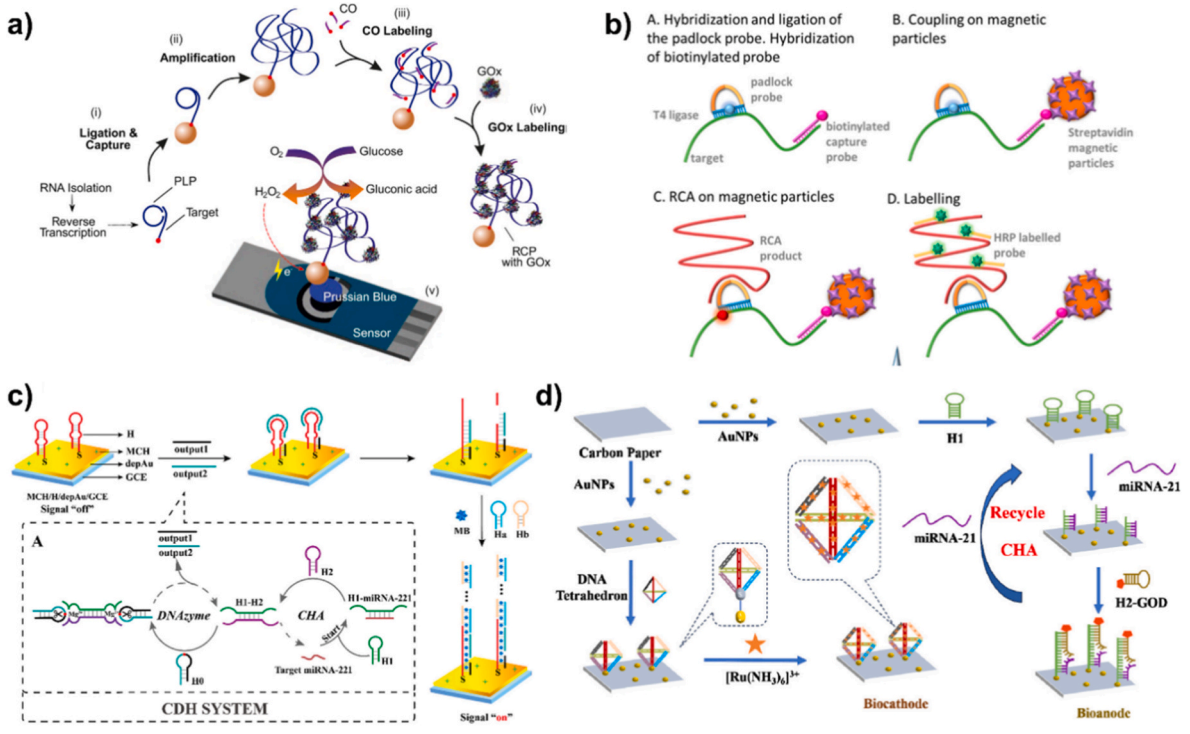

Fig. 7. Schematic representation of several state-of-the-art electrochemical genosensing strategies for nucleic acid detection: **a)** Step-by-step illustration of the RCA assay, i.e., ligase chain reaction and reverse transcription-based amplification with glucose oxidase (GOx) labeling for electrochemical signal generation on Prussian Blue-modified genosensor (image from Ref. [77] with permission from *Elsevier*), **b)** Padlock probe-based rolling circle amplification (RCA) on magnetic particles, including hybridization, ligation, coupling, amplification, and labeling steps (image from Ref. [78] with permission from *MDPI*), **c)** cascade DNAzyme and CHA system for dual-output signal transduction, integrating molecular recognition and amplification for sensitive miRNA detection (image [162] from permission from *ACS Publications*), **d)** DNA tetrahedron-assisted catalytic hairpin assembly (CHA) for miRNA-21 detection on AuNP-modified paper electrodes, enabling signal amplification through bioanode and biocathode design (image from Ref. [121] with permission from *ACS Publications*).

constant temperature and does not require thermal cycling, making it suitable for simple and portable diagnostic platforms. Ben Aissa et al. utilized streptavidin-coated magnetic beads for the affinity capture of biotinylated DNA probes specific to foodborne pathogens [78]. The amplification strategy in this electrochemical genosensor relies on RCA performed on magnetic particles after the target DNA is captured and circularized using highly specific padlock probes (Fig. 7b). The padlock probes hybridize to the *E. coli* 16 S rRNA gene and are ligated to form a circular template, which serves as the substrate for RCA by phi29 DNA polymerase under isothermal conditions. RCA generates long, repetitive DNA strands that collapse into dense structures, providing multiple binding sites for signal probes. For electrochemical detection, these RCA products are labeled either directly with HRP-modified probes or indirectly via digoxigenin-tagged probes followed by anti-DIG-HRP antibodies, with the direct HRP approach offering superior sensitivity. Importantly, this strategy amplifies the signal without thermocycling, enabling highly sensitive detection on disposable screen-printed electrodes using SWV.

Finally, the recent article published by Shunmugan et al. describes an amperometric electrochemical genosensor developed on a streptavidin-coated SPCE for detecting the ipaH gene, a molecular marker common to *Shigella* species and enteroinvasive *Escherichia coli*, using HRP/TMB enzymatic signal amplification following PCR-based target hybridization. The capture probe was anchored to the electrode surface through a biotin–streptavidin interaction, ensuring strong and specific immobilization for efficient hybridization [163].

Voltammetric sensors measure the current response as the potential applied to the working electrode is scanned in anodic or cathodic direction. These sensors are common in contemporary electroanalysis, including trace metal detection [164,165], pesticide analysis [166], glucose monitoring [167], cancer biomarker detection [168], corrosion studies [169], detection of gases or explosives [170,171], etc. **Cyclic voltammetry (CV)** is a widely used technique for studying redox processes, electrode reaction mechanisms, and surface phenomena. CV is particularly valuable for analyzing the reversibility of electrochemical reactions, determining formal redox potentials, and probing electron transfer kinetics. Importantly, beyond fundamental research, it is extensively applied in fields such as battery development, corrosion studies, electrocatalysis, and biosensing [172]. In recent years, it has also been used as an electrochemical detection technique in genosensing. CV can be used for this purpose only in the Faradaic operating regime, combined with redox systems, such as potassium ferri/ferrocyanide ($[Fe(CN)_6]^{3-/4-}$) couple [54,61,84–86], ferrocene [52], or other redox-active labels [61]. The $[Fe(CN)_6]^{3-/4-}$ is a well-known reversible redox system used in numerous electrochemical studies; it undergoes a one-electron transfer reaction, making it ideal for cyclic voltammetry, (bio)sensor, and electron transfer kinetics studies due to its stability, solubility, and well-defined redox behavior. For instance, Garcia-Mello et al. have demonstrated the applicability of CV in combination with $[Fe(CN)_6]^{3-/4-}$ in two recent articles, for the detection of the KRAS gene [85] and the p53 gene mutation [84]. Both articles report on the usage of SPAuEs associated with thiol-based chemistry for the immobilization of capture probes, and doxorubicin as the signalling probe, upon the hybridization event. In this case, the CV signal of $[Fe(CN)_6]^{3-/4-}$ was reduced due to the attachment of doxorubicin, enhancing a diffusion barrier for the redox species. As the analytical signal, the authors used the typical oxidation peak of this redox couple, positioned at ca. +0.2 V vs. an Ag|AgCl reference electrode.

Hadian-Ghazvini et al. used polyethyleneimine-stabilized silver nanoparticles to label the hybridization product of the capture probe and the target sequence on the gold electrode [61]. The authors opted for the oxidation peak of silver nanoparticles at ca. +0.19 V vs. an Ag|AgCl reference electrode as the analytical signal. The measurements were conducted in 0.1 M PBS (pH 7.4), from −0.6 to +0.6 V at a scan rate of 100 mV s^{-1}.

In a very interesting study, Shamsipur et al. developed an ultrasensitive, label-free electrochemical genosensor for the detection of HIV-1 pol gene using a CPE modified with lead ion-imprinted polymer (Pb-IIP) nanoparticles and AuNPs. DPV was employed as the detection technique to monitor changes in the oxidation current of lead ions, serving as the redox probe. The measurements were conducted in a 0.1 M PBS (pH 7.4), in the potential range of −0.8 V to −0.2 V. with a scan rate of 100 mV s^{-1}, a pulse width of 0.01 s, and a pulse amplitude of 0.1 V. Upon the hybridization event, the electron transfer of lead ions diminished, resulting in a decreased lead oxidation current, being reversely proportional to the concentration of the target DNA. The genosensor demonstrated excellent selectivity, reproducibility, and applicability in spiked serum samples [72].

Bishoyi et al. developed a paper-based electrochemical genosensor for detecting Zika virus (ZIKV) target DNA using the CV technique. A single-stranded DNA capture probe was immobilized on the AgNP-modified paper-based electrode, and MB was used as the redox indicator. The detection principle relied on the intercalation of MB into double-stranded DNA formed upon hybridization with the target DNA. This intercalation reduced the MB redox current, enabling quantification of hybridization events in 10 mM MB in 0.1 M KCl at 50 mV s^{-1} [68].

Similarly, Jaroenman et al. developed a voltammetric sensor for rapid on-site detection of *Mycobacterium tuberculosis*. Detection relies on the redox behavior of Hoechst 33258, a molecule that binds to double-stranded DNA. In the absence of the target DNA, free Hoechst molecules generate a high oxidation current during CV measurement. When the target DNA is present, LAMP amplifies the target sequence, and Hoechst binds to the resulting amplicons, reducing the number of free redox molecules and thus lowering the corresponding oxidation current. This current change is interpreted against a predefined cutoff, producing a simple positive/negative result. CV measurements were recorded using the scan rate of 100 mV s^{-1}, and the oxidation peak at ca. +0.55 V was used as the electroanalytical signal [93].

Gopal et al. used a gold electrode modified with rGO and metal-organic frameworks (MOFs) for the CV detection of miRNA-21, using ferrocene as the external redox probe. The measurements were conducted in the potential range of −1.0 to +1.0 V, with a scan rate of 50 mV s^{-1}. The authors opted for the ferrocene oxidation current at ca. +0.5 V vs. AgIAgCl as the analytical signal, being proportional to the concentration of the target sequence [52]. Notably, ferrocene is a stable organometallic redox probe with reversible Fe^{2+}/Fe^{3+} transitions; unlike the $[Fe(CN)_6]^{3-/4-}$ couple, ferrocene is neutral, less hydrophilic, and widely used in biosensing and organic electrochemistry [173].

Pulse voltammetric techniques, in contrast, offer significant advantages over CV, particularly in terms of sensitivity; by applying pulses rather than a continuous potential sweep, these methods enhance faradaic currents while suppressing background capacitive currents [174]. As a result, they can allow for lower detection limits, making them ideal for trace-level analysis, even in complex electrochemical systems. Similar to CV, these methods are viable only in the Faradaic operating regime, by using specific oxidation and/or reduction processes. In recent years, the prevalent pulse techniques used in genosensing were **square-wave voltammetry** and **differential pulse voltammetry**, combined with the utilization of electroactive species such as toluidine blue (TB) [76], $[Fe(CN)_6]^{3-/4-}$, ninhydrin [57], Co-porphyrin [63], methylene blue [45], ferrocene-based redox species [42], Pb nanoparticles as a signalling label [72], chlorogenic acid [43], and others. The main difference between SWV and DPV lies in their waveform and signal processing. SWV applies a symmetrical square-wave potential superimposed on a staircase waveform, measuring the current difference between forward and reverse pulses [175]. Such an approach effectively reduces capacitive currents, likely enhancing sensitivity, particularly for reversible redox systems, and enabling faster measurements. In contrast, DPV applies a series of potential pulses on a linear sweep and measures the current just before and just before the end of each pulse [176]. While DPV is also sensitive and reduces capacitive interferences, it is generally

slower than SWV due to its simpler pulse scheme. Moreover, SWV is particularly advantageous for rapid screening and low-concentration detection due to its high signal-to-noise ratio and potential scan speed; DPV, on the other hand, is often preferred when precise peak resolution is needed, especially in complex matrices. Recent genosensors based on SWV and DPV are presented in the following section. In a very recent study, a user-friendly, enzyme-assisted electrochemical point-of-care (POC) test for detecting miR-200a-5p, a biomarker associated with triple-negative breast cancer (TNBC), was demonstrated. The authors developed a signal-ON platform using duplex-specific nuclease (DSN) to selectively cleave DNA-RNA heteroduplexes. The DNA capture probe is tagged with methylene blue (MB), and upon hybridization with the target miRNA, DSN cleaves the duplex, releasing MB-labeled fragments. These fragments generate an electrochemical signal recorded by SWV, enabling sensitive detection without complex amplification or surface modification steps [177].

Another recent study presents an ultrasensitive electrochemical genosensor for miRNA-221 detection using a **triple cascade amplification system (CDH)**, i.e., catalytic hairpin assembly (CHA), Mg^{2+}-dependent DNAzyme, and hybridization chain reaction (HCR) (Fig. 7c). The target miRNA-221 initiates CHA, forming a DNAzyme that cleaves a substrate to release output DNAs. These outputs trigger HCR, forming long dsDNA polymers intercalated with MB, generating a strong electrochemical SWV signal [162].

Ben Aissa et al. employed SWV to detect RCA products generated from *E. coli* DNA using padlock probes. Two readout strategies were compared, i.e., direct labeling with HRP-tagged probes and indirect labeling using DIG-tagged probes followed by anti-DIG-HRP. The SWV was conducted in phosphate buffer containing 1 mM HQ as the redox mediator and 0.25 mM H_2O_2 as the substrate. The measurement was carried out in the potential range of +0.1 V to −0.7 V, with a step and amplitude of 10 mV and a frequency of 1 Hz [78]. Malla et al. developed a magneto-electrochemical genosensor using Au-decorated magnetic rGO for the detection of SARS-CoV-2 nucleocapsid (N) gene. SWV was employed as the detection technique, H_2O_2 was used as the substrate for HRP, and HQ served as the electron/redox mediator. The SWV parameters included an amplitude of 75 mV, a pulse period of 100 ms (corresponding to a frequency of 10 Hz), and a potential range from −0.2 V to +0.4 V. The genosensor demonstrated very high sensitivity and selectivity [73].

Flauzino et al. developed a genosensor using a graphite electrode modified with rGO and poly(3-hydroxybenzoic acid) for detecting mitochondrial DNA from beef. SWV was used to monitor hybridization events between immobilized DNA probes and target DNA from meat samples. The redox probe was the 5 mM $[Fe(CN)_6]^{3-/4-}$ in 0.1 M KCl. SWV parameters included a potential range of −0.1 V to +0.6 V, an amplitude of 25 mV, an increment of 4 mV, and a frequency of 15 Hz [152].

Kabinsing et al. used SWV to detect miRNA-183-5p using a dual-mode genosensor based on magnetic reduced graphene oxide (MrGO) modified with toluidine blue (TB), which served both as a redox probe and an intercalator; TB intercalated into the DNA/RNA duplex enabled a label-free detection. The optimized SWV parameters for the analytical performance tests were: an amplitude of 75 mV, a step potential of 20 mV, and a potential range of −0.6 V to +0.2 V [76].

Malecka et al. investigated the performance of electrochemical genosensors based on cobalt porphyrin-labeled DNA immobilized on either AuNPs or AgNPs. SWV was used to monitor the redox behavior of the Co(II)/Co(III) couple, which served as the integrated redox probe. The measurements were conducted in a phosphate buffer over a potential range of +0.1 V to +0.75 V, with a step potential of 1 mV, a frequency of 50 Hz, and an amplitude of 50 mV. The analyte was a 20-mer DNA sequence complementary to the capture probe. The study concluded that both nanoparticle systems performed similarly, with AgNPs offering a more cost-effective alternative [63].

Mokni et al. designed a label-free electrochemical genosensor for detecting PCA3, a prostate cancer biomarker, in urine samples. SWV was chosen over CV due to its superior signal resolution and lower capacitive background. The detection was performed without any external redox probe, relying instead on the intrinsic electroactivity of nucleobases. SWV was conducted in 0.3 M NaCl within a potential range of −0.6 V to +0.6 V, a step potential of 4 mV, an amplitude of 25 mV, and a frequency of 25 Hz. Such a simple, label-free approach offers a promising route for point-of-care diagnostics [87].

In the recent article by Razmi et al. [94], SWV was employed for detecting *Escherichia coli* O157:H7 DNA using a genosensor based on gold nanostars (AuNSs). The genosensor was constructed by immobilizing an aminated DNA capture probe onto a gold electrode modified with AuNSs, followed by blocking with mercaptoethanol and labeling with TB, a redox-active dye that binds to the DNA. The SWV measurements were conducted in a 10 mM $[Fe(CN)_6]^{4-/3-}$ solution, with 0.1 M KCl serving as the supporting electrolyte. The SWV parameters included a frequency of 1.0 Hz, an amplitude of 0.1 V, and a step size of 10 mV. This approach enabled rapid, sensitive, and specific detection of the target DNA, corroborating its suitability for environmental monitoring applications.

Asaadi et al. developed a biogatekeeper-based electrochemical genosensor for the detection of *Nocardia spp*. (multiple species within the *Nocardia* genus) using a porous carbon material derived from a metal-organic framework (PCMOF). The redox probe used was MB encapsulated within the PCMOF. The genosensor was constructed by immobilizing an ssDNA capture probe on the MB-loaded PCMOF, which was then deposited onto the GCE. In the absence of the target, MB remained trapped, producing a high DPV signal, while upon hybridization with the target DNA, the probe-target duplex detached from the PCMOF, releasing MB and reducing its signal. DPV was performed in 0.1 M PBS, pH 7.4, over a potential range of −0.6 to +0.1 V with a scan rate of 50 mV s^{-1} [45].

A multianalyte electrochemical genosensor for detecting high-risk HPV genotypes 16 and 18 in oral and cervical cancer samples was demonstrated, with DPV as the electrochemical detection technique [136]. The architecture involved silica nanoparticles doped with MB for HPV-16 and acridine orange (AO) for HPV-18 as redox indicators. These particles were conjugated to the specific reporter probes and used in a sandwich hybridization format with magnetic bead-bound capture probes. DPV was used to detect the redox signals; for HPV-16, the potential scan was in the range of −0.5 to +0.1 V, and for HPV-18, in the range of +0.2 to +1.0 V. The step potential was 10 mV, modulation amplitude 50 mV, interval time 0.05 s, and scan rate 100 mV s^{-1}. The genosensors showed high specificity and successful validation in clinical samples.

Crevillen et al. developed a 3D-printed microfluidic genosensor for detecting SARS-CoV-2 RNA within 7 min, involving the detection mechanism that relies on the oxidation of adenine residues in the ssDNA probe, which was monitored using DPV [66]. Upon hybridization with the target RNA, the ssDNA desorbs from the electrode surface, leading to a decrease in the DPV signal. DPV was conducted in PBS (pH 7.4) from 0.0 to +1.4 V, with a modulation time of 50 ms, an interval time of 0.5 s, a step potential of 10 mV, a modulation amplitude of 50 mV, and a scan rate of 20 mV s^{-1}.

Eskandari et al. developed a label-free electrochemical genosensor for detecting the p53 gene, using the hybridization between the immobilized ssDNA capture probe and its complementary target, which was monitored by DPV in the presence of $[Ru(bpy_3)]^{2+/3+}$ as the redox probe. The DPV measurements were conducted in 10 mM Tris-HCl buffer with 10 mM NaCl (pH 7.4), scanning the potential from +0.6 to +1.3 V vs. AgIAgCl, using a modulation amplitude of 25 mV and a modulation time of 50 ms. The genosensor demonstrated high sensitivity and selectivity, including discrimination of mismatched sequences [138].

A reusable genosensor for detecting *Candida auris* genomic DNA in urine, exploiting ninhydrin as a novel hybridization indicator, was

recently proposed. The gold electrode was modified with a thiolated DNA capture probe, and hybridization was detected indirectly by monitoring the oxidation peak of ninhydrin via DPV. The DPV was performed in 0.1 M PBS, pH 7.4, with a potential scan from −0.7 to +0.2 V, scan rate of 30 mV s^{-1}, modulation amplitude of 60 mV, and interval time of 0.2 s. The genosensor exhibited excellent selectivity, up to 8 times reusability, and stability of 100 % response after 80 days [57]. The same group presented an electrochemical genosensor for detecting miR-184 in human plasma; hybridization was detected both directly via guanosine oxidation and indirectly by using ethidium bromide (EB) as the redox probe. For indirect DPV detection, the potential was scanned from 0.0 to +0.8 V in 0.1 M PBS, pH 7.4, with a scan rate of 30 mV s^{-1}, a modulation amplitude of 60 mV, and an interval time of 0.2 s. The genosensor was reusable up to 10 times, stable for 50 days, and selective against non-complementary targets [56].

In the study presented by Moazampour et al., DPV was employed to monitor the electrochemical response of Fc-GO nanosheets, which were used as an electroactive label for detecting miR-200a. Measurements were performed in 0.1 M PBS (pH 7.4), and the signal was recorded before and after the hybridization event. The sensor demonstrated high sensitivity and selectivity, including discrimination of single-base mismatches [42].

DPV was used to detect guanine oxidation signals as a label-free method for identifying CRISPR-Cas9-induced mutations in the CIZ1 gene [70]. The genosensor was built on CNT/PGEs, with inosine-substituted capture probes immobilized via carbodiimide chemistry. Hybridization with complementary DNA restored guanine signals, which were absent in the probe due to inosine substitution. DPV scans were performed from +0.75 V to +1.40 V in acetate buffer (pH 4.8) at room temperature. The sensor could distinguish between entirely complementary, mismatched, and non-complementary sequences, while the method was validated using synthetic targets and PCR amplicons, showing high specificity and potential for mutation screening.

A recent article by Rizi et al. describes a PCR-free electrochemical genosensor for detecting MTB DNA using DPV to measure the peak current of MB, acting as a redox indicator. MB was intercalated into the DNA structure, and its signal decreased upon hybridization with the target DNA; DPV was conducted in 0.05 M phosphate buffer, pH 7.0, by scanning potential from +0.4 V to +0.1 V with a step potential of 5 mV, modulation time of 0.020 s, and an interval time of 0.0329 s. The genosensor showed excellent selectivity against mismatched and non-complementary sequences and was successfully applied to clinical sputum samples [41].

The three articles by Sohrabi et al. present a cohesive work focused on developing highly sensitive, label-free electrochemical genosensors for the detection of bacterial pathogens using DNA hybridization strategies and DPV as the electrochemical detection technique. Moreover, all three studies employed $[Fe(CN)_6]^{3-/4-}$ redox system, and the proposed genosensors were validated in real biological matrices, demonstrating their potential for clinical and environmental applications [58–60].

Finally, apart from the above-mentioned electrochemical techniques, a recent study has also demonstrated the applicability of **open-circuit voltage (OCV) measurements** in electrochemical genosensing, expanding the scope of signal transduction strategies [121]. The OCV measurements were used in an enzymatic biofuel cell (EBFC) configuration. The electroanalytical signal was generated by electron transfer during glucose oxidation at the bioanode and the redox conversion of $Ru(NH_3)_6^{3+}$ to $Ru(NH_3)_6^{2+}$ at the biocathode, with the amplified current recorded via a digital multimeter after capacitor discharge. The amplification strategy in this electrochemical genosensor combines three levels of signal enhancement, i.e., catalytic hairpin assembly (CHA) at the bioanode, DNA tetrahedra at the biocathode, and an external capacitor for electrical amplification (Fig. 7d). When miRNA-21 is present, it triggers CHA by opening hairpin H1, enabling the attachment of H2-glucose oxidase (H2-GOD) to the bioanode. GOD then catalyzes glucose oxidation, generating electrons that flow to the biocathode, where DNA tetrahedra capture large amounts of $Ru(NH_3)_6^{3+}$ complexes, further boosting conductivity. Finally, the capacitor stores and releases charge to amplify the electrical signal, resulting in a highly sensitive, "self-powered" genosensor. However, OCV measurements rely on equilibrium potential shifts that are inherently small, usually slow to stabilize, and highly susceptible to environmental fluctuations, which limits their sensitivity and reproducibility in complex samples. In contrast, pulse voltammetry, as reviewed, enables precise quantitative readout over a broad dynamic range and allows discrimination between specific hybridization events and nonspecific adsorption through well-defined peak potentials and peak shapes. In summary, the most common electroanalytical signals obtained via pulsed voltammetric techniques, reported in contemporary electrochemical genosensing, are depicted in Fig. 8.

In conclusion, while electrochemical techniques determine the mode by which a biorecognition event is converted into a measurable electroanalytical signal, the ultimate sensitivity, selectivity, and operational robustness of a genosensor are largely governed by the materials forming the sensing interface. Within this framework, nanomaterials should not be viewed as simple electrode modifiers, but rather as functional building blocks that regulate charge transfer, increase the effective electroactive surface, and facilitate signal amplification at the nanoscale. Accordingly, the following section focuses on the role of nanomaterials in contemporary electrochemical genosensing, emphasizing how their distinctive physicochemical characteristics are used to enhance analytical performance.

6. Nanomaterials in contemporary genosensing

It is widely accepted that nanomaterials play an important role in enhancing the performance of electrochemical sensors [178,179]. This

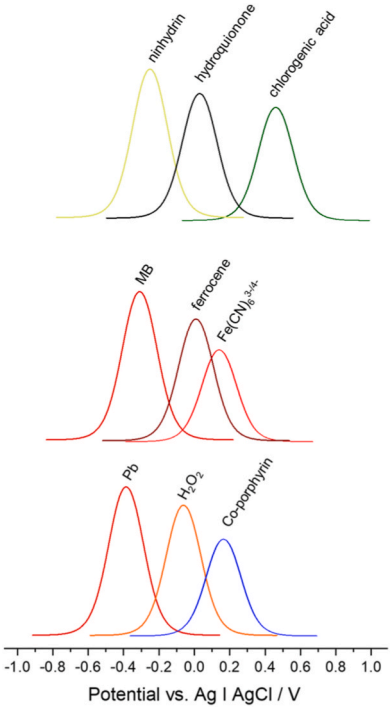

Fig. 8. The most commonly employed electroanalytical pulse voltammetric signals (e.g., DPV or SWV) used in genosensing in recent years, shown with respect to their peak potentials vs. AgIAgCl reference electrode. The signals include oxidation peak of Pb, reduction of H_2O_2, oxidation of Co-porphyrin, oxidation of MB, oxidation of ferrocene-based redox probe or tags, $[Fe(CN)_6]^{3-/4-}$ redox signalling, oxidation of chlorogenic acid, hydroquinone-based redox signalling, and ninhydrin redox activity.

also extends to genosensing applications, and the main reasons are the unique properties of nanomaterials, which include high surface area, excellent conductivity, biocompatibility, etc. Such characteristics enable more sensitive, selective, and rapid detection of genetic material. More importantly, nanomaterials improve the performance of genosensors by providing better immobilization platforms for nucleic acids, enhancing signal transduction, and offering (electro)catalytic properties that amplify electroanalytical signals. Various types of nanomaterials have been predominantly employed in state-of-the-art electrochemical genosensors. This subsection provides a thorough review of recent trends and advances in this context. Some of the most important nanomaterials used in contemporary genosensing are presented in Fig. 9.

Magnetic beads and magnetic nanoparticles, whether commercially available or synthesized, are widely employed, particularly in modern amperometric genosensors, to enable efficient target separation and pre-concentration, facilitating the detection process and enhancing selectivity and sensitivity [73,77,78,82,83,91,95,99,136]. Moreover, magnetic beads play an important role in the construction of electrochemical genosensors by serving as solid supports for capture probe immobilization and facilitating target sequence capture through magnetic separation. These beads, typically streptavidin-coated, e.g., Dynabeads MyOne Streptavidin T1 from Thermo Fisher Scientific, were used to bind biotinylated capture probes, enabling the formation of sandwich-type hybridization complexes with target nucleic acids and reporter probes [77,83,136]. The rationale for using magnetic beads lies in their high surface area, ease of manipulation via magnets, and facile washing and separation steps, which altogether enhance sensitivity and reduce background noise. However, challenges such as steric hindrance at high capture probe densities and the need for careful optimization of hybridization conditions were noted. Souza et al. developed an electrochemical magnetogenoassay using custom-synthesized core–shell Fe_3O_4@Au magnetic nanoparticles for detecting the HMGA gene in maize. These nanoparticles were synthesized in-house via thermal decomposition and gold coating, then functionalized with SAMs for covalent DNA capture probe immobilization. Similarly to the case of commercial magnetic beads, the reason for using Fe_3O_4@Au was to combine magnetic manipulability with excellent electrochemical properties of gold, enabling sensitive and reproducible DNA hybridization and enzymatic signal amplification. Advantages include high surface area, strong probe attachment, and enhanced signal-to-background ratio; however, somewhat complex synthesis and potential aggregation at high capture probe densities were the drawbacks [95].

On the other hand, there is an emerging trend of using **metal-organic frameworks (MOFs)** in genosensing that provide high surface area and tunable porosity for capture probe immobilization. In the above-discussed article by Asaadi et al., the use of PCMOF is highlighted as a key innovation in the development of a highly sensitive electrochemical genosensor for detecting *Nocardia spp.* PCMOF offers several advantages; besides high surface area, it provides a large and uniform pore volume, which is ideal for encapsulating electroactive molecules like MB, thereby assuring effective signal amplification. More importantly, its graphene-like π-rich structure facilitates strong π–π stacking interactions with ssDNA, enabling efficient and stable capture probe immobilization without the need for additional linkers. Furthermore, PCMOF exhibits excellent water solubility, biocompatibility, and electrochemical conductivity, all of which contribute to improved genosensor performance. These properties make PCMOF an ideal "nanocontainer" and signal amplifier in (bio)sensing applications, providing controlled release strategies and high sensitivity, even in complex biological matrices [45]. Similarly, in the article by Shishegari et al., the use of cerium-based metal–organic frameworks (Ce-MOFs) played an important role in enhancing the performance of the developed electrochemical genosensor for SARS-CoV-2 detection. The Ce-MOFs provided a high surface area and a unique straw-sheaf-like morphology, facilitating efficient biomolecule immobilization and improved electron transfer. The coordinatively unsaturated cerium centers acted as catalytic sites, contributing to the high sensitivity of the proposed genosensor. Although MOFs themselves possess generally low electrical conductivity, their integration with conductive layers like sulfur-doped reduced graphene oxide or dendritic palladium nanostructures creates synergistic effects, boosting the electrochemical performances of the genosensors. The Ce-MOF layer also enabled effective functionalization via EDC/NHS chemistry, allowing for stable and specific capture probe attachment. Overall, the incorporation of Ce-MOF into the genosensor architecture resulted in enhanced (electro)catalytic activity, increased current density, and improved electroanalytical performance [96]. Across two studies by Sohrabi et al., MOFs were highlighted as suitable materials for enhancing the performance of label-free electrochemical genosensors. In the first study, a Zn-based MOF was used in combination with CMC and AuNPs to modify a gold electrode, significantly improving the surface area, porosity, and electron transfer rate, which led to low detection limits for *Haemophilus influenzae* DNA in plasma samples [59]. The second study employed a bimetallic Fe/Mn MOF integrated with methyl-β-cyclodextrin and AuNPs stabilized on multi-walled carbon nanotubes (MWCNTs), forming a highly conductive and catalytically active nanocomposite. This configuration enabled sensitive detection of *Salmonella typhimurium*, likely benefiting from the synergistic effects of dual-metal centers and, therefore, enhanced charge transfer [58].

Noble metal nanostructures are widely utilized in electrochemical genosensing due to their exceptional conductivity, biocompatibility, and surface functionalization capabilities, which significantly enhance sensitivity and signal transduction. The incorporation of such nanostructures into composites or the introduction onto novel types of supporting electrodes has gained significant attention in recent years. For instance, Bishoyi et al. synthesized AgNPs and deposited them onto a paper-based graphene electrode to enhance electron transfer and provide a biocompatible surface for the DNA capture probe immobilization. This approach led to a twofold increase in current response and enabled the sensitive detection of the Zika virus [68]. Chaturvedi et al. constructed a ternary nanocomposite-based genosensor for MTB detection using AuNPs embedded in a reduced graphene oxide–polydopamine matrix. AuNPs contributed to improved conductivity and electron transfer, while polydopamine facilitated biomolecule immobilization [44]. Similarly, Ling Tan et al. designed a voltammetric genosensor for transgenic soybean analysis using a silica–gold nanoparticle (SiO_2–AuNP) composite. AuNPs were layered onto SPEs to enhance conductivity, while aminated silica nanospheres enabled high-density DNA capture probe immobilization via glutaraldehyde crosslinking [75]. Another electrochemical genosensor was developed for detecting the glycoprotein gene of VHSV using a PGE modified with rGO and AuNPs. The AuNPs were electrochemically deposited onto the rGO layer to enhance conductivity and facilitate thiol-based DNA capture probe immobilization. The genosensor also exhibited high selectivity against mismatched sequences [69]. As mentioned above in the section on the detection schemes, Malecka et al. compared electrochemical genosensors based on cobalt porphyrin-labeled DNA immobilized on either gold or silver nanoparticles. Both AuNP and AgNP systems were attached to gold electrodes via hybridization with corresponding capture probes. Interestingly, while AuNPs offered better separation and less aggregation, AgNPs provided a more cost-effective alternative with comparable sensitivity and selectivity, making them suitable for scalable applications [63]. In the study by Razmi et al. [94], AuNSs were employed in the design of a highly sensitive electrochemical genosensor for detecting *Escherichia coli* O157:H7 DNA. The AuNSs were deposited onto a gold electrode to significantly increase the surface area and enhance the immobilization of aminated DNA capture probes. The star-shaped morphology of the nanoparticles, i.e., nanostars, provided a high-density scaffold for capture probe attachment, which, combined with the use of SWV, enabled rapid, selective, and ultra-sensitive detection without the need for sample filtration. In the study by Shamsipur et al., AuNPs were electrodeposited onto a CPE modified with

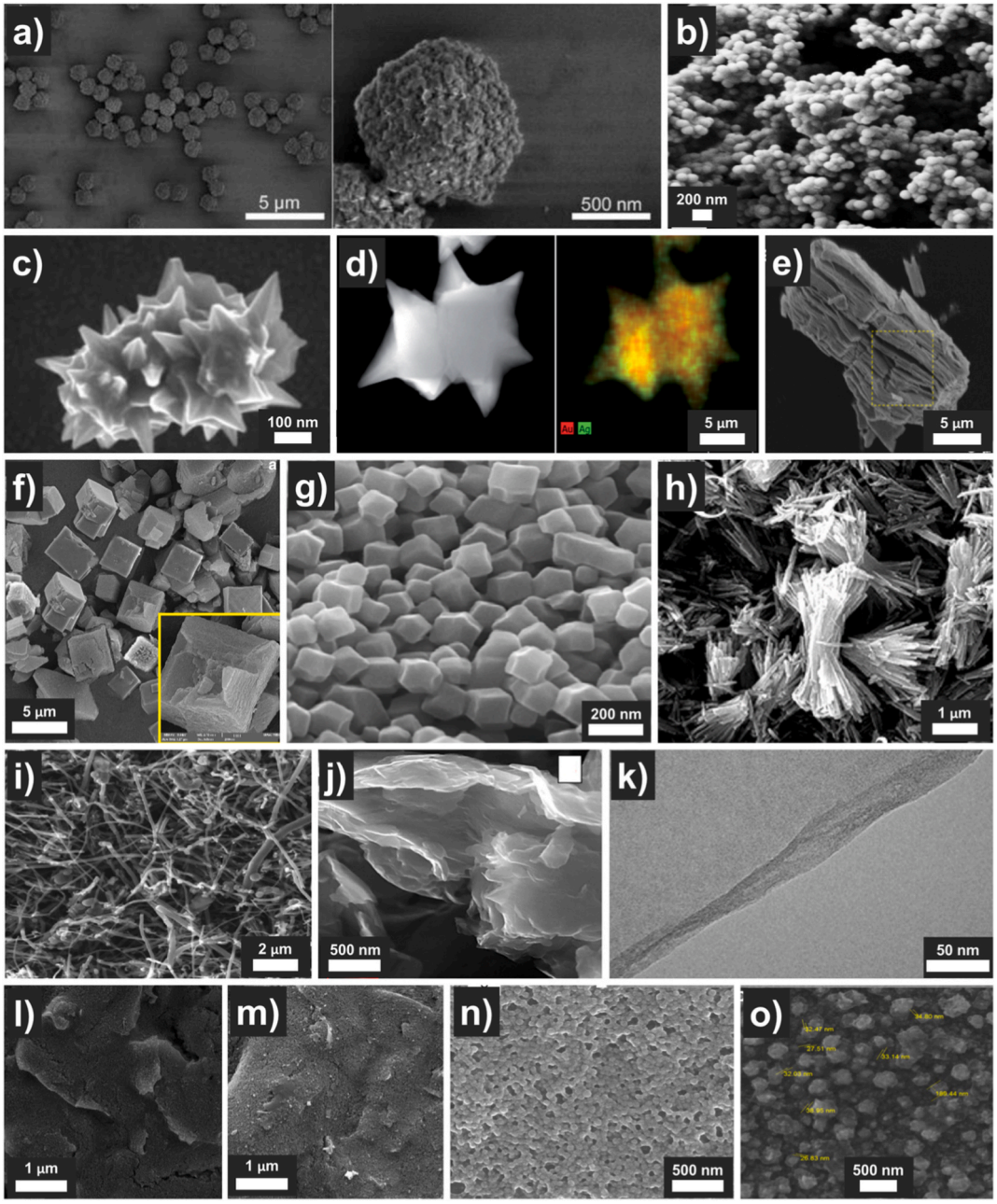

Fig. 9. Representative scanning electron microscopy (SEM) or transmission electron microscopy (TEM) micrographs illustrating the diversity of nanomaterials encountered in contemporary electrochemical genosensing platforms: **a)** Dynabeads™ MyOne™ Streptavidin T1 magnetic beads used in a glucose-based genosensor for the detection of viral nucleic acids via rolling cycle amplification and amperometry (images from Ref. [77] with permission from *Elsevier*), **b)** amino-modified silica nanospheres used in a voltammetric genosensor for the detection of the cauliflower mosaic virus (CaMV35S) gene (image from Ref. [75] with permission from *Elsevier*), **c),d)** Au nanostars used for fabrication of a genosensor for *Escherichia coli* O157:H7 DNA, characterized by FESEM-EDX, respectively (images from Ref. [94] with permission from *Royal Society of Chemistry*), **e)** $Ti_3C_2T_x$ MXenes used for fabrication of an impedimetric sensor for the detection of CBCVd RNA sequence (image from Ref. [21] with permission from *Elsevier*), **f)** Zn-based MOF used as an electrode modification material for voltammetric detection of *Haemophilus Influenzae* in human plasma samples (image from Ref. [59] with permission from *Springer Nature*), **g)** ZIF-8 MOF precursor for porous carbon used to fabricate a voltammetric genosensor for the detection of *Nocardia* strains (image from Ref. [45] with permission from *Elsevier*), **h)** Ce-MOF used in fabrication of voltammetric detection of SARS-CoV-2 target genes (image from Ref. [96] with permission from *Elsevier*), **i)** PLA/nanocarbon electrode material treated with DMF used for the voltammetric detection of target DNA (image from Ref. [67] with permission from *Elsevier*), **j)** GO used in the fabrication of a voltammetric genosensor for the detection of miR-200a (image from Ref. [42] with permission from *Elsevier; white square covers original notation*), **k)** rGO-polydopamine used in fabrication of voltammetric genosensor for detection of *Mycobacterium tuberculosis* (image from Ref. [44] with permission from *MDPI*), **l)** SPCE modified with graphene acid and **m)** SPCE modified with graphene acid and the DNA capture probe, used in fabrication of an impedimetric genosensor for the detection of meat adulteration (images from Ref. [80] with permission from *Elsevier*), **n)** GCE modified with carbon quantum dots and electropolymerized asparagine used in fabrication of voltammetric genosensor for detection of miR-106b (image from Ref. [43] with permission from *Elsevier*), **o)** Pd–Al LDH/FTO electrode surface used in fabrication of voltammetric detection of hepatitis B virus (image from Ref. [97] with permission from *Springer Nature*). Scale bars are indicated in each panel.

Pb-IIP nanoparticles to create a highly sensitive, label-free electrochemical genosensor for detecting the HIV-1 pol gene. The combination of AuNPs with Pb-IIP provided a novel dual-function platform: the Pb-IIP acted as a redox-active probe, while the AuNPs enhanced capture probe immobilization and signal transduction [72].

MXenes are a rapidly emerging class of 2D-layered transition metal carbides or nitrides, typically derived from the selective etching of precursor MAX phases [180]. Due to their unique combination of metallic conductivity, hydrophilicity, high surface area, and rich surface chemistry, MXenes have attracted considerable attention across various fields. In energy storage, they are widely explored for applications in supercapacitor and lithium-ion battery development due to their excellent charge transport properties. In sensor applications, particularly electrochemical gas sensors [170], humidity sensors [181], biosensors [182,183] and genosensors [21,49], MXenes offer enhanced signal transduction, attractive (electro)catalytic behavior, and facile functionalization for biomolecule attachment.

Sun et al. developed a ratiometric electrochemical genosensor for detecting sul2 using a hybrid nanomaterial composed of a Ti_3C_2-MXene monolayer decorated with AuNPs. The AuNPs were grown on the surface of the MXene via a seed-mediated method, which prevented restacking of the MXene nanosheets and enhanced their conductivity and surface area. This configuration significantly increased the DNA capture probe loading capacity and improved the electrochemical response [49].

In our recent study, $Ti_3C_2T_x$ MXene was employed as a key (electro) catalytic component in the development of a label-free impedimetric genosensor for the detection of CBCVd in hop plants. The MXene was synthesized via selective etching of the Al layer from Ti_3AlC_2 MAX phase, and its successful transformation was confirmed through scanning electron microscopy, energy-dispersive X-ray spectroscopy, Raman spectroscopy, X-ray diffraction, and FTIR analyses. Incorporated into the genosensor architecture alongside streptavidin–agarose beads and a biotinylated ssDNA capture probe, the 2D-layered $Ti_3C_2T_x$ significantly enhanced the electrochemical communication between the sensing interface and the supporting electrode. This integration led to a five-fold increase in sensitivity compared to the MXene-free architecture. The high conductivity, large surface area, and rich surface chemistry of MXene synergistically enabled efficient probe immobilization and signal transduction, resulting in a sensitive CBCVd detection in real total RNA samples obtained from the infected plants, even without the need for an amplification step [21].

Carbon-based nanomaterials, such as graphene, CNTs, nanocarbon, and carbon quantum dots, are known for their exceptional electrical conductivity, high surface area, mechanical strength, and chemical stability, making them highly valuable in a wide range of applications. Recently, in the field of electrochemical genosensing, carbon nanomaterials served as excellent transducer platforms, enhancing electron transfer and enabling sensitive and selective detection of various target sequences [40,43,52,58,66–70,73,76,80,99,117,152]. Graphene and its chemically modified forms, such as GO, rGO, and graphene acid, are widely employed for their high surface area and π–π stacking interactions, which facilitate the immobilization of ssDNA capture probes, as mentioned above. For example, Crevillen et al. used a graphene/PLA filament in a 3D-printing pen to produce electrodes for SARS-CoV-2 RNA detection, leveraging π–π stacking for capture probe immobilization [66]. PGE modified with graphene or carbon nanotubes also continues to serve as a low-cost, accessible platform for nucleic acid sensing [69]. Flauzino et al. demonstrated the effectiveness of rGO/poly (3-hydroxybenzoic acid) and graphene acid-modified electrodes for DNA hybridization-based detection of beef adulteration and pork DNA in meat samples, respectively [80,152]. Similarly, Eskandari et al. employed a CeO_2-rGO nanocomposite in a genosensor for the p53 gene, taking advantage of rGO surface characteristics and electron transfer [138]. CNTs, especially single-walled (SWCNTs) and multi-walled (MWCNTs) variants, have also been applied in genosensing due to their unique electrochemical and physico-chemical properties. Fortunati et al. utilized SWCNT-modified SPEs for detecting KRAS mutations in plasma, enabling point-of-care diagnostics [99]. Kivrak et al. fabricated label-free genosensors with CNT-modified PGEs for the detection of CRISPR-Cas9-induced mutations [70]. Ye et al. combined carboxylated MWCNTs with AuNPs to create a sandwich-type genosensor for detecting transgenes in genetically modified tomatoes [40]. Finally, carbon quantum dots (CQDs) offer additional advantages like photoluminescence and excellent surface chemistry; for example, Kuche-Meshki et al. synthesized CQDs from chitosan for genosensors targeting miR-106b, achieving high sensitivity through enhanced surface area and functional electropolymerization [43].

Layered double hydroxides (LDH) were recently introduced in the field of electrochemical genosensing. Namely, Heidari et al. employed a Pd–Al LDH film electrochemically deposited on an FTO electrode as a high-surface-area, conductive platform for immobilizing amino-labeled DNA capture probes, enabling sensitive detection of HBV DNA [97]. Similarly, Sohrabi et al. utilized Ni–Cr LDH nanosheets, synthesized via a co-precipitation method and combined with biochar to form a high-surface-area, conductive nanocomposite. The composite material was immobilized onto a gold electrode to enhance electron transfer and serve as a robust platform for the label-free electrochemical genosensing of *Haemophilus influenzae* DNA through hybridization-based detection [60].

7. Target sequences in contemporary electrochemical genosensing

The somewhat remarkable versatility of electrochemical genosensors has enabled the detection of a broad range of nucleic acid-based targets in recent years. These include pathogenic microorganisms, cancer biomarkers, food adulterants, genetic polymorphisms, and synthetic constructs, positioning electrochemical genosensing close or ahead of the standard laboratory methods in molecular diagnostics and environmental monitoring. Electrochemical genosensors have demonstrated excellent performance in the **detection of viral pathogens**, including SARS-CoV-2, through multiple genomic targets such as the N gene, RdRp gene, and combined RNA/DNA formats [66,73,82,96,127], hepatitis B virus (HBV) [97], HPV genotypes [48,54,136], Zika virus [68], Ebola virus [77], HIV-1 [72], HEV genotype 3 [83], VHSV [69], and CBCVd RNA in hop plants [21]; these examples span over clinical, environmental, and agricultural virology. In the **bacterial and parasitic pathogen domain**, targets include *E. coli* [78,94], *Salmonella typhimurium* [58], *Haemophilus influenzae* [59,60], *Campylobacter jejuni* [17], *Nocardia spp.* [45], *Mycobacterium tuberculosis*, targeting both general and IS6110 sequences [41,44,93,117], and Group B *Streptococcus* (clb gene) [52]. In **parasitology**, the DNA detection of several species of *Plasmodium* (*Plasmodium spp.*) supports malaria diagnostics [65]. **Fungal pathogens** such as *Candida auris* are also accessible through these genosensors [57]. In **oncology**, electrochemical genosensors detect a wide spectrum of genetic alterations and biomarkers, including mutations in KRAS [85,99], TP53 [51], and the p53 gene [84,138], as well as markers of microsatellite instability like BAT-26 [86]. Epigenetic markers, such as BMP3 gene methylation, also support colorectal cancer diagnostics [61]. Furthermore, **circulating RNA biomarkers** such as PCA3 long non-coding RNA, prostate-specific antigen messenger ribonucleic RNA, colon cancer-associated transcript 1 gene (CCAT1), GAPDH transcripts, and exosomal CD24 have been targeted for non-invasive prostate, colorectal, breast, and ovarian cancer diagnostics [79,87–89,91]. **MiRNAs,** including miR-106b [43], miR-200a [42], miR-183-5p [76], and miR-184 [56], are also commonly detected for applications in oncology and psychiatry. Importantly, in **pharmacogenetics**, electrochemical genosensors can detect single-nucleotide polymorphisms such as the brain-derived neurotrophic factors Val66Met (rs6265) and CYP2C9*3 [81,126], while Klotho gene mutations have relevance in aging and nephrology [90]. Electrochemical detection of

the sex-determining region Y gene allows for non-invasive prenatal sex determination [47]. **Applications in food safety** and authentication include detecting meat species through beef and pork DNA [80,152], GMO markers such as CaMV35S and HMGA genes [40,75,95], and plant DNA like *Erica arborea* for honey origin validation [50].

Finally, these genosensors also target **synthetic and engineered constructs**, such as synthetic DNA for influenza models [63], assay calibration [67], and CRISPR-Cas9-induced mutations [70], demonstrating their relevance in gene editing research. They have also been applied for detecting antibiotic resistance genes, e.g., sul2, specific for sulfonamide [49], further supporting their relevance in antimicrobial protection.

While considerable effort has been devoted to optimizing target sequence design and recognition, it needs to be noted that the subsequent performance and applicability of these genosensors remain constrained by the nature and complexity of the testing samples. Across all electrochemical genosensing studies analyzed for this review article, sample usage is dominated by simplified experimental systems, with a clear prevalence of buffer-based assays employing **synthetic nucleic acid targets**. Most of the studies rely exclusively on synthetic DNA or RNA measured in buffer solutions, while some articles provide insufficient detail to ascertain level of biological relevance. In these works, target analytes are most commonly synthetic oligonucleotides or PCR-derived amplicons, enabling precise analytical control but avoiding the complexities associated with real sample matrices. A smaller subset of investigations extend validation to spiked biological samples, most often serum or plasma with known target concentrations, representing an intermediate level of realism. Only limited number of studies explicitly report the use of **real biological samples**, indicating that genuine clinical or biological validation remains limited. These articles include, for instance, serum-derived DNA [184], unprocessed saliva [185], urine [186], clinical DNA from pediatric leukemia patients [187], clinical nasopharengyal swab samples [188], real pork and beef samples [80,152], upper respiratory specimens [127], raw sputum samples [117], RNA from fish samples [69], urine samples from patients scheduled for prostate biopsies [87], real hop samples [21], etc. More details on target sequences and tested samples are given in Table 1, which summarizes recent advances in electrochemical genosensing by organizing the latest research studies according to the key parameters discussed in this and previous sections, as well as in the following section concerning the emerging technologies, i.e., microfluidics and artificial intelligence. This structured comparison facilitates direct evaluation of different genosensing approaches, analytical performances, providing a concise overview of research directions in the field.

8. Emerging technologies in electrochemical genosensing

The integration of electrochemical genosensors with microfluidics and artificial intelligence (AI) is regarded as an emerging research direction, expected to gain a momentum [199]. This section provides an overview of the most recent, yet scarce, literature on this topic, with the expectation that continued progress in these technologies will ultimately pave the way for broader technology adoption. Notably, the synergy between isothermal amplification strategies and microfluidics in electrochemical genosensing has already been reviewed, covering nine articles published prior to 2020 [200]. Microfluidic platforms offer precise control over fluid handling, reaction kinetics, and assay timing, making them particularly well suited for general field of electrochemical biosensing [201]. By confining analytes within micrometer-scale channels, microfluidics enhances mass transport toward the sensing interface, accelerates hybridization, and reduces reagent and sample consumption. In electrochemical genosensing, the integration of microfluidic platforms has progressed beyond simple miniaturization. At the core of microfluidic platforms, as in static conditions, is a working electrode, which can be screen-printed gold, carbon, or graphene [184,188,195–198], interdigitated gold electrodes [193], gold microelectrode arrays [186,189], MEMS-fabricated glass chips with a gold working electrode [192], or planar gold electrodes on PET foil [194]. The detection principles are analogous to those employed under static conditions, i.e., direct or sandwich-type assays, with capture probes consisting of single-stranded DNA specific to the target, hairpin DNA, thiol- or biotin-modified DNA, or DNA aptamers. The anchoring strategies used in these devices follow the same principles observed in contemporary static sensing, including EDC/NHS coupling, physical adsorption, thiol–gold self-assembly chemistry, π–π stacking, glutaraldehyde cross-linking, and streptavidin–biotin affinity binding. Interestingly, most state-of-the-art microfluidic electrochemical genosensors do not incorporate additional nanomaterial modifications, as they strongly rely on the inherent advantages provided by bare gold electrodes, in various configurations, combined with thiol-based chemistry. Notable exception includes the use of MWCNTs, Fe_3O_4, or specific MOF compounds [198], as well as (paramagnetic) beads for enzyme-based amperometric detection approaches [189,197], described in detail above. Similar to static conditions, microfluidic devices also employ common electrochemical techniques such as EIS and pulse voltammetric methods operating in the Faradaic mode, in the presence of various redox-active systems, including MB, porphyrin, enzymatic conversion of naphthyl to napthol, ferrocene, etc.

Continuous-flow microfluidic platforms are typically fabricated from PDMS or thermoplastics, exploiting laminar flow of the target to reduce diffusion layer thickness and enhance analyte flux toward working electrode surfaces, thereby accelerating hybridization and stabilizing electrochemical responses. This effect is especially pronounced in impedance-based platforms, where flow-assisted hybridization yields more reproducible variation of R_{ct} and interfacial capacitance compared to static conditions [192]. Reportedly, microfluidic confinement also improves analytical robustness by promoting uniform capture probe immobilization and simultaneously limiting nonspecific adsorption, resulting in improved signal-to-noise ratios in biologically relevant matrices. Interestingly, reported limits of detection span several orders of magnitude, from micromolar concentrations in amplification-free, label-free systems to femtomolar or lower levels when biochemical amplification or nanostructured electrodes are employed. This variability in reported analytical performances show that there is still room for improvement of the technology itself. Perhaps the most attractive feature of microfluidic devices is the capillary-driven operation, providing an analytically attractive compromise between the analytical performance and operational simplicity. Although detection limits typically reside in the nano-to picomolar range, which is higher than in static conditions, assays are completed up to 45 min using minimal reagent volumes, making these systems particularly interesting for point-of-need applications where speed and robustness are more important than (ultra)sensitivity itself. On the other hand, more complex lab-on-chip architectures illustrate how microfluidics can encompass multistep workflows, including lysis, nucleic acid extraction, amplification, and electrochemical readout, into cohesive systems. Importantly, the newest studies in this field also integrate isothermal amplification or state-of-the-art CRISPR-based recognition with real-time electrochemical monitoring [185,191,195]. In these systems, microfluidics contributes not only confinement but also (i) contamination control, (ii) thermal management, and (iii) automated reagent handling, enabling operation within clinically relevant timeframes. In conclusion, the collective evidence from the most recent studies indicates that microfluidic integration delivers its most meaningful analytical contributions through improved kinetic efficiency, reproducibility, and workflow integration rather than through sensitivity enhancement, representing a good candidate for point-of-need diagnostics.

In parallel, artificial intelligence (AI) and machine learning techniques are being explored to address challenges across analytical chemistry, including signal complexity, noise, data abundance, and variability [202]. With that said, and given that electrochemical

Table 1
The most recent electrochemical genosensors listed based on their specific properties: supporting electrode used, electrochemical (EC) detection technique, genosensor/assay type, nanomaterials used in the fabrication process, biological recognition element (capture probe) used, anchoring/immobilization strategy employed, signal generation principle, redox system utilized, target sequence, type of tested samples, limit of detection (LOD), reference (REF).

Supporting electrode	EC detection technique	Assay type	Nanomaterials used	Capture probe	Anchoring/ immobilization strategy	Signal generation	Redox system	Target sequence	Tested sample	LOD	REF
μAuE	EIS	Direct type	None	Thiolated ssDNA capture probe	Thiol-gold chemistry with MCH blocking agent (SAM)	Change in charge transfer resistance	$Fe(CN)_6^{3-/4-}$	*Plasmodium* spp. DNA (malaria)	Synthetic in buffer and real blood lysate	18.7 aM (*P. falciparum*); 43.6 aM (*P. malariae*); 27.9 aM (*P. ovale*)	[65]
3D-printed nanocarbon electrode	LSV	Direct type (enzyme-linked hybridization)	Nanocarbon-PLA composite	Biotinylated DNA capture probe	Adsorption of target DNA	Enzymatic conversion of 1-naphthyl phosphate to 1-naphthol	1-naphthol (via ALP enzyme)	Synthetic DNA (model system)	Synthetic in buffer	0.95 μg mL^{-1}	[67]
3D-printed pen graphene/PLA electrode	DPV	Direct type	3D-printed graphene/PLA	Antisense ssDNA capture probe	Physical adsorption via π–π stacking between ssDNA and graphene	Adenine oxidation signal decrease upon hybridization	None	SARS-CoV-2 RNA (N gene)	Synthetic in buffer	15 nM	[66]
μAuE array (microfluidic device)	CV, EIS	Direct type	None	Hairpin DNA probe tagged with free-base porphyrin	Thiol-gold self-assembly	Signal-on mechanism: porphyrin exposure upon hairpin opening after hybridization	Porphyrin (intrinsic tag)	Bladder cancer methylation markers (E-Cadherin, DAPK, RARβ)	Synthetic in buffer and SurineTM Negative Urine Control	250 fM	[186]
μAuE (microfluidic device)	CA	Sandwich type	Paramagnetic beads	Biotinylated ssDNA capture probe	Streptavidin–biotin affinity on magnetic beads	Enzyme-linked amplification: alkaline phosphatase converts p-aminophenyl phosphate to p-aminophenol, detected electrochemically	p-aminophenyl phosphate (substrate for AP)	PCR-amplified fragment of Cor a 1.04 gene (hazelnut allergen)	Thermally denaturated PCR amplicons in buffer	0.2 nM	[189]
Au-coated electrospun polymeric fibers	DPV	Direct type	None	Phosphorothioated oligonucleotides	Covalent gold–sulfur bonding via phosphorothioate modification	MB intercalation in DNA duplex	MB	BCR/ABL fusion gene (Chronic Myeloid Leukemia)	Synthetic in buffer	ca. 5 fM	[100]
AuE	CA	Sandwich type	Fe_3O_4@Au MNPs	Aminated DNA capture probe targeting HMGA gene	EDC/NHS coupling	Enzymatic signal amplification (TMB by HRP)	TMB	HMGA gene (maize)	Synthetic in buffer	90 pM	[95]
AuE	CV, EIS	Sandwich type	PEI-stabilized AgNPs	Thiolated ssDNA capture probe for BMP3 methylation	Thiol-gold chemistry	AgNPs oxidation	AgNPs, $Fe(CN)_6^{3-/4-}$	BMP3 gene methylation (CRC biomarker)	Synthetic in buffer	1 fM	[61]
AuE	CV, EIS	Direct type	Polythiophene Acetic Acid (PTAA) film	Aminated DNA probe specific to the target	EDC/NHS coupling to carboxyl groups on PTAA	Charge transfer resistance and redox current changes	$Fe(CN)_6^{3-/4-}$	*Schistosoma mansoni* DNA	Cerebrospinal fluid, urine, plasma from infected patients	0.451 pg μL^{-1}	[64]
AuE	CV, SWV	Direct type	None	Thiolated ssDNA probes (Probe 1 and	Thiol-gold chemistry	Intrinsic oxidation/	None	PCA3 RNA (prostate cancer biomarker)	Urine samples (from patients	1.6 and 2.2 ng mL^{-1} depending on	[87]

(*continued on next page*)

Table 1 (*continued*)

Supporting electrode	EC detection technique	Assay type	Nanomaterials used	Capture probe	Anchoring/ immobilization strategy	Signal generation	Redox system	Target sequence	Tested sample	LOD	REF
				Probe 2) targeting PCA3 RNA		reduction of nucleobases			schedued for biopsies)	the capture probe	
AuE	DPASV	Direct type	Zn-MOF/CMC/ AuNPs	Thiolated ssDNA specific to the L-fuculokinase gene	Thiol-gold chemistry with MCH blocking agent (SAM)	Hybridization-induced current drop	$Fe(CN)_6^{3-/4-}$	*Haemophilus influenzae* (L-fuculokinase gene)	Spiked plasma	1.48 fM	[59]
AuE	DPV	Direct type	Fe/Mn-MOF/ MβCD/AuNPs/ MWCNTs	Thiolated ssDNA capture probe for the ViaB gene	Thiol-gold chemistry with MCH blocking agent (SAM)	Hybridization-induced current drop	$Fe(CN)_6^{3-/4-}$	*Salmonella typhimurium* (ViaB gene)	Spiked milk	0.07 pM	[58]
AuE	DPV	Direct type	NiCr-LDH/BC/ AuNPs	Thiolated ssDNA capture probe for L-fuculokinase gene	Thiol-gold chemistry with MCH blocking agent (SAM)	Hybridization-induced current drop	$Fe(CN)_6^{3-/4-}$	*Haemophilus influenzae* (L-fuculokinase gene)	Spiked urine	6.14 fM	[60]
AuE	DPV, CV, EIS	Direct type; ratiometric genosensor	$Ti_3C_2T_x$ MXene @ AuNPs	Hairpin DNA capture probe	Thiol-gold chemistry on $Ti_3C_2T_x$ MXene @ AuNPs with MCH	MB signal decrease, Fc signal increase upon hybridization	MB and Fc	sul2 gene (antibiotic resistance)	Synthetic in buffer and real tap water	2.04 fM	[49]
AuE	DPV, EIS	Direct type	None	Thiolated ssDNA capture probe for miR-184	Chemisorption on the Au surface	EB intercalation & guanosine oxidation	EB, $Ru(NH_3)_6^{2+/3+}$	miR-184 (Late-Life Depression biomarker)	Plasma samples	10^{-18} M	[56]
AuE	DPV, EIS	Direct type	None	Thiolated ssDNA capture probe specific to the target	Chemisorption on the Au surface	Ninhydrin oxidation peak	Ninhydrin, $Fe(CN)_6^{3-/4-}$	*Candida auris* genomic DNA	Urine samples	4.5 pg mL^{-1}	[57]
AuE	EIS, CV	Direct type	Polypyrrole and PAMAM-G5-AuNPs	Aminated MY09 degenerate DNA probe	Glutaraldehyde crosslinking on PAMAM dendrimer	Charge transfer resistance increase and peak current decrease upon hybridization	$Fe(CN)_6^{3-/4-}$	HPV genotypes (6, 16, 18, 31, 33)	Synthetic in buffer	0.04 pg μL^{-1} for plasmid DNA; 0.34 pg μL^{-1} for cDNA from clinical samples	[54]
AuE	SWV, CV, DPV	Direct type	AgNPs or AuNPs and Co-porphyrin-labeled DNA	Thiolated DNA capture probe	Thiol-gold chemistry	Co(II)/Co(III) redox current drop upon hybridization	Cobalt porphyrin (CoP) redox	Synthetic DNA (avian influenza H5N1 model)	Synthetic in buffer	3.8 aM (AuNP); 5.0 aM (AgNP)	[63]
AuE	SWV, CV, EIS	Direct type	None (uses DNA nanostructures)	DNA fishhook scaffold composed of Cp1 and Cp2	Hydrophobic interaction between cholesterol-modified DNA and HT SAM layer	Dual-signal electrocatalysis reaction (DEER) using MB and Fc mediated by potassium ferricyanide	MB, Fc	SARS-CoV-2 RDRP and N gene fragments; miRNA-21 and Met dimer	Synthetic in buffer	0.80 fM for T1 (SARS-CoV-2 RDRP gene); 3.55 fM for T2 (SARS-CoV-2 N gene)	[190]
AuE (microfluidic device)	DPV	Sandwich type	GO, Au NPs	DNA aptamer	π–π stacking on graphene oxide and Au–S bond	Enzymatic amplification with HRP catalysis	Hydroquinone	*Salmonella spp.*	Synthetic in buffer and real environmental samples	80 copies of the HF183 gene	[191]
AuE (microfluidic device)	EIS	Direct type	None	Thiolated ssDNA probe (specific to TP53 c.747G > T mutation)	Au–S chemisorption (thiol-gold SAM) with mercaptohexanol blocking	Hybridization-induced impedance change (label-free detection)	$Fe(CN)_6^{3-/4-}$	Hepatocellular carcinoma-specific ctDNA (TP53 mutation)	Synthetic in buffer	24.1 nM	[192]
AuE (microfluidic device)	SWV	CRISPR-based collateral cleavage (not direct or sandwich)	None	Reporter RNA tagged with ferrocene	Thiol-gold self-assembly	Decrease in ferrocene signal after Cas13a cleavage	Ferrocene	SARS-CoV-2 RNA	Real biological samples	50 aM	[185]

(*continued on next page*)

Table 1 (*continued*)

Supporting electrode	EC detection technique	Assay type	Nanomaterials used	Capture probe	Anchoring/ immobilization strategy	Signal generation	Redox system	Target sequence	Tested sample	LOD	REF
Carbon paper	CV, DPV, EIS	Direct type with triple signal amplification (CHA, DNA tetrahedra, capacitor)	Au NPs	Hairpin DNA strand with a thiol group	Thiol-gold chemistry	Electron transfer via GOx (bioanode); Ru $(NH_3)_6^{3+}$ reduction (biocathode), amplified by capacitor	$Ru(NH_3)_6^{2+/3+}$	miRNA-21	Synthetic in buffer	0.06 fM	[121]
CPE	DPV	Direct type	AuNPs and Pb-IIP	Thiolated ssDNA capture probe for HIV-1 pol gene	Thiol–gold chemistry	Pb oxidation current suppression	Pb^{2+} oxidation	HIV-1 pol gene	Synthetic in buffer	0.3 fM	[72]
FTO	SWV, DPV, EIS	Direct type	GO and AuNPs with CHI	Single-stranded miRNA-21 capture probe	Physical adsorption onto CHI-GO-AuNPs nanocomposite	Current change upon hybridization	$Fe(CN)_6^{3-/4-}$	miRNA-21 (Colorectal Cancer)	Synthetic in buffer	0.112 zM	[98]
FTO	CV, DPV, EIS	Direct type	S-doped rGO, Den-PdNS, Ce-MOF	Aminated ssDNA capture targeting RdRp SARS-CoV-2	EDC/NHS coupling on Ce-MOF	Hybridization-induced current drop	$Fe(CN)_6^{3-/4-}$	SARS-CoV-2 RdRp gene	Spiked saliva	0.2 fM	[96]
FTO	DPV, CV, EIS	Direct type	Pd–Al layered double hydroxide (LDH)	Aminated ssDNA capture probe for HBV DNA	EDC/NHS coupling on Pd–Al LDH film	Redox current change due to hybridization	$Fe(CN)_6^{3-/4-}$	Hepatitis B virus (HBV) DNA	Synthetic in buffer	1 fM	[97]
GCE	DPV	Direct type	PCMOF	ssDNA antisense oligonucleotide	π–π stacking of ssDNA on PCMOF	Release of MB from PCMOF	MB	Nocardia spp. DNA	Synthetic in buffer and sputum samples	0.54 aM (synthetic target); 4–7 copies per mL (real samples)	[45]
GCE	DPV	Direct type	$Ti_3C_2T_x$ MXene and polypyrrole (PPy)	ssDNA probe targeting the IS6110 sequence	Covalent bonding to PPY/MXene composite	MB intercalation	MB	*Mycobacterium tuberculosis* DNA (IS6110)	Synthetic in buffer and sputum samples	11.24 fM	[41]
GCE	DPV, CV, EIS	Direct type	Carbon quantum dots (CQDs)	Aminated ssDNA capture probe for miR-106b	EDC/NHS coupling	CGA oxidation current change upon hybridization	Chlorogenic acid (CGA)	miR-106b (gastric cancer biomarker)	Synthetic in buffer and spiked serum samples	0.39 fM	[43]
GCE	DPV, CV, EIS	Sandwich type	Fe_3O_4–Au@Ag core-shell MNPs	Thiolated DNA capture probe	Thiol-gold chemistry	H_2O_2 reduction catalysis	H_2O_2	CaMV35S gene (GMO marker)	Synthetic in buffer	10^{-17} M	[40]
GCE	DPV, EIS	Direct type	Amino-functionalized CuO nanoparticles, MnO_2 nanorods, ferrocene-functionalized graphene oxide (Fc-GO)	Aminated ssDNA capture probe complementary to miR-200a	Glutaraldehyde crosslinking and π-stacking with Fc-GO	Redox current change due to hybridization	Ferrocene (Fc) redox label	miR-200a (ovarian cancer biomarker)	Synthetic in buffer and spiked serum samples	0.29 fM	[42]
GCE	EIS	Direct type	$Ti_3C_2T_x$ MXene	Biotinylated ssDNA capture probe for CBCVd RNA	Biotin-streptavidin/ agarose interaction	Charge transfer resistance upon hybridization	$Fe(CN)_6^{3-/4-}$	CBCVd RNA (hop viroid)	Total RNA samples from hop plants	5.5 fM	[21]
GCE	EIS, CV	Direct type	$Cu(OH)_2$@N–C nanoboxes	Aminated DNA capture probe targeting SRY	Amine-Cu interaction	Change in charge transfer resistance	$Fe(CN)_6^{3-/4-}$	SRY gene (fetal sex determination)	Plasma samples	0.16 fM	[47]
GCE	LSV	Direct type	rGO–PDA–AuNP nanocomposite	Biotinylated ssDNA capture probe specific to the target	Biotin-avidin interaction on rGO–PDA–AuNP-modified GCE	Current suppression due to hybridization	$Fe(CN)_6^{3-/4-}$	*Mycobacterium tuberculosis* DNA	Synthetic in buffer	10^{-14} M	[44]

(*continued on next page*)

Table 1 (*continued*)

Supporting electrode	EC detection technique	Assay type	Nanomaterials used	Capture probe	Anchoring/ immobilization strategy	Signal generation	Redox system	Target sequence	Tested sample	LOD	REF
GCE	SWV	Direct type with triple cascade amplification (CHA-DNAzyme-HCR)	Au NPs electrodeposited	Double-loop hairpin DNA capture probe	Thiol-gold chemistry	MB intercalation into HCR product	MB	miRNA-221	Cancer cell lysates	9.25 aM	[162]
Glass micropipette (dual functionalized)	IC, SERS	Direct type (dual-functionalized micropipette sensor)	SiNWs (inner), AuNPs (outer)	Cp DNA (miRNA), Aptamer (protein)	EDC/NHS coupling for DNA probe, thiol-gold chemistry for aptamer	Ionic current change (miRNA), Raman intensity change (protein)	MB	miRNA-1246, PSA (protein); miRNA-106a, CD44 (protein)	Synthetic in buffer	1 aM for miRNA; 0.001 ng mL^{-1} for protein	[101]
Gold-coated glass electrode	SWV	Direct type	Au nanostars (AuNSs)	Aminated DNA capture probe targeting the Z3276 gene	Amine–gold affinity binding	TB intercalation into dsDNA	TB	*E. coli* O157:H7 DNA (Z3276 gene)	Synthetic in buffer	0.01 zM	[94]
Graphite electrode	EIS, SWV	Direct type	rGO	Aminated ssDNA probe (cattle-mitochondrial DNA specific)	EDC/NHS coupling	Change in charge transfer resistance and peak current upon hybridization	$Fe(CN)_6^{3-/4-}$	Beef DNA (adulteration with pork)	Real mixture of pork and beef	1 % w/w pork content in beef	[152]
Interdigitated gold electrodes (microfluidic device)	EIS	Direct type	None	DNA probe specific for HPV16	EDC/NHS covalent coupling on chitosan/ chondroitin sulfate LbL film	Change in capacitance/ impedance upon hybridization	None (label-free impedance)	HPV16 ssDNA	Synthetic in buffer	10.5 pM	[193]
ITO	CV, DPV	Direct type	Graphene oxide–chitosan (GO–CHI) composite	ssDNA capture probe with an amino linker	Glutaraldehyde crosslinking to amine groups on GO-CHI	Charge transfer resistance change upon hybridization	$Fe(CN)_6^{3-/4-}$	*Mycobacterium tuberculosis* (IS6110) DNA	Raw sputum samples	3.4 pM	[117]
m-GEC	CA	Sandwich type (double-tagging PCR with biotin/ digoxigenin labeling)	Magnetic particles	GAPDH-specific primers with biotin and digoxigenin tags	Biotin–streptavidin interaction on magnetic particles	HRP-catalyzed H_2O_2/HQ redox	HQ	GAPDH transcripts in breast cancer exosomes	Serum samples	415 exosomes per µL (CD81 IMS); 1225 exosomes per µL (CD326 IMS)	[91]
Paper-based graphene electrode	CV	Direct type	AgNPs	ssDNA capture probe targeting ZIKV target DNA	Drop-casting onto AgNP-modified paper	MB intercalation	MB	Zika virus target DNA	Synthetic in buffer	0.1 µM	[68]
PGE	CV, DPV, EIS	Direct type	RGO - AuNPs composite	Thiolated single-stranded DNA capture probe targeting the VHSV glycoprotein gene	Thiol-gold chemistry on Au/RGO-modified PGE	Rct increase and change in current upon hybridization	$Fe(CN)_6^{3-/4-}$	VHSV RNA (fish virus)	Real biological samples: extracts from fish	125 pM	[69]
PGE	DPV	Direct type	CNTs	Inosine-substituted ssDNA capture probe	EDC/NHS coupling to CNTs	Guanine oxidation signal (yes/no detection)	None	CRISPR-Cas9-induced mutations (CIZ1 gene)	Synthetic in buffer	213.7 nM	[70]
Polycrystalline AuE	DPV	Direct type	None	Hairpin DNA capture probe with MB label	Thiol-gold chemistry with MCH blocking agent (SAM)	MB redox signal change upon hybridization	MB	TP53 gene mutation (SNP)	Synthetic in buffer and simulated real samples	10 nM	[51]
Printed planar AuE on PET foil	SWV	Direct type	None	Thiol-modified DNA probe	Self-assembled monolayer via Au–S bond and	Redox current from methylene	MB	vanB gene (vancomycin resistance marker)	Synthetic in buffer	<50 nM (synthetic target);	[194]

(*continued on next page*)

Table 1 (*continued*)

Supporting electrode	EC detection technique	Assay type	Nanomaterials used	Capture probe	Anchoring/ immobilization strategy	Signal generation	Redox system	Target sequence	Tested sample	LOD	REF
(microfluidic device)				complementary to vanB gene	mercaptohexanol backfilling	blue tag on PCR amplicons				qualitative detection of asymmetric PCR products	
SPAuE	CA	Sandwich type	Magnetic beads (streptavidin-coated)	Biotinylated DNA capture probe complementary to HEV genotype 3	Biotin-streptavidin interaction on magnetic beads	Enzymatic reduction of TMB by HRP, measured electrochemically	TMB + H_2O_2	Hepatitis E Virus (HEV) genotype 3	Synthetic in buffer	1.2 pM	[83]
SPAuE	CA	Sandwich type	None	Thiolated DNA capture probe and FITC-labeled signaling probe	Thiol-gold chemistry with MCH blocking agent (SAM)	Enzymatic amplification via anti-FITC-POD	TMB	CYP2C9*2 SNP	Synthetic in buffer	13.03 pM (DNA-Target G), 22.58 pM (DNA-Target A)	[160]
SPAuE	CA	Sandwich type	Magnetic particles (maleimide-coated)	Thiolated capture probe and biotinylated signaling probes	Thiol-maleimide chemistry	HRP-catalyzed TMB reduction	TMB	SARS-CoV-2 RNA	Synthetic in buffer and RNA extracted from SARS-CoV-2 cell culture	0.6 pM	[82]
SPAuE	CA	Sandwich type	None	Thiolated capture probe and FITC-labeled signal probe	Thiol-gold chemistry with MCH blocking agent (SAM)	HRP-catalyzed TMB oxidation	TMB + H_2O_2	BDNF Val66Met SNP (rs6265)	Synthetic in buffer	Not explicitly stated	[126]
SPAuE	CA	Sandwich type	None	Thiolated DNA capture probe specific to the target	Thiol-gold chemistry with MCH blocking agent (SAM)	HRP-catalyzed TMB/H_2O_2 redox reaction	TMB + H_2O_2	*Alexandrium minutum* DNA (toxic algae)	Synthetic in buffer	24.78 pM	[157]
SPAuE	CA	Sandwich type	None	Thiolated DNA capture probe specific to the target	Thiol-gold chemistry with MCH blocking agent (SAM)	HRP-catalyzed TMB/H_2O_2 redox reaction	TMB + H_2O_2	CYP2C9*3 SNP (pharmacogenetics)	Synthetic in buffer	42 and 87 pM	[81]
SPAuE	CA	Sandwich type	None	Thiolated DNA capture probe specific to the target	Thiol-gold chemistry with MCH blocking agent (SAM)	HRP-catalyzed TMB/H_2O_2 redox reaction	TMB + H_2O_2	*Erica arborea* DNA (honey authentication)	Real plant samples	30 pM	[50]
SPAuE	CA	Sandwich type	None	Thiolated capture DNA probes for PCA3 and PSA	Thiol-gold chemistry with p-aminothiophenol (SAM)	HRP-catalyzed TMB oxidation	TMB	PCA3 lncRNA and PSA mRNA (prostate cancer)	Real urine samples from biopsy positive patients	4.4 pM (PCA3); 1.5 pM (PSA)	[89]
SPAuE	CA	Sandwich type	None	Thiolated capture DNA probes for CCAT1 and GAPDH	Thiol-gold chemistry with p-aminothiophenol (SAM)	HRP-catalyzed TMB oxidation	TMB	CCAT1 lncRNA (colorectal cancer)	Spiked plasma	990 fM (CCAT1); 1830 fM (GAPDH)	[88]
SPAuE	CV	Direct type	None	Thiolated ssDNA capture probe specific to the target	SAM using 11-mer-captoundecanoic acid (MUA)	Doxorubicin intercalation signal suppression	$Fe(CN)_6^{3-/4-}$	K-ras gene mutation (k12p.1)	Synthetic in buffer	7.96 fM	[85]
SPAuE	CV	Direct type	None	Thiolated ssDNA capture probe specific to the target	SAM using 11-mer-captoundecanoic acid (MUA)	Doxorubicin intercalation signal suppression	$Fe(CN)_6^{3-/4-}$	p53 gene mutation (175p2)	Synthetic in buffer	175 aM	[84]
SPAuE	CV, DPV	Direct type	None	Thiolated ssDNA capture probe	SAM using 11-mer-captoundecanoic acid (MUA)	Dox intercalation signal suppression	$Fe(CN)_6^{3-/4-}$	BAT-26 microsatellite instability marker	Synthetic in buffer	71.74 aM	[86]
SPAuE	DPV	Sandwich type	None	Thiolated DNA capture probe specific to Klotho mRNA	Thiol–gold chemistry	Enzymatic conversion of naphthyl phosphate to naphthol	1-naphthol (via ALP enzyme)	Klotho gene (kidney disease)	Synthetic in buffer	0.5 nM	[90]

(*continued on next page*)

Table 1 (*continued*)

Supporting electrode	EC detection technique	Assay type	Nanomaterials used	Capture probe	Anchoring/ immobilization strategy	Signal generation	Redox system	Target sequence	Tested sample	LOD	REF
SPAuE	EIS, DPV	Direct type	CeO_2 NPs and rGO and PANI	ssDNA capture probe	Physical adsorption via CeO_2 electrostatics and π–π stacking	Redox signal decrease upon hybridization	$Ru(bpy)_3^{2+/3+}$	p53 tumor suppressor gene (DNA)	Synthetic in buffer	1.3 fM	[138]
SPAuE	EIS, DPV, CV	Direct type	None (focus on BSA treatment)	ssDNA capture probe	Thiol-gold chemistry	Change in charge transfer resistance and peak current upon hybridization	$Fe(CN)_6^{3-/4-}$	*Campylobacter jejuni* DNA	Synthetic in buffer	200 nM (threshold concentration for detectable signal shift)	[17]
SPAuE	SWV	Direct type; ratiometric genosensor	AgNPs	MB-tagged peptide nucleic acid (PNA) capture probe	Thiol-gold chemistry with MCH blocking agent (SAM)	Dual-signal: MB and AgNPs	MB and AgNPs	*Mycobacterium tuberculosis* (MTB) genomic DNA	Simulated sputum with isolated MTB	1.59 fM (non-amplified MTB genomic DNA)	[92]
SPAuE (microfluidic device)	SWV	Collateral cleavage-based CRISPR sensor (not direct/ sandwich)	None	PolyU reporter tagged with methylene blue (MB)	Thiol-gold self-assembly on electrode surface	Decrease in MB redox current upon Cas13a collateral cleavage	MB	SARS-CoV-2 RNA	Synthetic in buffer and nasopharyngeal swab samples	10.0 aM	[195]
SPCE	CA	Sandwich (RCA-based)	Magnetic beads	Padlock probe and biotinylated capture oligonucleotide	Streptavidin-biotin interaction accompanied by RCA on magnetic beads	H_2O_2 generation from GOx + glucose oxidation	PB	Ebola virus RNA (clinical samples)	Synthetic in buffer	1 pM (synthetic target); clinical detection demonstrated	[77]
SPCE	CA	Sandwich type	None	Biotinylated DNA capture probe targeting the ipaH gene	Streptavidin-biotin interaction	HRP-TMB enzymatic reaction (current signal)	TMB	*ipaH* gene (Shigella spp. & EIEC)	Synthetic in buffer	4 nM	[163]
SPCE	CV, LSV	Direct type	Chitosan-butein conjugate (CSB)	Aminated DNA aptamer for exosomal CD24	Mix&Go bioaffinity layer drop-casted on CSB-modified electrode	Redox current quenching upon hybridization	Intrinsic redox of CSB was used	Exosomal CD24 (ovarian cancer biomarker)	Synthetic in buffer	2.24 pM	[79]
SPCE	DPV	Sandwich	Magnetic beads, silica nanoparticles with MB (HPV-16) and AO (HPV-18)	Biotinylated capture probe and redox-dye-labeled signal probe	Biotin-avidin interaction on magnetic beads	Redox dye release (MB/AO) from silica nanoparticles	MB, AO	HPV-16 and HPV-18 DNA (oral & cervical)	Synthetic in buffer and clinical (oral and cervical) samples	22 fM for HPV-16; 20 fM for HPV-18	[136]
SPCE	DPV, CV	Direct type	Silica nanospheres - AuNPs composite	Aminated ssDNA capture probe for CaMV35S gene	Glutaraldehyde crosslinking	AQMS intercalation into dsDNA	AQMS redox indicator	CaMV35S gene (GMO soybean marker)	Synthetic in buffer and extracted from soybean and soy food samples	2.37 fM	[75]
SPCE	DPV, CV, EIS	Direct type	None (uses DNA nanostructures)	Human telomeric G-quadruplex DNA with RNA loop	Diazonium coupling and EDC/NHS coupling on SPCE	MB redox current enhanced by RNA-induced unfolding	Methylene blue (MB)	SARS-CoV-2 RNA	Synthetic in buffer and upper respiratory specimens confirmed positive for SARS-CoV-2	0.59 zM (synthetic RNA); 1.4 copies (plasmid)	[127]
SPCE	EIS (non-Faradaic)	Direct type	Graphene Acid	Aminated ssDNA capture probe (pork-mitochondrial DNA specific)	EDC/NHS coupling to graphene acid carboxyl groups	Admittance and impedance change upon hybridization	None	Pork mitochondrial DNA (meat adulteration)	Synthetic in buffer, pure beef and pork meat extracts, mixtures of beef	9 % w/w pork content in beef	[80]

(*continued on next page*)

Table 1 (*continued*)

Supporting electrode	EC detection technique	Assay type	Nanomaterials used	Capture probe	Anchoring/ immobilization strategy	Signal generation	Redox system	Target sequence	Tested sample	LOD	REF
									and pork extracts		
SPCE	SWV	Sandwich (RCA-based)	Magnetic beads (streptavidin-coated)	Biotinylated oligonucleotide specific to the target	Biotin-streptavidin interaction on magnetic particles	Enzymatic reaction of HRP with H_2O_2 and HQ, detected via SWV	HQ	*E. coli* 16 S rRNA gene	Synthetic in buffer and DNA extracts from cultured *E.coli*	0.67 pM (synthetic DNA); 3×10^3 CFU in 10 μL (bacterial sample)	[78]
SPCE (double electrode system)	DPV	Direct type	None	DNA capture probe targeting HPV-16 E6/E7 oncogene	Electrochemical immobilization on SPE via chronoamperometry	MB intercalation into dsDNA and oxidation	MB	HPV-16 DNA (cervical cancer)	Synthetic in buffer and 40 cervical tissue samples	0.23 copies per μL	[48]
SPCE (microfluidic device)	ASWV	Direct type	AuNPs (formed during metallization)	acpcPNA (pyrrolidinyl peptide nucleic acid)	Physical adsorption on nitrocellulose (hydrophobic interactions)	Gold metallization on DNA backbone followed by stripping voltammetry	Gold ions (Au^{3+})	HBV DNA	Synthetic in buffer and real serum samples	7.23 pM	[196]
SPCE (microfluidic device)	DPV	Sandwich-type	Magnetic beads (streptavidin-coated)	Biotinylated DNA probe complementary to sul1/sul4	Streptavidin–biotin interaction on magnetic beads	Enzymatic conversion of α-naphthyl phosphate to α-naphthol by AlkP	α-naphthol (generated electroactive species)	Sulfonamide resistance genes (sul1, sul4)	Synthetic in buffer	44.2 pmol L^{-1} (sul1), 48.5 pmol L^{-1} (sul4)	[197]
SPE	CV	Direct type	GO	ssDNA capture probe targeting the clb gene	EDC/NHS coupling	Current suppression upon hybridization	$Fe(CN)_6^{3-/4-}$	Group B *Streptococcus* (GBS) clb gene (Neonatal Sepsis marker)	Synthetic in buffer	10^{-12} M	[52]
SPE	SWV	Direct type	None	MB-tagged DNA capture probe specific to anti-miR-2001-5p	No immobilization on the electrode; detection in solution via enzymatic cleavage	MB release via DSN cleavage	MB	miR-200a-5p	Synthetic in buffer and spiked serum samples	26 fM	[177]
SPE	SWV, EIS, CV	Sandwich and direct (dual mode)	MrGO	DNA capture probe complementary to miRNA-183-5p	EDC/NHS coupling	HRP catalysis or TBO intercalation signal amplification	TBO (intercalator) or H_2O_2/HQ (HRP)	miRNA-183-5p (prostate cancer biomarker)	Synthetic in buffer and spiked serum and urine samples	0.86 aM (intercalator method); 3.73 aM (HRP method)	[76]
SPE	SWV, EIS, CV	Sandwich type	Au-decorated magnetic rGO (AMrGO)	DNA capture probe complementary to the SARS-CoV-2 N-gene	EDC/NHS coupling	HRP-catalyzed H_2O_2/HQ redox reaction	H_2O_2/HQ (HRP)	SARS-CoV-2 N-gene RNA/DNA	Spiked serum, urine, and saliva samples	0.19 fM (serum); 0.33 fM (urine); 0.37 fM (saliva)	[73]
SPE (microfluidic device)	DPV	Direct type	MWCNTs, Fe3O4, MOF	ssDNA aptamer specific to H5N1 DNA	EDC/NHS covalent coupling on carboxylated MWCNT-Fe_3O_4@TMU-8 composite	Catalytic redox recycling of Ru $(NH_3)_6^{3+}$ mediated by Fe_3O_4@TMU-8/MWCNT composite	$Ru(NH_3)_6^{2+/3+}$	H5N1 influenza virus DNA	Spiked serum	0.16 fM	[198]
SPE/graphene	CV	Direct type (based on DNA amplification and redox probe interaction)	Graphene	LAMP amplicons targeting the IS6110 gene of MTB	Drop-cast the LAMP product and redox probe onto the SPE/graphene	Hoechst redox current quenched by DNA binding	Hoechst 33258	*Mycobacterium tuberculosis* DNA	Synthetic in buffer and 104 sputum samples	1 pg DNA or 40 genome equivalents	[93]

(*continued on next page*)

Table 1 (*continued*)

Supporting electrode	EC detection technique	Assay type	Nanomaterials used	Capture probe	Anchoring/ immobilization strategy	Signal generation	Redox system	Target sequence	Tested sample	LOD	REF
SPE/graphene (microfluidic device)	CA	Direct type	None	acpcPNA probe (specific for HIV-1 and HCV DNA)	Chitosan coating + glutaraldehyde crosslinking for PNA immobilization	Electrostatic interaction between Ru(III) complex and PNA-DNA duplex (current increase upon hybridization)	$Ru(NH_3)_6^{2+/3+}$	HIV-1 and HCV cDNA (coinfection detection)	Real biological sample: serum derived cDNA	HIV: 1.45 nM; HCV: 1.20 nM	[184]
SPE/SWCNTs	DPV	Sandwich type	Magnetic microbeads	Peptide nucleic acid (PNA) capture probes	EDC/NHS coupling on magnetic beads	ALP-catalyzed conversion of HQDP to HQ	HQ	KRAS p.G12D SNV (liquid biopsy)	Spiked plasma samples	818 fM for KRAS p.G12D; 1.98 pM for KRAS wild-type	[99]

genosensors often generate rich datasets that are laborious to interpret using conventional analytical methods, AI and machine learning approaches are expected to play an important role in facilitating data processing and interpretation, at least. Interestingly, the bond between AI and electrochemistry has been already established. Recent reports highlight the use of machine learning in voltammetric mechanistic studies [203] and in the quantitative analysis of voltammetric reduction processes of model compounds for thermodynamic and kinetic investigations [204]. AI has also been employed for the prediction of voltammetric responses and in-depth analysis of model reactions [205]. Furthermore, the application of AI to the interpretation of EIS datasets has recently gained attention, particularly given the successful deployment of these techniques in chromatography, Raman spectroscopy, IR spectroscopy, and XRD [206]. Overall, these examples illustrate the strong susceptibility of the analytical community to AI-based innovations. At present, however, many of these research efforts remain at the stage of conceptualization rather than full realization. It is therefore expected that more focused and application-driven studies integrating AI within the framework of electrochemical genosensing will emerge in the coming years, with the potential for unprecedented impact, analogous to developments already seen in other analytical fields such as chromatography and spectroscopy.

9. Challenges and future prospects

Regardless of the impressive progress that electrochemical genosensing has achieved, several important challenges still prevent its full transformation from laboratory and proof-of-concept studies into commercialization and routine use in real-life settings. One of the most persistent concerns is the need to preserve both sensitivity and specificity when operating in real, complex biological samples. Notably, validation is mostly restricted to synthetic or spiked samples, while systematic studies in relevant real matrices remain scarce. Biological fluids such as blood, saliva, or urine, as well as food and environmental extracts, contain various interfering species that can mask or mimic the signal corresponding to the target sequence. For instance, single-nucleotide polymorphism discrimination has been reported, but reliably detecting such discrete deviations in highly heterogeneous matrices remains a difficult task. This applies particularly to clinical diagnostics, where false positives or false negatives can cause serious practical consequences. Another persistent challenge lies in reproducibility and standardization; many genosensing platforms are based on sophisticated electrode modifications, nanomaterials, nanostructured composite coatings, and multi-step capture probe anchoring/immobilization strategies. These procedures frequently vary between laboratories and can produce significant differences in electroanalytical performance. The absence of universal protocols makes it difficult to compare results across studies and complicates the path toward regulatory endorsement. For instance, under the European regulatory framework, electrochemical genosensors intended for medical use are classified as in vitro diagnostic medical devices (IVDs) and therefore fall under Regulation (EU) 2017/746 (IVDR) [207]. **The IVDR introduces very strict requirements for market access, shifting the focus from analytical feasibility, toward demonstrated clinical value and long-term reliability.** However, critical practical aspects of electrochemical genosensors such as long-term stability, shelf life, and performance under dynamic conditions, i.e., field, hospital, bedside, are rarely addressed in academia, despite their importance. The long-term stability of functionalized electrodes and biological recognition elements poses clear limitations; DNA/RNA probes, enzymes, or even nanomaterials may degrade during storage or transportation, reducing the shelf life of devices that are intended for point-of-care or field applications. Manufacturing scalability presents an additional barrier. For instance, screen-printed electrodes indeed offer highly desired cost efficiency, but their integration into robust, engaging analytical platforms is still challenging. Looking to the future, however, the field of electrochemical

genosensing is ripe with opportunities. Emerging supporting electrodes, including 3D-printed nanocarbon electrodes, SPEs, and transparent conductive substrates such as ITO and FTO glass, demonstrate promising directions by offering enhanced adaptability, integration with nanomaterials, portability, and cost-effective fabrication routes. Advances in nanomaterials and surface engineering are expected to further enhance both the sensitivity and selectivity of genosensors. Graphene-based compounds, metal–organic frameworks, MXenes, and hybrid nanocomposites provide tunable surface properties that can improve probe immobilization, may reduce nonspecific binding, and allow for multiplexed detection within a single device. Parallel to this, the integration of electrochemical sensing with microfluidics and lab-on-a-chip technologies offers the promise of automated, miniaturized platforms capable of handling sample preparation, detection, and analysis in a portable manner. Equally exciting is the prospect of coupling genosensors with emerging nucleic acid technologies, as mentioned above; it needs to be noted, however, that the integration of RCA, CDH, CRISP-R–Cas systems, or isothermal amplification methods with electrochemical genosensors still faces the challenge of balancing high sensitivity and selectivity with operational simplicity and device practical applicability.

Finally, to summarize this review, while challenges relating to reproducibility, stability, scalability, and clinical validation remain significant, the pace of innovation is steady, arguably accelerating. The integration of novel materials and cutting-edge nucleic acid technologies points toward a future in which genosensors could become valuable tools mainly across medicine, food safety, and environmental monitoring. Of course, realizing this potential will require close(r) collaboration between (electro)chemistry, molecular biology, computational sciences, and engineering. The trajectory of progress suggests that electrochemical genosensing is perhaps maturing from a laboratory setup into a practical, real-life technology.

CRediT authorship contribution statement

Alnilan Lobato: Writing – review & editing, Writing – original draft, Visualization, Conceptualization. **Mitja Koderman:** Writing – review & editing, Writing – original draft, Visualization. **Nika Vranešič:** Writing – original draft. **Samo B. Hočevar:** Writing – review & editing, Writing – original draft, Funding acquisition. **Nikola Tasić:** Writing – review & editing, Writing – original draft, Visualization, Supervision, Conceptualization.

Declaration of competing interest

The authors declare that they have no known competing financial interests or personal relationships that could have appeared to influence the work reported in this paper.

Acknowledgments

The funding from the Slovenian Research Agency (Research Program P1-0034, Research Projects J1-3017, J1-50019, and the Slovenian Research Agency's Young Researchers Program - grant agreements No. 56119 (AL) and No. 59876 (MK)) is greatly acknowledged.

List of abbreviations (by order of appearance)

PCR	polymerase chain reaction
RT-PCR	reverse transcription PCR
qPCR	quantitative PCR
LAMP	loop-mediated isothermal amplification
FISH	fluorescence in situ hybridization
DNA	deoxyribonucleic acid
RNA	ribonucleic acid
ss-DNA	single-stranded DNA
MB	methylene blue
ALP	alkaline phosphatase
HRP	horseradish peroxidase
POD	peroxidase
G6PDH	glucose-6-phosphate dehydrogenase
miRNA	micro RNA
ALL	acute lymphocytic leukemia
GMOs	genetically modified organisms
LOD	limit of detection
GCE	glassy carbon electrode
CE	carbon electrodes
AuE	gold electrodes
μAuE	gold microelectrodes
PGE	pencil graphite electrodes
CPE	carbon paste electrodes
SPCE	screen-printed carbon electrodes
SPAuE	screen-printed gold electrodes
FTO	fluorine-doped tin oxide
SPE	screen-printed electrode
FDM	fused deposition modeling
PLA	polylactic acid
LSV	linear sweep voltammetry
PDMS	polydimethylsiloxane
DPV	differential pulse voltammetry
EIS	electrochemical impedance spectroscopy
SWV	square-wave voltammetry
CNT	carbon nanotube
CRISPR	clustered regularly interspaced short palindromic repeats
EDC	1-ethyl-3-(3-dimethylaminopropyl)carbodiimide
NHS	N-hydroxysuccinimide
GO	graphene oxide
rGO	reduced graphene oxide
BHB	3-hydroxybutyric acid
m-GEC	magneto-actuated graphite-epoxy composite electrodes
DIG	digoxigenin
HIV	human immunodeficiency virus
RT	reverse transcriptase
PR	protease
IN	integrase
TCEP	tris(2-carboxyethyl)phosphine
ITO	indium tin oxide
GA	glutaraldehyde
BSA	bovine serum albumin
S-rGO	sulfur-doped reduced graphene oxide
Den-PdNS	dendritic palladium nanostructures
Ce-MOF	cerium-based metal-organic framework
Pd–Al LDH	palladium-aluminum layered double hydroxide
MCH	6-mercapto-1-hexanol
PMMA	Poly(methyl methacrylate)
PET	Polyethylene terephthalate
AgNP	silver nanoparticle
t-DNA	target DNA
SALP	streptavidin-alkaline phosphatase
SPGE	screen-printed graphene electrode
CV	cyclic voltammetry
SAM	self-assembled monolayer
AuNP	gold nanoparticle
PAMAM	poly(amidoamine)
HPV	human papilloma virus
FTIR	Fourier-transform infrared spectroscopy
CMC	carboxymethylcellulose
PDA	polydopamine
MTB	*Mycobacterium tuberculosis*
HEV	Hepatitis E virus
RCA	rolling circle amplification
GOx	glucose oxidase

PoC	point-of-care
PNA	peptide nucleic acid
KRAS	Kirsten rat sarcoma viral oncogene homolog
CSB	chitosan-butein
PCMOF	porous carbon metal–organic framework
Fc-GO	ferrocene-functionalized graphene oxide
CBCVd	Citrus bark cracking viroid
R_{ct}	charge transfer resistance
NLSF	nonlinear least squares fitting
R_S	solution resistance
Q_{dl}	constant phase element; notably, the constant phase element can also be abbreviated as CPE, which was already assigned to carbon paste electrode in this manuscript
Z_W	Warburg element
VHSV	viral hemorrhagic septicemia virus
RR	relative response
Z_{CPE}	CPE (Q_{dl}) impedance
Y_{CPE}	CPE (Q_{dl}) admittance
PBS	phosphate-buffered saline
HMGA	high-mobility group protein
TMB	3,3′,5,5′-tetramethylbenzidine
HQ	hydroquinone
CA	chronoamperometry
MMB	modified magnetic beads
FITC	fluorescein isothiocyanate
Pb-IIP	lead ion-imprinted polymer
ZIKV	Zika virus
MOF	metla-organic framework
TB	toluidine blue
CDH	triple cascade amplification system
CHA	catalytic hairpin assembly
HCR	hybridization chain reaction
MrGO	magnetic reduced graphene oxide
AuNSs	gold nanostars
AO	acridine orange
EB	ethidium bromide
SEM	scanning electron microscopy
TEM	transmission electron microscopy
FESEM	field-emission scanning electron microscopy
EDX	energy-dispersive X-ray spectroscopy
DMF	dimethylformamide
MWCNTs	multi-walled carbon nanotubes
SWCNTs	single-walled carbon nanotubes
CQDs	carbon quantum dots
LDH	layered double hydroxides
EC	electrochemical (abbreviation used only in Table 1)
PDMS	polydimethylsiloxane
MEMS	microelectromechanical systems
IVDs	in vitro diagnostic medical devices

Data availability

Data will be made available on request.

References

[1] H. Zhu, H. Zhang, Y. Xu, S. Laššáková, M. Korabečná, P. Neužil, PCR past, present and future, Biotechniques 69 (2020) 317–325, https://doi.org/10.2144/btn-2020-0057.

[2] J. Murphy, S.A. Bustin, Reliability of real-time reverse-transcription PCR in clinical diagnostics: gold standard or substandard? Expert Rev. Mol. Diagn 9 (2009) 187–197, https://doi.org/10.1586/14737159.9.2.187.

[3] D.A. Forero, Y. González-Giraldo, L.J. Castro-Vega, G.E. Barreto, qPCR-Based methods for expression analysis of miRNAs, Biotechniques 67 (2019) 192–199, https://doi.org/10.2144/btn-2019-0065.

[4] F. Postollec, H. Falentin, S. Pavan, J. Combrisson, D. Sohier, Recent advances in quantitative PCR (qPCR) applications in food microbiology, Food Microbiol. 28 (2011) 848–861, https://doi.org/10.1016/j.fm.2011.02.008.

[5] L. Becherer, N. Borst, M. Bakheit, S. Frischmann, R. Zengerle, F. von Stetten, Loop-mediated isothermal amplification (LAMP) – review and classification of methods for sequence-specific detection, Anal. Methods 12 (2020) 717–746, https://doi.org/10.1039/C9AY02246E.

[6] T.J. Moehling, G. Choi, L.C. Dugan, M. Salit, R.J. Meagher, LAMP diagnostics at the Point-of-Care: emerging trends and perspectives for the developer community, Expert Rev. Mol. Diagn 21 (2021) 43–61, https://doi.org/10.1080/14737159.2021.1873769.

[7] K. Josefsen, H. Nielsen, Northern blotting analysis, 87–105, https://doi.org/10.1007/978-1-59745-248-9_7, 2011.

[8] L.L.M. Hoopes, Nucleic acid blotting: southern and northern, Curr. Protoc. Essent. Lab Tech. 6 (2012), https://doi.org/10.1002/9780470089941.et0802s6.

[9] J.M. Levsky, R.H. Singer, Fluorescence in situ hybridization: past, present and future, J. Cell Sci. 116 (2003) 2833–2838, https://doi.org/10.1242/jcs.00633.

[10] F.R.R. Teles, L.P. Fonseca, Trends in DNA biosensors, Talanta 77 (2008) 606–623, https://doi.org/10.1016/J.TALANTA.2008.07.024.

[11] J.D. Watson, F.H.C. Crick, The structure of DNA, Cold Spring Harbor Symp. Quant. Biol. 18 (1953) 123–131, https://doi.org/10.1101/SQB.1953.018.01.020.

[12] S. Cosnier, P. Mailley, Recent advances in DNA sensors, Analyst 133 (2008) 984–991, https://doi.org/10.1039/B803083A.

[13] C.L. Manzanares-Palenzuela, B. Martín-Fernández, M. Sánchez-Paniagua López, B. López-Ruiz, Electrochemical genosensors as innovative tools for detection of genetically modified organisms, TrAC, Trends Anal. Chem. 66 (2015) 19–31, https://doi.org/10.1016/j.trac.2014.10.006.

[14] V.C. Diculescu, A.M. Chiorcea-Paquim, A.M. Oliveira-Brett, Applications of a DNA-electrochemical biosensor, TrAC, Trends Anal. Chem. 79 (2016) 23–36, https://doi.org/10.1016/J.TRAC.2016.01.019.

[15] E. Povedano, E. Vargas, V.R.-V. Montiel, R.M. Torrente-Rodríguez, M. Pedrero, R. Barderas, P.S. Segundo-Acosta, A. Peláez-García, M. Mendiola, D. Hardisson, S. Campuzano, J.M. Pingarrón, Electrochemical affinity biosensors for fast detection of gene-specific methylations with no need for bisulfite and amplification treatments, Sci. Rep. 8 (2018) 6418, https://doi.org/10.1038/s41598-018-24902-1.

[16] T.G. Drummond, M.G. Hill, J.K. Barton, Electrochemical DNA sensors, Nat. Biotechnol. 21 (2003) 1192–1199, https://doi.org/10.1038/nbt873.

[17] S. Bonaldo, L. Franchin, E. Pasqualotto, E. Cretaio, C. Losasso, A. Peruzzo, A. Paccagnella, Influence of BSA protein on electrochemical response of genosensors, IEEE Sens. J. 23 (2023) 1786–1794, https://doi.org/10.1109/JSEN.2022.3230290.

[18] R. Sánchez-Salcedo, R. Miranda-Castro, N. de-los-Santos-Álvarez, M.J. Lobo-Castañón, Dual electrochemical genosensor for early diagnosis of prostate cancer through lncRNAs detection, Biosens. Bioelectron. 192 (2021) 113520, https://doi.org/10.1016/J.BIOS.2021.113520.

[19] S. Ciftci, R. Cánovas, F. Neumann, T. Paulraj, M. Nilsson, G.A. Crespo, N. Madaboosi, The sweet detection of rolling circle amplification: Glucose-based electrochemical genosensor for the detection of viral nucleic acid, Biosens. Bioelectron. 151 (2020) 112002, https://doi.org/10.1016/J.BIOS.2019.112002.

[20] M. Khater, A. de la Escosura-Muñiz, L. Altet, A. Merkoçi, In situ plant virus nucleic acid isothermal amplification detection on gold nanoparticle-modified electrodes, Anal. Chem. 91 (2019) 4790–4796, https://doi.org/10.1021/acs.analchem.9b00340.

[21] A. Lobato, I. Konjević, S. Radišek, J. Jakše, H. Volk, M. Hermanová, M. Fojta, J. Paštika, Z. Sofer, R. Gusmão, S.B. Hočevar, N. Tasić, Label-free and sensitive detection of Citrus Bark cracking Viroid in hop using Ti3C2Tx MXene-modified genosensor, Sensor. Actuator. B Chem. 423 (2025), https://doi.org/10.1016/j.snb.2024.136762.

[22] L.S. Oliveira, K.Y.P.S. Avelino, S.R.D.E. Oliveira, N. Lucena-Silva, H.P. de Oliveira, C.A.S. Andrade, M.D.L. Oliveira, Flexible genosensors based on polypyrrole and graphene quantum dots for PML/RARα fusion gene detection: a study of acute promyelocytic leukemia in children, J. Pharm. Biomed. Anal. 235 (2023), https://doi.org/10.1016/j.jpba.2023.115606.

[23] F. Farabullini, F. Lucarelli, I. Palchetti, G. Marrazza, M. Mascini, Disposable electrochemical genosensor for the simultaneous analysis of different bacterial food contaminants, Biosens. Bioelectron. 22 (2007) 1544–1549, https://doi.org/10.1016/j.bios.2006.06.001.

[24] I. Palchetti, M. Mascini, Nucleic acid biosensors for environmental pollution monitoring, Analyst 133 (2008) 846, https://doi.org/10.1039/b802920m.

[25] P. Yáñez-Sedeño, L. Agüí, R. Villalonga, J.M. Pingarrón, Biosensors in forensic analysis. A review, Anal. Chim. Acta 823 (2014) 1–19, https://doi.org/10.1016/j.aca.2014.03.011.

[26] M. Pedrero, S. Campuzano, J.M. Pingarrón, Electrochemical genosensors based on PCR strategies for microorganisms detection and quantification, Anal. Methods 3 (2011) 780, https://doi.org/10.1039/c0ay00755b.

[27] S. Campuzano, M. Pedrero, J.M. Pingarrón, Electrochemical genosensors for the detection of cancer-related miRNAs, Anal. Bioanal. Chem. 406 (2014) 27–33, https://doi.org/10.1007/s00216-013-7459-z.

[28] H. Mohammadi, G. Yammouri, A. Amine, Current advances in electrochemical genosensors for detecting microRNA cancer markers, Curr. Opin. Electrochem. 16 (2019) 96–105, https://doi.org/10.1016/j.coelec.2019.04.030.

[29] S. Campuzano, P. Yáñez-Sedeño, J. Pingarrón, Electrochemical genosensing of circulating biomarkers, Sensors 17 (2017) 866, https://doi.org/10.3390/s17040866.

[30] S. Campuzano, V. Serafín, M. Gamella, M. Pedrero, P. Yáñez-Sedeño, J. M. Pingarrón, Opportunities, challenges, and prospects in electrochemical biosensing of circulating tumor DNA and its specific features, Sensors 19 (2019) 3762, https://doi.org/10.3390/s19173762.

[31] S. Campuzano, M. Pedrero, P. Yánez-Sedeño, J.M. Pingarrón, Advances in electrochemical (Bio)Sensing targeting epigenetic modifications of nucleic acids, Electroanalysis 31 (2019) 1816–1832, https://doi.org/10.1002/elan.201900180.
[32] E.E. Ferapontova, Hybridization biosensors relying on electrical properties of nucleic acids, Electroanalysis 29 (2017) 6–13, https://doi.org/10.1002/elan.201600593.
[33] D. Sadighbayan, K. Sadighbayan, A.Y. Khosroushahi, M. Hasanzadeh, Recent advances on the DNA-based electrochemical biosensing of cancer biomarkers: analytical approach, TrAC, Trends Anal. Chem. 119 (2019) 115609, https://doi.org/10.1016/j.trac.2019.07.020.
[34] J. Orozco, L.K. Medlin, Review: advances in electrochemical genosensors-based methods for monitoring blooms of toxic algae, Environ. Sci. Pollut. Control Ser. 20 (2013) 6838–6850, https://doi.org/10.1007/s11356-012-1258-5.
[35] M. Hasanzadeh, N. Shadjou, (Nano)-materials and methods of signal enhancement for genosensing of p53 tumor suppressor protein: novel research overview, Mater. Sci. Eng. C 76 (2017) 1424–1439, https://doi.org/10.1016/j.msec.2017.02.038.
[36] A. Babaei, A. Pouremamali, N. Rafiee, H. Sohrabi, A. Mokhtarzadeh, M. de la Guardia, Genosensors as an alternative diagnostic sensing approaches for specific detection of virus species: a review of common techniques and outcomes, TrAC, Trends Anal. Chem. 155 (2022), https://doi.org/10.1016/j.trac.2022.116686.
[37] K. Thapa, W. Liu, R. Wang, Nucleic acid-based electrochemical biosensor: recent advances in probe immobilization and signal amplification strategies, Wiley Interdiscip. Rev. Nanomed. Nanobiotechnol. 14 (2022), https://doi.org/10.1002/WNAN.1765.
[38] Y. El Goumi, Electrochemical genosensors: definition and fields of application, Int. J. Biosens. Bioelectron. 3 (2017), https://doi.org/10.15406/ijbsbe.2017.03.00080.
[39] M. Kaushik, S. Khurana, K. Mehra, N. Yadav, S. Mishra, S. Kukreti, Emerging trends in advanced nanomaterials based electrochemical genosensors, Curr. Pharm. Des. 24 (2019) 3697–3709, https://doi.org/10.2174/1381612824666181109154919.
[40] Y. Ye, S. Mao, S. He, X. Xu, X. Cao, Z. Wei, S. Gunasekaran, Ultrasensitive electrochemical genosensor for detection of CaMV35S gene with Fe3O4-Au@Ag nanoprobe, Talanta 206 (2020) 120205, https://doi.org/10.1016/j.talanta.2019.120205.
[41] K. Salimiyan Rizi, B. Hatamluyi, M. Darroudi, Z. Meshkat, E. Aryan, S. Soleimanpour, M. Rezayi, PCR-free electrochemical genosensor for Mycobacterium tuberculosis complex detection based on two-dimensional Ti3C2 Mxene-polypyrrole signal amplification, Microchem. J. 179 (2022) 107467, https://doi.org/10.1016/j.microc.2022.107467.
[42] M. Moazampour, H.R. Zare, Z. Shekari, S. Mohammad Moshtaghioun, Development of an electrochemical genosensor for quantitative determination of miR-200a based on the current response of ferrocene-functionalized graphene oxide nanosheets, Microchem. J. 185 (2023) 108202, https://doi.org/10.1016/j.microc.2022.108202.
[43] M. Kuche-Meshki, H.R. Zare, A. Akbarnia, S. Mohammad Moshtaghioun, A sensitive electrochemical genosensor for measuring gastric cancer biomarker, microRNA-106b, based on asparagine polymerization on carbon quantum dots modified electrode, Microchem. J. 191 (2023) 108846, https://doi.org/10.1016/j.microc.2023.108846.
[44] M. Chaturvedi, M. Patel, N. Bisht, Shruti, M. Das Mukherjee, A. Tiwari, D. P. Mondal, A.K. Srivastava, N. Dwivedi, C. Dhand, Reduced graphene oxide-polydopamine-gold nanoparticles: a ternary nanocomposite-based electrochemical genosensor for rapid and early Mycobacterium tuberculosis detection, Biosensors (Basel) 13 (2023) 342, https://doi.org/10.3390/bios13030342.
[45] H. Asaadi, A. vojdani, Z. Meshkat, M. Sankian, H. Farsiani, S.B. Tavakoly Sany, E. Aryan, B. Hatamluyi, Nucleic acid-functionalized nanoscale porous carbon-based electrochemical genosensor for detection of Nocardia spp. in real samples, Talanta 280 (2024) 126706, https://doi.org/10.1016/j.talanta.2024.126706.
[46] B.M. Gunasekaran, S. Srinivasan, M. Ezhilan, N. Nesakumar, Nucleic acid-based electrochemical biosensors, Clin. Chim. Acta 559 (2024) 119715, https://doi.org/10.1016/j.cca.2024.119715.
[47] P. Tahmasebi, S. Farokhi, G. Ahmadi, M. Roushani, Electrochemical impedance biosensor based on Y chromosome–specific sequences for fetal sex determination, Microchim. Acta 190 (2023) 483, https://doi.org/10.1007/s00604-023-06061-x.
[48] P. Nakowong, P. Chatchawal, T. Chaibun, N. Boonapatcharoen, C. Promptmas, W. Buajeeb, S.Y. Lee, P. Jearanaikoon, B. Lertanantawong, Detection of high-risk HPV 16 genotypes in cervical cancers using isothermal DNA amplification with electrochemical genosensor, Talanta 269 (2024) 125495, https://doi.org/10.1016/j.talanta.2023.125495.
[49] P. Sun, K. Niu, H. Du, R. Li, J. Chen, X. Lu, Ultrasensitive rapid detection of antibiotic resistance genes by electrochemical ratiometric genosensor based on 2D monolayer Ti3C2@AuNPs, Biosens. Bioelectron. 240 (2023) 115643, https://doi.org/10.1016/j.bios.2023.115643.
[50] S.L. Morais, M. Castanheira, M. Santos, V.F. Domingues, C. Delerue-Matos, M. F. Barroso, Electrochemical genosensors as a new approach to plant DNA detection and quantification for honey authentication, in: ECSA-11, MDPI, Basel Switzerland, 2024, p. 79, https://doi.org/10.3390/ecsa-11-20353.
[51] P. Sun, K. Niu, H. Du, R. Li, J. Chen, X. Lu, Sensitive electrochemical biosensor for rapid screening of tumor biomarker TP53 gene mutation Hotspot, Biosensors (Basel) 12 (2022) 658, https://doi.org/10.3390/bios12080658.
[52] N. Gopal, N. Chauhan, U. Jain, S.K. Dass, R. Chandra, Nanomaterial modified screen printed electrode based electrochemical genosensor for efficient detection of neonatal sepsis, Indian J. Microbiol. (2024), https://doi.org/10.1007/s12088-024-01348-w.
[53] X. Fuku, M.P. Bilibana, E. Iwuoha, Genosensor design and strategies towards electrochemical deoxyribonucleic acid (DNA) signal transduction: mechanism of interaction, J. Mol. Struct. 1269 (2022) 133810, https://doi.org/10.1016/j.molstruc.2022.133810.
[54] H.B. Dantas, A.G. Silva-Junior, N.L.C.L. Silva, A. Errachid, M.D.L. Oliveira, C.A. S. Andrade, Genosensor based on polypyrrole and dendrimer-coated gold nanoparticles for human papillomavirus detection, Biochem. Eng. J. 213 (2025) 109551, https://doi.org/10.1016/j.bej.2024.109551.
[55] E. Birgusova, J. Navratil, E. Dostalova, A.M. Ashrafi, Z. Bytesnikova, J. Pribyl, L. Richtera, TP53 detection based on electrochemical genosensors with different types of gold nanoparticles, Microchem. J. 209 (2025) 112856, https://doi.org/10.1016/j.microc.2025.112856.
[56] P.H.G. Guedes, J.G. Brussasco, A.C.R. Moço, D.D. Moraes, M. Segatto, J.M. R. Flauzino, A.P. Mendes-Silva, C.U. Vieira, J.M. Madurro, A.G. Brito-Madurro, A highly reusable genosensor for late-life depression diagnosis based on microRNA 184 attomolar detection in human plasma, Talanta 258 (2023) 124342, https://doi.org/10.1016/j.talanta.2023.124342.
[57] P.H.G. Guedes, J.G. Brussasco, A.C.R. Moço, D.D. Moraes, J.M.R. Flauzino, L.F. G. Luz, M.T.G. Almeida, M.M.C.N. Soares, R.J. Oliveira, J.M. Madurro, A.G. Brito-Madurro, Ninhydrin as a novel DNA hybridization indicator applied to a highly reusable electrochemical genosensor for Candida auris, Talanta 235 (2021) 122694, https://doi.org/10.1016/j.talanta.2021.122694.
[58] H. Sohrabi, M.R. Majidi, K. Asadpour-Zeynali, A. Khataee, A. Mokhtarzadeh, Bimetallic Fe/Mn MOFs/MβCD/AuNPs stabilized on MWCNTs for developing a label-free DNA-based genosensing bio-assay applied in the determination of Salmonella typhimurium in milk samples, Chemosphere 287 (2022) 132373, https://doi.org/10.1016/j.chemosphere.2021.132373.
[59] H. Sohrabi, M.R. Majidi, F. Nami, K. Asadpour-Zeynali, A. Khataee, A. Mokhtarzadeh, A novel engineered label-free Zn-based MOF/CMC/AuNPs electrochemical genosensor for highly sensitive determination of Haemophilus Influenzae in human plasma samples, Microchim. Acta 188 (2021) 100, https://doi.org/10.1007/s00604-021-04757-6.
[60] H. Sohrabi, M.R. Majidi, K. Asadpour-Zeynali, A. Khataee, A. Mokhtarzadeh, Self-assembled monolayer-assisted label-free electrochemical genosensor for specific point-of-care determination of Haemophilus influenzae, Microchim. Acta 190 (2023) 112, https://doi.org/10.1007/s00604-023-05687-1.
[61] S. Hadian-Ghazvini, F. Dashtestani, F. Hakimian, H. Ghourchian, An electrochemical genosensor for differentiation of fully methylated from fully unmethylated states of BMP3 gene, Bioelectrochemistry 142 (2021) 107924, https://doi.org/10.1016/j.bioelechem.2021.107924.
[62] K. Ondraskova, R. Sebuyoya, L. Moranova, J. Holcakova, P. Vonka, R. Hrstka, M. Bartosik, Electrochemical biosensors for analysis of DNA point mutations in cancer research, Anal. Bioanal. Chem. 415 (2023) 1065–1085, https://doi.org/10.1007/s00216-022-04388-7.
[63] K. Malecka, B. Kaur, D.A. Cristaldi, C.S. Chay, I. Mames, H. Radecka, J. Radecki, E. Stulz, Silver or gold? A comparison of nanoparticle modified electrochemical genosensors based on cobalt porphyrin-DNA, Bioelectrochemistry 138 (2021) 107723, https://doi.org/10.1016/j.bioelechem.2020.107723.
[64] M.S.M.L. Oliveira, R.P.S. Lucena, A.G. Silva-Júnior, F.L. Melo, B.M. Silva, E.C. S. Gomes, C.A.S. Andrade, M.D.L. Oliveira, A simple electrochemical genosensor based on polythiophene acetic acid film for detection of Schistosoma mansoni, Biotechnol. Prog. 41 (2025), https://doi.org/10.1002/btpr.70048.
[65] F. Ansah, F. Krampa, J.K. Donkor, C. Owusu-Appiah, S. Ashitei, V.E. Kornu, R. K. Danku, J.D. Chirawurah, G.A. Awandare, Y. Aniweh, P. Kanyong, Ultrasensitive electrochemical genosensors for species-specific diagnosis of malaria, Electrochim. Acta 429 (2022) 140988, https://doi.org/10.1016/j.electacta.2022.140988.
[66] A.G. Crevillen, C.C. Mayorga-Martinez, J.V. Vaghasiya, M. Pumera, 3D-Printed SARS-CoV-2 RNA genosensing microfluidic System, Adv. Mater. Technol. 7 (2022), https://doi.org/10.1002/admt.202101121.
[67] M. Fojta Jyoti, M. Hermanová, H. Pivoňková, O. Alduhaish, M. Pumera, Genosensing on a 3D-printed nanocarbon electrode, Electrochem. Commun. 151 (2023) 107508, https://doi.org/10.1016/j.elecom.2023.107508.
[68] A. Bishoyi, MdA. Alam, MohdR. Hasan, M. Khanuja, R. Pilloton, J. Narang, Cyclic voltammetric-paper-based genosensor for detection of the target DNA of zika virus, Micromachines 13 (2022) 2037, https://doi.org/10.3390/mi13122037.
[69] G. Moattari, Z. Izadi, M. Shakhsi-Niaei, Development of an electrochemical genosensor for detection of viral hemorrhagic septicemia virus (VHSV) using glycoprotein (G) gene probe, Aquaculture 536 (2021) 736451, https://doi.org/10.1016/j.aquaculture.2021.736451.
[70] E. Kivrak, T. Pauzaite, N. Copeland, J. Hardy, P. Kara, M. Firlak, A. Yardimci, S. Yilmaz, F. Palaz, M. Ozsoz, Detection of CRISPR-Cas9-Mediated mutations using a carbon nanotube-modified electrochemical genosensor, Biosensors (Basel) 11 (2021) 17, https://doi.org/10.3390/bios11010017.
[71] V.P. Egorova, H.V. Grushevskaya, N.G. Krylova, E.V. Vaskovtsev, A.S. Babenka, I. V. Anufreyonak, S.Yu Smirnov, G.G. Krylov, High-sensitivity label-free electrochemical genosensors for carbon nanotube plasmon-assisted detection of somatic mutations in nucleic acids from formalin-fixed paraffin-embedded tissues, Microchem. J. 208 (2025) 112234, https://doi.org/10.1016/j.microc.2024.112234.
[72] M. Shamsipur, L. Samandari, L. Farzin, A. Besharati-Seidani, Development of an ultrasensitive electrochemical genosensor for detection of HIV-1 pol gene using a gold nanoparticles coated carbon paste electrode impregnated with lead ion-

imprinted polymer nanomaterials as a novel electrochemical probe, Microchem. J. 160 (2021) 105714, https://doi.org/10.1016/j.microc.2020.105714.
[73] P. Malla, C.-H. Liu, W.-C. Wu, P. Kabinsing, P. Sreearunothai, Synthesis and characterization of Au-decorated graphene oxide nanocomposite for magneto-electrochemical detection of SARS-CoV-2 nucleocapsid gene, Talanta 262 (2023) 124701, https://doi.org/10.1016/j.talanta.2023.124701.
[74] K. Malecka-Baturo, I. Grabowska, Efficiency of electrochemical immuno- vs. apta (geno)sensors for multiple cancer biomarkers detection, Talanta 281 (2025) 126870, https://doi.org/10.1016/j.talanta.2024.126870.
[75] L.L. Tan, D. Futra, L.Y. Heng, A. Ulianas, A.A.A. Kadir, Z. Ishak, Voltammetric genosensor from silica nanocomposites for transgenic soybean analysis, J. Food Compos. Anal. 140 (2025) 107277, https://doi.org/10.1016/j.jfca.2025.107277.
[76] P. Kabinsing, P. Malla, C.-H. Liu, W.-C. Wu, P. Sreearunothai, Magnetic graphene oxide nanocomposite as dual-mode genosensor for ultrasensitive detection of oncogenic microRNA, Microchem. J. 191 (2023) 108775, https://doi.org/10.1016/j.microc.2023.108775.
[77] S. Ciftci, R. Cánovas, F. Neumann, T. Paulraj, M. Nilsson, G.A. Crespo, N. Madaboosi, The sweet detection of rolling circle amplification: glucose-based electrochemical genosensor for the detection of viral nucleic acid, Biosens. Bioelectron. 151 (2020) 112002, https://doi.org/10.1016/j.bios.2019.112002.
[78] A. Ben Aissa, N. Madaboosi, M. Nilsson, M.I. Pividori, Electrochemical genosensing of E. coli based on padlock probes and rolling circle amplification, Sensors 21 (2021) 1749, https://doi.org/10.3390/s21051749.
[79] V. Krishnan, G.R. Pandey, K.A. Babu, S. Paramasivam, S.S. Kumar, S. Balasubramanian, V. Ravichandiran, G.P. Pazhani, M. Veerapandian, Chitosan grafted butein: a metal-free transducer for electrochemical genosensing of exosomal CD24, Carbohydr. Polym. 269 (2021) 118333, https://doi.org/10.1016/j.carbpol.2021.118333.
[80] J.M.R. Flauzino, E.P. Nguyen, Q. Yang, G. Rosati, D. Panáček, A.G. Brito-Madurro, J.M. Madurro, A. Bakandritsos, M. Otyepka, A. Merkoçi, Label-free and reagentless electrochemical genosensor based on graphene acid for meat adulteration detection, Biosens. Bioelectron. 195 (2022) 113628, https://doi.org/10.1016/j.bios.2021.113628.
[81] S.L. Morais, J.M.C.S. Magalhães, V.F. Domingues, C. Delerue-Matos, J. Ramos-Jesus, H. Ferreira-Fernandes, G.R. Pinto, M. Santos, M.F. Barroso, Development of an electrochemical DNA-based biosensor for the detection of the cardiovascular pharmacogenetic-altering SNP CYP2C9*3, Talanta 264 (2023) 124692, https://doi.org/10.1016/j.talanta.2023.124692.
[82] S. Cajigas, D. Alzate, M. Fernández, C. Muskus, J. Orozco, Electrochemical genosensor for the specific detection of SARS-CoV-2, Talanta 245 (2022) 123482, https://doi.org/10.1016/j.talanta.2022.123482.
[83] D. Alzate, M.C. Lopez-Osorio, F. Cortés-Mancera, M.-C. Navas, J. Orozco, Detection of hepatitis E virus genotype 3 in wastewater by an electrochemical genosensor, Anal. Chim. Acta 1221 (2022) 340121, https://doi.org/10.1016/j.aca.2022.340121.
[84] L.F. Garcia-Melo, N.A. Chagoya Pio, M. Morales-Rodríguez, E. Madrigal-Bujaidar, E.O. Madrigal-Santillán, I. Álvarez-González, R.N. Pineda Cruces, N. Batina, Detection of the p53 gene mutation using an ultra-sensitive and highly selective electrochemical DNA biosensor, J. Mex. Chem. Soc. 67 (2023) 33–45, https://doi.org/10.29356/jmcs.v67i1.1880.
[85] L.F. Garcia-Melo, M. Morales-Rodríguez, E. Madrigal-Bujaidar, E.O. Madrigal-Santillán, J.A. Morales-González, R.N. Pineda Cruces, J.A. Campoy Ramírez, P. Damian-Matsumura, A. Tellez-Plancarte, N. Batina, I. Álvarez-González, Development of a nanostructured electrochemical genosensor for the detection of the K-ras gene, J. Anal. Methods Chem. 2022 (2022) 1–12, https://doi.org/10.1155/2022/6575140.
[86] L.F. Garcia-Melo, N.A. Chagoya Pio, J.A. Campoy Ramírez, E. Madrigal-Bujaidar, I. Álvarez-González, J.A. Morales-González, E.O. Madrigal-Santillán, N. Batina, Development of the BAT-26 mutation-based electrochemical genosensor for identifying microsatellite instability in relationship to cancer, Sens. Biosens. Res. 44 (2024) 100651, https://doi.org/10.1016/j.sbsr.2024.100651.
[87] M. Mokni, A. Tlili, Y. Khalij, G. Attia, C. Zerrouki, W. Hmida, A. Othmane, A. Bouslama, A. Omezzine, N. Fourati, Designing a simple electrochemical genosensor for the detection of urinary PCA3, a prostate cancer biomarker, Micromachines 15 (2024) 602, https://doi.org/10.3390/mi15050602.
[88] R. Sánchez-Salcedo, R. Miranda-Castro, N. de-los-Santos-Álvarez, D. Fernández-Martínez, L.J. García-Flórez, M.J. Lobo-Castañón, An electrochemical genosensing platform for the relative quantification of the circulating long noncoding RNA CCAT1 to aid in the diagnosis of colorectal cancer, Sensor. Actuator. B Chem. 376 (2023) 132940, https://doi.org/10.1016/j.snb.2022.132940.
[89] R. Sánchez-Salcedo, R. Miranda-Castro, N. de-los-Santos-Álvarez, M.J. Lobo-Castañón, Dual electrochemical genosensor for early diagnosis of prostate cancer through lncRNAs detection, Biosens. Bioelectron. 192 (2021) 113520, https://doi.org/10.1016/j.bios.2021.113520.
[90] M. Sánchez-Paniagua, S. Palenzuela-Batista, C.L. Manzanares-Palenzuela, B. López-Ruiz, Electrochemical genosensor for Klotho detection based on aliphatic and aromatic thiols self-assembled monolayers, Talanta 212 (2020) 120735, https://doi.org/10.1016/j.talanta.2020.120735.
[91] A. Pallares-Rusiñol, S.L. Moura, M. Martí, M.I. Pividori, Electrochemical genosensing of overexpressed GAPDH transcripts in breast cancer exosomes, Anal. Chem. 95 (2023) 2487–2495, https://doi.org/10.1021/acs.analchem.2c04773.
[92] S. Bunyarataphan, T. Prammananan, PCR-Free self-calibrated ratiometric electrochemical genosensor utilizing a dual-signal amplification approach for genomic detection of Mycobacterium tuberculosis, J. Electrochem. Soc. 172 (2025) 017520, https://doi.org/10.1149/1945-7111/adacb1.
[93] W. Jaroenram, J. Kampeera, N. Arunrut, C. Karuwan, A. Sappat, P. Khumwan, S. Jaitrong, K. Boonnak, T. Prammananan, A. Chaiprasert, A. Tuantranont, W. Kiatpathomchai, Graphene-based electrochemical genosensor incorporated loop-mediated isothermal amplification for rapid on-site detection of Mycobacterium tuberculosis, J. Pharm. Biomed. Anal. 186 (2020) 113333, https://doi.org/10.1016/j.jpba.2020.113333.
[94] N. Razmi, M. Hasanzadeh, M. Willander, O. Nur, Electrochemical genosensor based on gold nanostars for the detection of *Escherichia coli* O157:H7 DNA, Anal. Methods 14 (2022) 1562–1570, https://doi.org/10.1039/D2AY00056C.
[95] J.B. Sousa, J. Ramos-Jesus, L.C. Silva, C. Pereira, N. de-los-Santos-Álvarez, R.A. S. Fonseca, R. Miranda-Castro, C. Delerue-Matos, J.R. Santos Júnior, M. F. Barroso, Fe3O4@Au nanoparticles-based magnetoplatform for the HMGA maize endogenous gene electrochemical genosensing, Talanta 206 (2020) 120220, https://doi.org/10.1016/j.talanta.2019.120220.
[96] N. Shishegari, A. Tadjarodi, E. Omidinia, An electrochemical nano-genosensor for SARS-CoV-2 detection utilizing Ce-metal organic framework, dendritic palladium nano-structure, and sulfur-doped graphene oxide, Talanta 287 (2025) 127662, https://doi.org/10.1016/j.talanta.2025.127662.
[97] M. Heidari, A. Ghaffarinejad, E. Omidinia, Screening of hepatitis B virus DNA in the serum sample by a new sensitive electrochemical genosensor-based Pd-Al LDH substrate, J. Solid State Electrochem. 26 (2022) 1445–1454, https://doi.org/10.1007/s10008-022-05176-0.
[98] V. Khazaei, S. Javani, M. Golalipour, M. Sheikharabi, M. Arefi, S. Mirmohammadi, H. Shahbazmohammadi, A. Kianmehr, An ultrasensitive microRNA-21 electrochemical nano-genosensor for early detection of colorectal cancer, Int. J. Electrochem. Sci. 20 (2025) 101152, https://doi.org/10.1016/j.ijoes.2025.101152.
[99] S. Fortunati, C. Giliberti, M. Giannetto, A. Bertucci, S. Capodaglio, E. Ricciardi, P. Giacomini, V. Bianchi, A. Boni, I. De Munari, R. Corradini, M. Careri, A highly sensitive electrochemical magneto-genosensing assay for the specific detection of a single nucleotide variation in the KRAS oncogene in human plasma, Biosens. Bioelectron. X 15 (2023) 100404, https://doi.org/10.1016/j.biosx.2023.100404.
[100] A. Aldea, M. Onea, E. Matei, N. Apostol, D. Botta, I. Enculescu, V.C. Diculescu, Phosphorothioated oligonucleotides on gold-coated electrospun polymeric fibers for electrochemical genosensors, Electrochim. Acta 524 (2025) 146006, https://doi.org/10.1016/j.electacta.2025.146006.
[101] G. Wang, S. Xu, Y. Feng, L. Huang, Y. Wang, N. Liu, Dual-functionalized glass micropipette sensor for simultaneous high sensitivity detection of cancer biomarkers, ACS Appl. Mater. Interfaces 17 (2025) 20717–20725, https://doi.org/10.1021/acsami.4c22311.
[102] K. Kerman, Y. Morita, Y. Takamura, E. Tamiya, Label-free electrochemical detection of DNA hybridization on gold electrode, Electrochem. Commun. 5 (2003) 887–891, https://doi.org/10.1016/j.elecom.2003.08.013.
[103] M. Pasta, F. La Mantia, Y. Cui, A new approach to glucose sensing at gold electrodes, Electrochem. Commun. 12 (2010) 1407–1410, https://doi.org/10.1016/j.elecom.2010.07.033.
[104] S.N. Topkaya, M. Azimzadeh, M. Ozsoz, Electrochemical biosensors for cancer biomarkers detection: recent advances and challenges, Electroanalysis 28 (2016) 1402–1419, https://doi.org/10.1002/elan.201501174.
[105] M. Fiałek, M. Grabarczyk, Application of an 800 gold microelectrode array for rapid voltammetric detection of nitrite pollution in environmental waters, J. Electrochem. Soc. 171 (2024) 117517, https://doi.org/10.1149/1945-7111/ad9062.
[106] C. Wang, C. Yu, Detection of chemical pollutants in water using gold nanoparticles as sensors: a review, Rev. Anal. Chem. 32 (2013) 1–14, https://doi.org/10.1515/revac-2012-0023.
[107] B. Uslu, S. Ozkan, Solid electrodes in electroanalytical chemistry: present applications and prospects for high throughput screening of drug compounds, Comb. Chem. High Throughput Screen. 10 (2007) 495–513, https://doi.org/10.2174/138620707782152425.
[108] J. Hedlund, A. Lundgren, B. Lundgren, H. Elwing, A new compact electrochemical method for analyzing complex protein films adsorbed on the surface of modified interdigitated gold electrodes, Sensor. Actuator. B Chem. 142 (2009) 494–501, https://doi.org/10.1016/j.snb.2009.08.037.
[109] W.E. Van der Linden, J.W. Dieker, Glassy carbon as electrode material in electro-analytical chemistry, Anal. Chim. Acta 119 (1980) 1–24, https://doi.org/10.1016/S0003-2670(00)00025-8.
[110] H. Wang, M. La Russa, L.S. Qi, CRISPR/Cas9 in genome editing and beyond, Annu. Rev. Biochem. 85 (2016) 227–264, https://doi.org/10.1146/annurev-biochem-060815-014607.
[111] W.S. Hummers, R.E. Offeman, Preparation of graphitic oxide, J. Am. Chem. Soc. 80 (1958) 1339, https://doi.org/10.1021/ja01539a017, 1339.
[112] R.G. Morris, M.J. Arends, P.E. Bishop, K. Sizer, E. Duvall, C.C. Bird, Sensitivity of digoxigenin and biotin labelled probes for detection of human papillomavirus by in situ hybridisation, J. Clin. Pathol. 43 (1990) 800–805, https://doi.org/10.1136/jcp.43.10.800.
[113] S.B. Hočevar, I. Švancara, K. Vytřas, B. Ogorevc, Novel electrode for electrochemical stripping analysis based on carbon paste modified with bismuth powder, Electrochim. Acta 51 (2005) 706–710, https://doi.org/10.1016/j.electacta.2005.05.023.
[114] T. Mutić, D. Stanković, D. Manojlović, D. Petrić, F. Pastor, V.V. Avdin, M. Ognjanović, V. Stanković, Micromolar levofloxacin sensor by incorporating highly crystalline Co3O4 into a carbon paste electrode structure, Electrochem 5 (2024) 45–56, https://doi.org/10.3390/electrochem5010003.

[115] V. Stanković, S. Đurđić, M. Ognjanović, G. Zlatić, D. Stanković, Triangle-shaped cerium tungstate nanoparticles used to modify carbon paste electrode for sensitive hydroquinone detection in water samples, Sensors 24 (2024) 705, https://doi.org/10.3390/s24020705.
[116] I. Švancara, K. Vytřas, K. Kalcher, A. Walcarius, J. Wang, Carbon paste electrodes in facts, numbers, and notes: a review on the occasion of the 50-Years jubilee of carbon paste in electrochemistry and electroanalysis, Electroanalysis 21 (2009) 7–28, https://doi.org/10.1002/elan.200804340.
[117] A. Javed, S.R. Abbas, M.U. Hashmi, N.U.A. Babar, I. Hussain, Graphene oxide based electrochemical genosensor for label free detection of Mycobacterium tuberculosis from raw clinical samples, Int. J. Nanomed. 16 (2021) 7339–7352, https://doi.org/10.2147/IJN.S326480.
[118] N. Tasić, A. Bezerra Martins, X. Yifei, M. Sousa Góes, D. Martín-Yerga, L. Mao, T. R.L.C. Paixão, L. Moreira Gonçalves, Insights into electrochemical behavior in laser-scribed electrochemical paper-based analytical devices, Electrochem. Commun. 121 (2020), https://doi.org/10.1016/j.elecom.2020.106872.
[119] V.N. Ataide, L.F. Mendes, L.I.L.M. Gama, W.R. de Araujo, T.R.L.C. Paixão, Electrochemical paper-based analytical devices: ten years of development, Anal. Methods 12 (2020) 1030–1054, https://doi.org/10.1039/C9AY02350J.
[120] C. Desmet, C.A. Marquette, L.J. Blum, B. Doumèche, Paper electrodes for bioelectrochemistry: biosensors and biofuel cells, Biosens. Bioelectron. 76 (2016) 145–163, https://doi.org/10.1016/j.bios.2015.06.052.
[121] J. Zhan, F. Wang, Y. Li, J. Li, S. Xiang, Y. Yang, K. Chen, H. Yang, R. Cai, A triple signal amplification strategy for accurate and ultrasensitive miRNA-21 detection, Anal. Chem. 96 (2024) 14464–14470, https://doi.org/10.1021/acs.analchem.4c02355.
[122] D. Bizzotto, I.J. Burgess, T. Doneux, T. Sagara, H.Z. Yu, Beyond simple cartoons: challenges in characterizing electrochemical biosensor interfaces, ACS Sens. 3 (2018) 5–12, https://doi.org/10.1021/acssensors.7b00840.
[123] J.I.A. Rashid, N.A. Yusof, The strategies of DNA immobilization and hybridization detection mechanism in the construction of electrochemical DNA sensor: a review, Sens. Biosens. Res. 16 (2017) 19–31, https://doi.org/10.1016/j.sbsr.2017.09.001.
[124] M.I. Pividori, A. Merkoçi, S. Alegret, Electrochemical genosensor design: immobilisation of oligonucleotides onto transducer surfaces and detection methods, Biosens. Bioelectron. 15 (2000) 291–303, https://doi.org/10.1016/S0956-5663(00)00071-3.
[125] M. Pividori, Electrochemical genosensor design: immobilisation of oligonucleotides onto transducer surfaces and detection methods, Biosens. Bioelectron. 15 (2000) 291–303, https://doi.org/10.1016/S0956-5663(00)00071-3.
[126] R. Caldevilla, S. Morais, S. Carvalho, R. Medeiros, C. Delerue-Matos, A. Cruz, M. Santos, M.F. Barroso, Design of an electrochemical genosensor for BDNF gene polymorphism sequence detection using an enzymatically labeled DNA probe, in: CSAC 2023, MDPI, Basel Switzerland, 2023, p. 39, https://doi.org/10.3390/CSAC2023-14913.
[127] N. Ibrahim, K.B. Gan, N.Y. Mohd Yusof, C.T. Goh, N. Krupa B, L.L. Tan, Electrochemical genosensor based on RNA-Responsive human telomeric G-quadruplex DNA: a proof-of-concept with SARS-CoV-2 RNA, Talanta 274 (2024) 125916, https://doi.org/10.1016/j.talanta.2024.125916.
[128] W.-W. Zhao, J.-J. Xu, H.-Y. Chen, Photoelectrochemical DNA biosensors, Chem. Rev. 114 (2014) 7421–7441, https://doi.org/10.1021/cr500100j.
[129] J.I.A. Rashid, N.A. Yusof, The strategies of DNA immobilization and hybridization detection mechanism in the construction of electrochemical DNA sensor: a review, Sens. Biosens. Res. 16 (2017) 19–31, https://doi.org/10.1016/J.SBSR.2017.09.001.
[130] M. Chahma, C. Carruthers, Electrochemical detection of oligonucleotides using polypyrroles, Sens. Acutators Rep. 3 (2021) 100039, https://doi.org/10.1016/J.SNR.2021.100039.
[131] D. Futra, L.L. Tan, S.Y. Lee, B. Lertanantawong, L.Y. Heng, An ultrasensitive voltammetric genosensor for the detection of bacteria Vibrio cholerae in vegetable and environmental water samples, Biosensors (Basel) 13 (2023), https://doi.org/10.3390/bios13060616.
[132] M.L. Bochman, K. Paeschke, V.A. Zakian, DNA secondary structures: stability and function of G-quadruplex structures, Nat. Rev. Genet. 13 (2012) 770–780, https://doi.org/10.1038/nrg3296.
[133] D. Voccia, M. Sosnowska, F. Bettazzi, G. Roscigno, E. Fratini, V. De Franciscis, G. Condorelli, R. Chitta, F. D'Souza, W. Kutner, I. Palchetti, Direct determination of small RNAs using a biotinylated polythiophene impedimetric genosensor, Biosens. Bioelectron. 87 (2017) 1012–1019, https://doi.org/10.1016/J.BIOS.2016.09.058.
[134] C.M. Dundas, D. Demonte, S. Park, Streptavidin–biotin technology: improvements and innovations in chemical and biological applications, Appl. Microbiol. Biotechnol. 97 (2013) 9343–9353, https://doi.org/10.1007/s00253-013-5232-z.
[135] M. Ortiz, M. Torréns, N. Canela, A. Fragoso, C.K. O'Sullivan, Supramolecular confinement of polymeric electron transfer mediator on gold surface for picomolar detection of DNA, Soft Matter 7 (2011) 10925–10930, https://doi.org/10.1039/c1sm06300f.
[136] T. Chaibun, P. Thanasapburachot, P. Chatchawal, L. Su Yin, S. Jiaranuchart, P. Jearanaikoon, C. Promptmas, W. Buajeeb, B. Lertanantawong, A multianalyte electrochemical genosensor for the detection of high-risk HPV genotypes in oral and cervical cancers, Biosensors (Basel) 12 (2022) 290, https://doi.org/10.3390/bios12050290.
[137] H. Pei, N. Lu, Y. Wen, S. Song, Y. Liu, H. Yan, C. Fan, A DNA nanostructure-based biomolecular probe carrier platform for electrochemical biosensing, Adv. Mater. 22 (2010) 4754–4758, https://doi.org/10.1002/ADMA.201002767.
[138] M. Eskandari, F. Faridbod, A sensitive electrochemical genosensor for the detection of p53, a tumor suppressor gene using A simple method for tag-free ssDNA immobilization based on Ceria nanoparticles, Anal. Bioanal. Electrochem. 16 (2024) 344–359, https://doi.org/10.22034/abec.2024.712922.
[139] W. Choi, H.-C. Shin, J.M. Kim, J.-Y. Choi, W.-S. Yoon, Modeling and applications of Electrochemical Impedance Spectroscopy (EIS) for lithium-ion batteries, J. Electrochem. Sci. Technol. 11 (2020) 1–13, https://doi.org/10.33961/jecst.2019.00528.
[140] M. Zunic, L. Chevallier, E. Di Bartolomeo, A. D'Epifanio, S. Licoccia, E. Traversa, Anode supported protonic solid oxide fuel cells fabricated using electrophoretic deposition, Fuel Cells 11 (2011) 165–171, https://doi.org/10.1002/fuce.200900104.
[141] N. Tasic, Z. Marinkovic-Stanojevic, Z. Brankovic, M. Zunic, U. Lacnjevac, M. Gilic, T. Novakovic, G. Brankovic, Mesoporous TiO2 spheres as a photoanodic material in dye-sensitized solar cells, Process. Appl. Ceram. 12 (2018) 374–382, https://doi.org/10.2298/PAC1804374T.
[142] G. Šekularac, I. Milošev, Electrochemical behavior and self-sealing ability of zirconium conversion coating applied on aluminum alloy 3005 in 0.5 M NaCl solution, J. Electrochem. Soc. 167 (2020) 021509, https://doi.org/10.1149/1945-7111/ab6b0d.
[143] Y. Hamlaoui, F. Pedraza, L. Tifouti, Corrosion monitoring of galvanised coatings through electrochemical impedance spectroscopy, Corros. Sci. 50 (2008) 1558–1566, https://doi.org/10.1016/j.corsci.2008.02.010.
[144] R. Kötz, M. Hahn, R. Gallay, Temperature behavior and impedance fundamentals of supercapacitors, J. Power Sources 154 (2006) 550–555, https://doi.org/10.1016/j.jpowsour.2005.10.048.
[145] M. Smiljanić, S. Panić, M. Bele, F. Ruiz-Zepeda, L. Pavko, L. Gašparič, A. Kokalj, M. Gaberšček, N. Hodnik, Improving the HER activity and stability of Pt nanoparticles by titanium oxynitride support, ACS Catal. 12 (2022) 13021–13033, https://doi.org/10.1021/acscatal.2c03214.
[146] G. Bolat, J. Izquierdo, D. Mareci, D. Sutiman, R.M. Souto, Electrochemical characterization of ZrTi alloys for biomedical applications. Part 2: the effect of thermal oxidation, Electrochim. Acta 106 (2013) 432–439, https://doi.org/10.1016/j.electacta.2013.05.093.
[147] M. Grossi, B. Riccò, Electrical impedance spectroscopy (EIS) for biological analysis and food characterization: a review, J. Sens. Sens. Syst. 6 (2017) 303–325, https://doi.org/10.5194/jsss-6-303-2017.
[148] J. Hu, Oxygen evolution reaction on IrO2-based DSA® type electrodes: kinetics analysis of Tafel lines and EIS, Int. J. Hydrogen Energy 29 (2004) 791–797, https://doi.org/10.1016/j.ijhydene.2003.09.007.
[149] MdM. Ahmed, R. Zhao, J. Du, J. Li, Review—nanostructural ZnO-Based electrochemical sensor for environmental application, J. Electrochem. Soc. 169 (2022) 020573, https://doi.org/10.1149/1945-7111/ac534d.
[150] P. Jolly, P. Zhurauski, J.L. Hammond, A. Miodek, S. Liébana, T. Bertok, J. Tkáč, P. Estrela, Self-assembled gold nanoparticles for impedimetric and amperometric detection of a prostate cancer biomarker, Sensor. Actuator. B Chem. 251 (2017) 637–643, https://doi.org/10.1016/j.snb.2017.05.040.
[151] A. Bogomolova, E. Komarova, K. Reber, T. Gerasimov, O. Yavuz, S. Bhatt, M. Aldissi, Challenges of electrochemical impedance spectroscopy in protein biosensing, Anal. Chem. 81 (2009) 3944–3949, https://doi.org/10.1021/ac9002358.
[152] J.M.R. Flauzino, E.L. Pimentel, L.M. Alves, J.M. Madurro, A.G. Brito-Madurro, A novel and reusable electrochemical genosensor for detection of beef adulteration, Electroanalysis 33 (2021) 296–303, https://doi.org/10.1002/elan.202060029.
[153] S.M. Gateman, O. Gharbi, H. Gomes de Melo, K. Ngo, M. Turmine, V. Vivier, On the use of a constant phase element (CPE) in electrochemistry, Curr. Opin. Electrochem. 36 (2022) 101133, https://doi.org/10.1016/j.coelec.2022.101133.
[154] M.M. Patrick, J.M. Grillot, Z.M. Derden, D.W. Paul, Long–term drifts in sensitivity caused by biofouling of an amperometric oxygen sensor, Electroanalysis 29 (2017) 998–1005, https://doi.org/10.1002/elan.201600653.
[155] B.L. Hanssen, S. Siraj, D.K.Y. Wong, Recent strategies to minimise fouling in electrochemical detection systems, Rev. Anal. Chem. 35 (2016) 1–28, https://doi.org/10.1515/revac-2015-0008.
[156] P. Bollella, L. Gorton, Enzyme based amperometric biosensors, Curr. Opin. Electrochem. 10 (2018) 157–173, https://doi.org/10.1016/j.coelec.2018.06.003.
[157] S.L. Morais, P. Barros, M. Santos, C. Delerue-Matos, A.C. Gomes, M. Fátima Barroso, Electrochemical genosensor for the detection of Alexandrium minutum dinoflagellates, Talanta 222 (2021) 121416, https://doi.org/10.1016/j.talanta.2020.121416.
[158] A. Frey, B. Meckelein, D. Externest, M.A. Schmidt, A stable and highly sensitive 3,3′,5,5′-tetramethylbenzidine-based substrate reagent for enzyme-linked immunosorbent assays, J. Immunol. Methods 233 (2000) 47–56, https://doi.org/10.1016/S0022-1759(99)00166-0.
[159] B.H. Northrop, S.H. Frayne, U. Choudhary, Thiol–maleimide "click" chemistry: evaluating the influence of solvent, initiator, and thiol on the reaction mechanism, kinetics, and selectivity, Polym. Chem. 6 (2015) 3415–3430, https://doi.org/10.1039/C5PY00168D.
[160] T. Barbosa, S.L. Morais, E. Pereira, J.M.C.S. Magalhães, V.F. Domingues, H. Ferreira-Fernandes, G. Pinto, M. Santos, M.F. Barroso, Warfarin pharmacogenomics: designing electrochemical DNA-based sensors to detect CYP2C9*2 gene variation, Genes 16 (2025) 372, https://doi.org/10.3390/genes16040372.
[161] T. Barbosa, S.L. Morais, R. Carvalho, J.M.C.S. Magalhães, V.F. Domingues, C. Delerue-Matos, H. Ferreira-Fernandes, G.R. Pinto, M. Santos, M.F. Barroso, Vitamin K epoxide Reductase Complex (VKORC1) electrochemical genosensors:

towards the identification of 1639 G>A genetic polymorphism, Chemosensors 13 (2025) 248, https://doi.org/10.3390/chemosensors13070248.
[162] X. Wang, W.-W. Liu, L.-L. Long, S.-Y. Tan, Y.-Q. Chai, R. Yuan, Ultrasensitive electrochemical biosensor with powerful triple Cascade signal amplification for detection of MicroRNA, Anal. Chem. 96 (2024) 15066–15073, https://doi.org/10.1021/acs.analchem.4c03766.
[163] P. Shunmugam, N. Ahmed, K.K.B. Singh, ipaH-Targeted electrochemical genosensor: a fast and reliable diagnostic approach for simultaneous detection of Shigella species and enteroinvasive Escherichia coli, Microchem. J. 216 (2025) 114794, https://doi.org/10.1016/j.microc.2025.114794.
[164] D. Obrez, M. Kolar, N. Tasić, S.B. Hočevar, Study of different types of copper electrodes for anodic stripping voltammetric detection of trace metal ions, Electrochim. Acta 457 (2023) 142480, https://doi.org/10.1016/j.electacta.2023.142480.
[165] J. Wang, S.B. Hocevar, R.P. Deo, B. Ogorevc, Carbon-fiber microsensor for in vivo monitoring of trace zinc(II) based on electrochemical stripping analysis, Electrochem. Commun. 3 (2001) 352–356, https://doi.org/10.1016/S1388-2481(01)00175-8.
[166] R. Šelešovská, K. Schwarzová-Pecková, R. Sokolová, K. Krejčová, P. Martinková-Kelíšková, The first study of triazole fungicide difenoconazole oxidation and its voltammetric and flow amperometric detection on boron doped diamond electrode, Electrochim. Acta 381 (2021) 138260, https://doi.org/10.1016/j.electacta.2021.138260.
[167] B. Šljukić, C.E. Banks, C. Salter, A. Crossley, R.G. Compton, Electrochemically polymerised composites of multi-walled carbon nanotubes and poly (vinylferrocene) and their use as modified electrodes: application to glucose sensing, Analyst 131 (2006) 670–677, https://doi.org/10.1039/B601299J.
[168] F. Cui, Z. Zhou, H.S. Zhou, Review—Measurement and analysis of cancer biomarkers based on electrochemical biosensors, J. Electrochem. Soc. 167 (2020) 037525, https://doi.org/10.1149/2.0252003JES.
[169] A. Cranny, N.R. Harris, M. Nie, J.A. Wharton, R.J.K. Wood, K.R. Stokes, Sensors for corrosion detection: measurement of copper ions in 3.5% sodium chloride using screen-printed platinum electrodes, IEEE Sens. J. 12 (2012) 2091–2099, https://doi.org/10.1109/JSEN.2012.2183867.
[170] J. Isailović, A. Oberlintner, U. Novak, M. Finšgar, F.M. Oliveira, J. Paštika, Z. Sofer, N. Tasić, R. Gusmão, S.B. Hočevar, Study of chitosan-stabilized Ti 3 C 2 T x MXene for ultrasensitive and Interference-Free Detection of Gaseous H 2 O 2, ACS Appl. Mater. Interfaces 15 (2023) 31643–31651, https://doi.org/10.1021/acsami.3c05314.
[171] J. Wang, Electrochemical sensing of explosives, Electroanalysis 19 (2007) 415–423, https://doi.org/10.1002/elan.200603748.
[172] N. Elgrishi, K.J. Rountree, B.D. McCarthy, E.S. Rountree, T.T. Eisenhart, J. L. Dempsey, A practical beginner's guide to cyclic voltammetry, J. Chem. Educ. 95 (2018) 197–206, https://doi.org/10.1021/acs.jchemed.7b00361.
[173] D. Astruc, Why is ferrocene so Exceptional? Eur. J. Inorg. Chem. 2017 (2017) 6–29, https://doi.org/10.1002/ejic.201600983.
[174] A.J. Bard, L.R. Faulkner, Electrochemical Methods : Fundamentals and Applications, John Wiley & Sons, Inc., 2001.
[175] V. Mirceski, S. Skrzypek, L. Stojanov, Square-wave voltammetry, Chem. Texts 4 (2018) 17, https://doi.org/10.1007/s40828-018-0073-0.
[176] B. Kashyap, R. Kumar, A novel multi-set differential pulse voltammetry technique for improving precision in electrochemical sensing, Biosens. Bioelectron. 216 (2022) 114628, https://doi.org/10.1016/j.bios.2022.114628.
[177] P.M. Kalligosfyri, W. Cimmino, N. Normanno, S. Cinti, Enzyme-Assisted electrochemical point-of-care test for miRNA detection in liquid biopsy, Anal. Chem. 96 (2024) 19202–19206, https://doi.org/10.1021/acs.analchem.4c04127.
[178] C. Zhu, G. Yang, H. Li, D. Du, Y. Lin, Electrochemical sensors and biosensors based on nanomaterials and nanostructures, Anal. Chem. 87 (2014) 230–249, https://doi.org/10.1021/AC5039863.
[179] Y. Song, Y. Luo, C. Zhu, H. Li, D. Du, Y. Lin, Recent advances in electrochemical biosensors based on graphene two-dimensional nanomaterials, Biosens. Bioelectron. 76 (2016) 195–212, https://doi.org/10.1016/J.BIOS.2015.07.002.
[180] V. Kotasthane, D.E. Holta, X. Zhao, J.L. Lutkenhaus, M.J. Green, M. Radovic, Core–shell mechanism of etching V2AlC MAX phase to V2CTz MXenes, J. Mater. Res. 38 (2023) 1527–1542, https://doi.org/10.1557/s43578-023-00915-z.
[181] H. An, T. Habib, S. Shah, H. Gao, A. Patel, I. Echols, X. Zhao, M. Radovic, M. J. Green, J.L. Lutkenhaus, Water sorption in MXene/Polyelectrolyte multilayers for ultrafast humidity sensing, ACS Appl. Nano Mater. 2 (2019) 948–955, https://doi.org/10.1021/acsanm.8b02265.
[182] T. Vessella, H. Zhang, Z. Zhou, F. Cui, H.S. Zhou, In-situ synthesized V2CTx MXene-based immune tag for the electrochemical detection of Interleukin 6 (IL-6) from breast cancer cells, Biosens. Bioelectron. 237 (2023) 115512, https://doi.org/10.1016/j.bios.2023.115512.
[183] N. Tasić, I. Konjević, A. Lobato, D. Metarapi, M. Finšgar, F.M. Oliveira, Z. Sofer, R. Gusmão, X. Zhang, S.B. Hočevar, Study of V 2 CT x -MXene based immunosensor for sensitive label-free impedimetric detection of SARS-CoV-2 spike protein, ACS Appl. Mater. Interfaces (2024), https://doi.org/10.1021/acsami.4c04567.
[184] K. Chittuam, S. Jampasa, T. Vilaivan, P. Tangkijvanich, N. Chuaypen, A. Avihingsanon, M. Sain, Y. Panraksa, O. Chailapakul, Electrochemical capillary-driven microfluidic DNA sensor for HIV-1 and HCV coinfection analysis, Anal. Chim. Acta 1265 (2023) 341257, https://doi.org/10.1016/j.aca.2023.341257.
[185] D. Najjar, J. Rainbow, S. Sharma Timilsina, P. Jolly, H. de Puig, M. Yafia, N. Durr, H. Sallum, G. Alter, J.Z. Li, X.G. Yu, D.R. Walt, J.A. Paradiso, P. Estrela, J. J. Collins, D.E. Ingber, A lab-on-a-chip for the concurrent electrochemical detection of SARS-CoV-2 RNA and anti-SARS-CoV-2 antibodies in saliva and plasma, Nat. Biomed. Eng. 6 (2022) 968–978, https://doi.org/10.1038/s41551-022-00919-w.
[186] J.P. Pursey, Y. Chen, E. Stulz, M.K. Park, P. Kongsuphol, Microfluidic electrochemical multiplex detection of bladder cancer DNA markers, Sensor. Actuator. B Chem. 251 (2017) 34–39, https://doi.org/10.1016/j.snb.2017.05.006.
[187] L.S. Oliveira, N. Lucena-Silva, C.A.S. Andrade, M.D.L. Oliveira, Flexible electrochemical biochip for multianalyte detection in childhood leukemia diagnosis, Bioelectrochemistry 168 (2026) 109134, https://doi.org/10.1016/j.bioelechem.2025.109134.
[188] S. Naorungroj, C. Srisomwat, W. Khamcharoen, S. Jampasa, E. Pasomsub, K. Shin, T. Vilaivan, O. Chailapakul, Sequential flow controllable microfluidic device for G-Quadruplex DNAzyme-Based electrochemical detection of SARS-CoV-2 using a pyrrolidinyl peptide nucleic acid, Anal. Chem. 95 (2023) 12794–12801, https://doi.org/10.1021/acs.analchem.3c01758.
[189] F. Berti, S. Laschi, I. Palchetti, J. Rossier, F. Reymond, M. Mascini, G. Marrazza, Microfluidic-based electrochemical genosensor coupled to magnetic beads for hybridization detection, Talanta 77 (2009) 971–978, https://doi.org/10.1016/j.talanta.2008.07.064.
[190] G. Chen, L. Xu, Z. Chen, L. Lin, W. Wang, M. Chen, W. Sun, X. Huang, X. Zhang, J. Chen, A DNA fishhook electrochemical sensor based on a potassium ferricyanide-mediated dual-signal-correlation enhanced electrocatalysis reaction for a simultaneous and correlation assay of multiple biomarkers, ACS Sens. 10 (2025) 3909–3920, https://doi.org/10.1021/acssensors.4c03142.
[191] Y. Liu, B. Lu, Y. Tang, Y. Du, B. Li, Real-time gene analysis based on a portable electrochemical microfluidic system, Electrochem. Commun. 111 (2020) 106665, https://doi.org/10.1016/j.elecom.2020.106665.
[192] Z. Çağlayan Arslan, M. Okan, H. Külah, Pre-enrichment-free detection of hepatocellular carcinoma-specific ctDNA via PDMS and MEMS-based microfluidic sensor, Microchim. Acta 191 (2024) 229, https://doi.org/10.1007/s00604-024-06315-2.
[193] A.C. Soares, J.C. Soares, V.C. Rodrigues, H.D.M. Follmann, L.M.R.B. Arantes, A. C. Carvalho, M.E. Melendez, J.H.T.G. Fregnani, R.M. Reis, A.L. Carvalho, O. N. Oliveira, Microfluidic-based genosensor to detect human papillomavirus (HPV16) for head and neck cancer, ACS Appl. Mater. Interfaces 10 (2018) 36757–36763, https://doi.org/10.1021/acsami.8b14632.
[194] A. Skiba, A. Szymczyk-Drozd, K.M. Serafin, M. Olszewski, E.E. Ferapontova, J. Krzemiński, M. Prygiel, M. Polak, K. Tokarska, E. Malinowska, R. Ziółkowski, Foil-based lab-on-chip electrochemical genosensors for rapid antimicrobial resistance testing, Measurement 259 (2026) 119668, https://doi.org/10.1016/j.measurement.2025.119668.
[195] Y. Zhang, Y. Song, Z. Weng, J. Yang, L. Avery, K.D. Dieckhaus, R.Y. Lai, X. Gao, Y. Zhang, A point-of-care microfluidic biosensing system for rapid and ultrasensitive nucleic acid detection from clinical samples, Lab Chip 23 (2023) 3862–3873, https://doi.org/10.1039/D3LC00372H.
[196] C. Srisomwat, A. Yakoh, N. Chuaypen, P. Tangkijvanich, T. Vilaivan, O. Chailapakul, Amplification-free DNA sensor for the one-step detection of the hepatitis B virus using an automated paper-based lateral flow electrochemical device, Anal. Chem. 93 (2021) 2879–2887, https://doi.org/10.1021/acs.analchem.0c04283.
[197] P.S. Sfragano, E.C. Reynoso, N.E. Rojas-Ruíz, S. Laschi, G. Rossi, M. Buchinger, E. Torres, I. Palchetti, A microfluidic card-based electrochemical assay for the detection of sulfonamide resistance genes, Talanta 271 (2024) 125718, https://doi.org/10.1016/j.talanta.2024.125718.
[198] H. Ehzari, M. Amiri, R. Hallaj, M. Sadeghi, Rapid, flexible fabrication of a microfluidic electrochemical chip nucleic acid target for selective, label-free detection of influenza virus DNA using catalytic redox-recycling, Anal. Biochem. 700 (2025) 115771, https://doi.org/10.1016/j.ab.2025.115771.
[199] A. Dehghan, M.J. Kiani, A. Gholizadeh, J. Aminizadeh, A. Rahi, I. Zare, E. Pishbin, H. Heli, Electrochemical genosensors on-a-chip: applications in early diagnosis of pathogens, Sens. Acutators Rep. 9 (2025) 100335, https://doi.org/10.1016/j.snr.2025.100335.
[200] C. Patiti, P.S. Sfragano, S. Laschi, S. Pillozzi, A. Boddi, O. Crociani, A. Bernini, I. Palchetti, Chip-based and wearable tools for isothermal amplification and electrochemical analysis of nucleic acids, Chemosensors 10 (2022) 278, https://doi.org/10.3390/chemosensors10070278.
[201] G. Luka, A. Ahmadi, H. Najjaran, E. Alocilja, M. DeRosa, K. Wolthers, A. Malki, H. Aziz, A. Althani, M. Hoorfar, Microfluidics integrated biosensors: a leading technology towards Lab-on-a-Chip and sensing applications, Sensors 15 (2015) 30011–30031, https://doi.org/10.3390/s151229783.
[202] R. Cardoso Rial, AI in analytical chemistry: advancements, challenges, and future directions, Talanta 274 (2024) 125949, https://doi.org/10.1016/j.talanta.2024.125949.
[203] A.M. Bond, J. Zhang, L. Gundry, G.F. Kennedy, Opportunities and challenges in applying machine learning to voltammetric mechanistic studies, Curr. Opin. Electrochem. 34 (2022) 101009, https://doi.org/10.1016/j.coelec.2022.101009.
[204] H. Chen, D. Li, E. Kätelhön, R. Miao, R.G. Compton, Experimental voltammetry analyzed using artificial intelligence: thermodynamics and kinetics of the dissociation of acetic acid in aqueous solution, Anal. Chem. 94 (2022) 5901–5908, https://doi.org/10.1021/acs.analchem.2c00110.
[205] H. Chen, E. Kätelhön, H. Le, R.G. Compton, Use of artificial intelligence in electrode reaction mechanism studies: predicting voltammograms and analyzing

the dissociative CE reaction at a hemispherical electrode, Anal. Chem. 93 (2021) 13360–13372, https://doi.org/10.1021/acs.analchem.1c03154.
[206] M.E. Orazem, B. Ulgut, Can interpretation of electrochemical impedance spectroscopy data be automated? Where do artificial intelligence algorithms stand? Curr. Opin. Electrochem. 55 (2026) 101788 https://doi.org/10.1016/j.coelec.2025.101788.
[207] Regulation (EU), 2017/746 of the European Parliament and of the Council of 5 April 2017 on in vitro diagnostic medical devices and repealing Directive 98/79/EC and Commission Decision 2010/227/EU. https://eur-lex.europa.eu/eli/reg/2017/746/oj/eng.